Analysis of drug resistance mechanisms in intact *Plasmodium falciparum*-infected red blood cells

Sarah Julia Reiling

Institute of Parasitology

McGill University, Montreal

August 2015

A thesis submitted to McGill University in partial fulfillment of the requirements of the degree of Doctor of Philosophy

Abstract

Malaria is a major global health concern, with half of the world's population being at risk of infection. Among the *Plasmodium* species that infect humans, *P. falciparum* causes most fatalities. Chloroquine (CQ) was the drug of choice for decades and considered safe, affordable and easy-to-use until resistance emerged. No other antimalarial drug has been able to avoid emergence of resistance as long as CQ, and although resistance against *P. falciparum* is widespread, CQ is still effective against *P. vivax*. However, the exact mechanism of CQ resistance is not known. It is of high importance to understand the mechanism of resistance to drugs such as CQ, especially since resistance is starting to emerge for the currently used artemisinin-based combination therapies only a few years after their introduction. CQ is suggested to accumulate in the parasite's digestive vacuole due to its weak base properties, where it exerts its antimalarial action.

Several transporters are involved in intracellular distribution of antimalarial drugs. Among them are the *P. falciparum* chloroquine resistance transporter (PfCRT) and the *P. falciparum* multidrug resistance 1 transporter (PfMDR1). Both are located in the digestive vacuolar membrane but transport substrates in opposing directions. While the PfCRT variant harboring the K76T mutation transports substrates out of the digestive vacuole (DV), PfMDR1 transports substrates into the DV. PfMDR1 contains five polymorphisms that are suggested to be involved in altered drug transport, although the exact role of each amino acid mutation remains unknown. To gain more insight into the transport functions of PfMDR1, variants with different mutation patterns were analyzed using the fluorescent substrate Fluo-4. We found a crucial role for asparagine (N) at residue 1042 in Fluo-4 transport, while substitution with aspartic acid (D) abolished all transport. In addition, we showed an association of the PfMDR1 N1042D mutation with increased mefloquine but decreased quinine sensitivity. Furthermore, competition studies of Fluo-4 with the antimalarial drugs chloroquine, mefloquine and quinine showed distinct transport inhibition patterns for parasites of different genetic background. This can be used as a tool to evaluate parasite susceptibility to antimalarial drugs.

Next, we investigated the mechanism of resistance to CQ in more detail. We showed that parasite survival is higher in CQ-resistant strains compared to CQ-sensitive strains in the initial 10 hours

after exposure to equally lethal CQ concentrations. Moreover, dark cytosolic structures appeared in CQ-sensitive strains that were later confirmed as hemozoin-containing compartments surrounded by a membrane bilayer. Leakage of hemozoin crystals out of the DV was ruled out since lysis of the digestive vacuolar membrane did not occur during that time frame. These data suggest that CQ resistance is not linked to reduced drug concentrations in the DV alone, and additional regulatory mechanisms in the parasite must play a crucial role during CQ exposure.

To pursue these findings, a commercially available fluorescent tagged CQ analogue, LynxTag™-CQ_{GREEN} (CQ_{GREEN}), was examined for its suitability in studying CQ transport and intracellular drug accumulation. While CQ_{GREEN} was half as effective in parasite killing of CQ-sensitive strains compared to unmodified CQ, no significant changes in parasite killing were observed in CQ-resistant strains. However, live cell imaging showed that CQ_{GREEN} accumulated in the parasite cytosol and not the DV. These results show for the first time a potential target for a CQ analogue outside the digestive vacuole. Moreover, intracellular CQ_{GREEN} uptake rates were reduced in CQ-resistant strains compared to CQ-sensitive strains. This, too, suggests that CQ-resistant strains must have evolved a regulatory mechanism to decrease intracellular CQ accumulation.

The results presented in this thesis expand our understanding of substrate transport by PfMDR1. Furthermore, a novel phenotype was described for CQ-sensitive strains upon drug exposure that was not seen in CQ-resistant strains. These data suggest that altered regulatory mechanisms play a role in CQ resistance and are likely located in the parasite cytosol.

Abrégé

Avec la moitié de la population mondiale à risque d'infection, le paludisme est un problème important de santé mondiale. Parmi les espèces de *Plasmodium* qui infectent les humains, *P. falciparum* provoque la majorité des décès. Pendant des décennies, la chloroquine (CQ) a été le médicament privilégié. Elle était considérée sécuritaire, abordable et facile à utiliser jusqu'au jour où la résistance a émergé. À ce jour, aucun autre médicament antipaludique a été en mesure d'éviter l'émergence de la résistance aussi longtemps que la chloroquine. Le mécanisme exact de la résistance à la CQ n'est pas encore connu. Actuellement, la résistance aux antipaludiques commence à émerger aussi dans les thérapies combinées à base d'artémisinine at ceci seulement quelques années après leur introduction sur le marché. Il est donc important de comprendre le mécanisme de la résistance aux antipaludiques, particulièrement dont la chloroquine. Il a été proposé que la CQ s'accumulait dans la vacuole digestive du parasite en raison de ses propriétés de faible base, où elle déploie son action antipaludique.

Plusieurs transporteurs sont impliqués dans la distribution intracellulaire des médicaments antipaludiques dont le *P. falciparum* chloroquine resistance transporter (PfCRT) et le *P. falciparum* multidrug resistance 1 transporter (PfMDR1). Tous les deux sont situés dans la membrane de la vacuole digestive, mais ils transportent des substrats dans des directions opposées. Alors que la variante PfCRT porteuse de la mutation de la chloroquine K76T transporte la CQ hors de la vacuole digestive (VD), PfMDR1 transporte des substrats dans la VD. PfMDR1 contient cinq polymorphismes proposés comme étant impliqués dans le transport altéré de la drogue. Le rôle exact de chaque mutation dans ces acides aminés reste inconnu. Les variantes polymorphiques composées des divers types de mutations ont été analysées en utilisant le substrat fluorescent Fluo-4 pour identifier les fonctions de transport de PfMDR1. Nous avons trouvé un rôle primordial de transport de Fluo-4 au niveau de l'asparagine (N) localisée au résidu 1042, alors que la substitution de cet acide aminé par un acide aspartique (D) abolissait tous les transports. Nous avons aussi montré une association de la mutation PfMDR1 N1042D avec une sensibilité accrue pour la méfloquine. De plus, des études de compétition de Fluo-4 avec les antipaludiques tels que la chloroquine, méfloquine et quinine ont montré des profils d'inhibition de transport distincts

pour les parasites d'origines génétiques différentes. Ceci peut être utilisé comme un outil pour évaluer la sensibilité des parasites aux médicaments antipaludiques.

Ensuite, nous avons étudié le mécanisme de la résistance à la chloroquine plus en détail. Nous avons montré que la survie des parasites était plus élevée chez les parasites CQ-résistants (CQR) par rapport aux parasites CQ-sensibles (CQS) dans les premières 10 heures après exposition à des concentrations de CQ également létales. Par ailleurs, des structures cytosoliques sombres ont été observées dans les parasites CQS. Des compartiments contenant de l'hémozoïne entouré d'une membrane bicouche ont été ensuite confirmés. L'hypothèse de perforations de la VD entraînant la fuite ultérieure des cristaux des hémozoïnes n'a pas été retenue car lyse de la membrane vacuolaire digestive n'a pas eu lieu au cours de ce laps de temps. Ces données suggèrent que la résistance à la CQ n'est pas seulement liée à des concentrations de médicament réduites dans la VD. Des mécanismes de régulation supplémentaires dans les parasites semblent jouer un rôle primordial lors de l'exposition à la CQ.

Par ailleurs, un analogue fluorescent de la chloroquine disponible dans le commerce LynxTag™-CQ_{GREEN} (CQ_{GREEN}) a été examiné étant approprié pour l'étudie du transport de la CQ et de l'accumulation intracellulaire du médicament. La CQ_{GREEN} était à moitié efficace pour tuer les parasites CQS que la CQ non modifiée, mais nous n'avons pas observé de changement significatif dans la destruction des parasites CQR. De plus, l'imagerie des cellules vivantes a permis de montrer que la CQ_{GREEN} s'accumulait dans le cytosol des parasites et non dans la VD. Ces résultats montrent pour la première fois une cible potentielle d'un analogue à la CQ hors de la VD. Les quantités d'accumulation intracellulaire de CQ_{GREEN} ont été réduites chez les parasites CQR par rapport aux parasites CQS et ainsi suggère que les parasites CQR semblent avoir développés un mécanisme régulateur pour diminuer l'accumulation de CQ intracellulaire.

Les résultats présentés dans cette thèse élargissent notre compréhension du transport de substrat de PfMDR1. Un nouveau phénotype a été observé et décrit uniquement chez les parasites CQS lors de l'exposition au médicament. Ces données suggèrent que des mécanismes de régulation modifiés, probablement situés dans le cytosol des parasites, jouent un rôle dans la résistance à la CQ.

Acknowledgements

This work would not have been possible without the mentorship of my thesis supervisor, Prof. Petra Rohrbach. I greatly value the independence that she has given me in the design and execution of projects. When I got sidetracked by the numerous options provided by each individual project, her careful evaluation has brought me back on track to successfully finish this thesis. I am deeply grateful for Petra's constructive editing of all my writing during the course of my thesis. Her positive feedback has highly improved my spelling style to obtain an excellent academic level.

I would like to thank the former and current members of the Rohrbach lab, who have much added to the joy of everyday routine. I will gladly remember the great time I have had with Maren Heimhalt, Georgi Tadeus and Jill Arnold, who all have astonished me with their amazing personalities, high intelligence and powerful charm. Many thanks to Juliane and her loving emails.

I am especially grateful to Sonia Edaye and Karen Geukers for their introduction into culturing malaria parasites and everything they have taught me about being passionate about the wellbeing of these creatures. Thank you Sonia for always being there whenever I had the feeling of being stuck. Your dedication to research was wonderful to witness.

Lots of thanks to the warm welcome that I have received from Prof. John Dalton and the members of his laboratory when I started working at the Institute of Parasitology. Rency Mathew has been a great friend when I arrived at this institute and has made my start in this country much more pleasant. Through her, I have learned how important it is to have one friend who will always be there, and to have faith in myself. Dr. Karine Thivierge was a wonderful mentor in molecular techniques. I will also happily remember the time that John Dalton and I have spent in the tropical malaria culture room on cold winter weekends, feeding parasites in the malaria incubator and the wave bioreactor.

Through the DAAD Exchange program, I had the opportunity to work with many talented young researchers from Germany who much added to the joy of the quiet summer months at Macdonald campus: Yamila Betz, whom I could tell to either feed the parasites or bake cookies; Felix Gilbert, who has sent the first postcard that I have received at this institute, which is a constant reminder

to visit Canada's East Coast; Laura Sellmer and Ricarda Hoffmann who were almost inseparable; Georgi Tadeus, without whom I would know nothing about Igor; and Jakob Wirbel who has become a close friend and companion.

I am very grateful for the support that I have received from Prof. Elias Georges. His knowledge and guidance have greatly pushed my research objectives forward, more than I could have wished for.

The joint laboratory meetings with Prof. Jerry Aldridge and his laboratory members were always interesting to attend, and have much contributed to my knowledge about experimental controls, influenza immunology and teaching strategies of a supervisor.

Prof. Timothy Geary has made me feel at home at the institute from the day I have arrived. His care and geniality are heartwarming. His amazing passion and ideas about research projects have always inspired me to dig deeper into the unknown at the edge of science.

The administrative support and motherly care from Shirley Mongeau was fabulous. Getting familiar with the institute and its equipment was made easy with the help of Serghei Dernovici, Gordon Bingham and Jenny Eng. Furthermore, I have never felt lonely during long evenings at the institute through the cheerful presence of Mike.

Prof. Georg Krohne has introduced me to the world of electron microscopy. His unlimited friendliness and patience during long days at the Biocenter, University of Würzburg, Germany has made my stay in Bavaria unforgettable. It was a great pleasure to work on joint projects with Prof. Oliver Friedrich, Dr. Barbara Kappes and Dr. Nina Simon from the Friedrich-Alexander University of Erlangen-Nuremberg, Germany.

Merci beaucoup à Dr. Catherine Bourguinat, qui m'a aidé énormément avec la traduction française de l'abrégé.

The generosity from Douglas and Mari Harpur was wonderful. Getting to know them personally has made me incredibly proud to have been awarded the Robert P. Harpur Fellowship.

Paul Sauer has supported me throughout the years during my thesis. His reassurance and support have driven me to conclude this work. He has never failed to believe in the successful completion of my PhD.

Maude Ouellette-Dubé has inspired me to stay positive and to look at life from a more philosophical point of view. Andreas Harmeling has given me incredible support during the final year of my thesis and beyond.

My lovely parents Doris and Michael, and my sister Miriam Reiling have supported me during every step of my thesis. Their pride in the work I am doing has driven me to give my best.

Statement of Originality

The following aspects presented in this thesis are considered original contributions to knowledge:

Chapter 2 - Manuscript I:

Sarah J. Reiling and Petra Rohrbach

'Monitoring PfMDR1 transport in *Plasmodium falciparum*.'

Malaria Journal 2015. 14(1):270

This manuscript describes for the first time a functional association of an amino acid mutation in the *P. falciparum* multidrug resistance 1 transporter (PfMDR1), located in the proposed substrate binding pocket, with altered substrate transport. Fluo-4 has already been identified as a substrate that was transported by most PfMDR1 variants but no single amino acid mutation could be identified for Fluo-4 transport from the cytosol into the digestive vacuole. For this manuscript, detailed analysis was performed with *P. falciparum* parasite strains of different genetic background and varying PfMDR1 mutation patterns to narrow down which mutation sites may be involved in abolished Fluo-4 transport. The importance of residue 1042 in Fluo-4 transport was confirmed using clones derived from two *P. falciparum* strains that display either a chloroquine-sensitive or chloroquine-resistant phenotype and were stably transfected to generate a single amino acid mutation at residue 1042. For the first time, we showed distinct competition patterns of Fluo-4 with the antimalarial drugs chloroquine, quinine and mefloquine in parasites that were sensitive or resistant to these drugs. Furthermore, this study supports a potential role of asparagine at residue 1042 in altered parasite susceptibility to mefloquine and quinine.

Chapter 3 - Manuscript II:

Sarah J. Reiling, Georgi Tadeus, Georg Krohne and Petra Rohrbach

'Chloroquine induces formation of cytosolic hemozoin-containing compartments in chloroquine-sensitive *Plasmodium falciparum* parasites.'

The exact mechanism of chloroquine (CQ)-induced parasite killing is not fully understood. Although the PfCRT K76T mutation plays an important role, this hypothesis cannot explain by itself why CQ-resistant parasites tolerate higher intracellular CQ concentrations compared to sensitive strains. This study uses for the first time an assay that is based on the IC_{50} values of each strain to quantitatively determine the amount of CQ necessary for equal killing of CQ-sensitive versus -resistant strains in a time-dependent manner. Live cell microscopy of CQ-sensitive and CQ-resistant strains exposed to CQ concentrations equal to their 20x IC_{50} values revealed the appearance of cytosolic hemozoin-containing compartments in CQ-sensitive strains, which were not observed in CQ-resistant strains and have not been described before. Using Fluo-4 as a fluorescent substrate that accumulates in the digestive vacuole (DV) and subsequent CQ exposure of sensitive parasites, this study proposes that the hemozoin-containing compartments originate from the DV. This manuscript demonstrates that CQ-sensitive parasites exhibit features of programmed cell death that occur prior to lysis of the DV membrane and without activation of classical apoptosis cascades, such as the loss of the mitochondrial membrane potential. Furthermore, these features were absent in CQ-resistant parasites exposed to lethal CQ concentrations, indicating that regulatory pathways may be involved in CQ resistance.

Chapter 4 - Manuscript III:

Sarah J. Reiling and Petra Rohrbach

'Fluorescently tagged chloroquine accumulates in the *Plasmodium falciparum* cytosol.'

This manuscript critically investigates the usefulness of a commercially available fluorescently tagged chloroquine, LynxTag-CQ™$_{GREEN}$ (CQ_{GREEN}), for experiments on *P. falciparum* parasites. Although one study has described the suitability of CQ_{GREEN} using microsomes that carry either sensitive- or resistant-type PfCRT [92], the effect of CQ_{GREEN} on live parasites is not known. This manuscript reveals discrepancies between reported accumulation of CQ_{GREEN} in the parasite's digestive vacuole (DV) and our own measurements, displaying strong accumulation in the parasite cytosol but not the DV. The possibility that cleavage of the fluorescent BODIPY moiety from CQ occurred was excluded through our experiments. Furthermore, accumulation of CQ_{GREEN} in the parasite's cytosol was independent of pH, which is the main contributor to accumulation of unmodified CQ in the DV, suggesting that an intracellular target is likely influencing the localization of CQ_{GREEN} to the cytosol. This manuscript suggests that accumulation of CQ within the parasite may not only be pH dependent but also determined by the affinity of CQ for cytosolic proteins.

Contribution of Authors

Experiments presented in this thesis have been designed and executed by the author under the supervision of Prof. Petra Rohrbach, with contributions as follows:

In the first manuscript, the clones SDD^{GC03}, SND^{GC03}, SDD^{3BA6} and SND^{3BA6} were kindly provided by Prof. David Fidock. All experiments presented in this manuscript were executed by Sarah J. Reiling.

In the second manuscript, IC_{50} values were determined using a custom made procedure for Igor Pro 6.2 written by Georgi Tadeus, based on an R script kindly provided by Hervé Le Nagard. Preparation of parasites for electron microscopy was done by the Sarah J. Reiling at the Friedrich-Alexander University of Erlangen-Nuremberg, Germany in the laboratory of Dr. Barbara Kappes. Staining of fixed parasites with OsO_4, embedding in epon 812 and ultrathin cuts were done by Prof. Georg Krohne and his laboratory at the Biocenter, University of Würzburg, Germany. Electron microscopy images were taken by Prof. Georg Krohne together with Sarah J. Reiling.

In the third manuscript, all experiments were performed by the Sarah J. Reiling. Georgi Tadeus kindly assisted in the analysis of CQ_{GREEN} uptake rates.

Table of Contents

List of Figures

List of Tables

List of Abbreviations

ABC	ATP-binding cassette
ACT	artemisinin-based combination therapy
AQ	amodiaquine
ART	artemisinin
ATG	autophagy-related genes
Baf-A1	bafilomycin A1
CFI	Canada Foundation for Innovation
CHPI	Centre for Host-Parasite Interactions
CQ	chloroquine
CQR	chloroquine-resistant
CQS	chloroquine-sensitive
DAAD	German Academic Exchange Service
DHA	dihydroartemisinin
DIC	differential interference contrast
DMSO	dimethyl sulfoxide
DNA	deoxyribonucleic acid
DV	digestive vacuole
EL	external loop
EM	electron microscopy
Fluo-4 AM	Fluo-4 acetoxymethyl ester
FPIX	ferriprotoporphyrin IX
GFP	green fluorescent protein
GSH	glutathione
HF	halofantrine
Hz	hemozoin
IH	internal helix
iRBC	infected red blood cell
LF	lumefantrine

LSM	laser scanning microscope
MDR	multidrug resistance
MQ	mefloquine
MRP	multidrug resistance associated protein
MW	molecular weight
NBD	nucleotide binding domain
NSERC	Natural Sciences and Engineering Research Council
PBS	phosphate buffered saline
PCD	programmed cell death
PCR	polymerase chain reaction
PfCRT	*Plasmodium falciparum* chloroquine resistance transporter
PfMDR1	*Plasmodium falciparum* multi-drug resistance 1 transporter
Pgh1	P-glycoprotein homologue 1
Pgp	P-glycoprotein
PV	parasitophorous vacuole
PVM	parasitophorous vacuole membrane
QC	quinacrine
QN	quinine
RBC	red blood cell
RNA	ribonucleic acid
RT	room temperature
SDCM	spinning disk confocal microscopy
SNP	single nucleotide polymorphism
TMD	transmembrane domain
TQ	tariquidar
uRBC	uninfected red blood cell
VP	verapamil
WHO	World Health Organization
ψ_m	mitochondrial membrane potential

General Introduction

Malaria is a common and potentially life-threatening disease in many tropical and subtropical regions. It is caused by parasites of the *Plasmodium* genus and transmitted through female *Anopheles* mosquitoes. Elimination of *Plasmodium* parasites was successful in several regions with low transmission rates, but they are still endemic in more than 100 countries, putting half of the world's population at risk of infection. Most of the severe malaria cases are associated with *P. falciparum* infections. If left untreated, the disease can lead to serious complications, including death. In 2014, roughly 600,000 people succumbed to malaria infections, averaging one death every 50 seconds.

Extensive use of single drug treatment regimens has resulted in widespread resistance of *P. falciparum* to commonly used antimalarial drugs. To date, artemisinin-based combination therapies (ACTs) are the treatment of choice in most countries. ACTs are still effective in Africa and South America, but resistance has started to emerge in Southeast Asia only a few years after their introduction. It is imperative to find new solutions to combat drug resistance and make antimalarial treatment a viable option.

Chloroquine (CQ) was the drug of choice for decades until resistance emerged. No other antimalarial drug has avoided resistance in parasites as long as CQ. Moreover, studies on parasite populations in the field revealed that *P. falciparum* parasites in formerly CQ-resistant regions have reverted back to sensitivity [1]. Genetic modifications may enhance the parasite's survival in the human host during CQ pressure but most likely lead to a fitness disadvantage compared to wild-type parasites. This could explain why CQ resistance took decades to manifest itself in the field and is unfavorable to maintain in the absence of drug pressure. However, the exact mechanism(s) of CQ resistance are not known.

Two transporters are involved in CQ resistance: the *P. falciparum* chloroquine resistance transporter (PfCRT) and the *P. falciparum* multidrug resistance 1 transporter (PfMDR1). A single amino acid mutation in PfCRT at residue 76 from lysine to threonine (K76T) enhances resistance to

CQ [2]. The transporter PfMDR1 contains five polymorphisms that are linked to increased resistance to various antimalarial drugs, including CQ, but their exact role has not been elucidated.

The aim of this thesis is to better understand drug resistance mechanisms in intact *P. falciparum*-infected red blood cells (RBCs). The first objective was to determine which PfMDR1 amino acid mutation(s) influence substrate transport. For this, *P. falciparum* strains with varying amino acid mutations were analyzed for their ability to transport the fluorescent dye Fluo-4. Furthermore, stably transfected parasites harboring an asparagine (N) or aspartic acid (D) at position 1042 were used to verify the importance of this residue. In addition, the role of residue 1042, which is located in the substrate binding pocket, in altered drug sensitivity was analyzed.

CQ accumulates in all *P. falciparum* parasites but to higher extent in CQ-sensitive (CQS) strains compared to CQ-resistant (CQR) strains. However, increasing extracellular CQ concentrations to obtain similar intracellular drug concentrations was not sufficient to achieve equivalent levels of parasite killing [3, 4]. The second objective of this thesis was to investigate the effects of varying CQ concentrations on CQS and CQR strains. A novel phenotype was described for CQS strains that was not seen in CQR strains and was further characterized in this thesis.

Due to its weak base properties, CQ accumulates in acidic compartments such as the parasite's DV, where it gets trapped in its diprotonated form. However, these assumptions are based on diffusion models, while affinity of CQ to molecules, such as ferriprotoporphyrin IX (FPIX), was not taken into account. A fluorescently tagged CQ analogue, called LynxTag™CQ_{GREEN}, is commercially available and can be used to analyze its intracellular distribution in live parasites. The third objective of this thesis was to investigate the suitability of CQ_{GREEN} for live cell imaging of intact *P. falciparum*-infected RBCs and determine its efficacy and intracellular localization.

These studies provide new insight into CQ's mode of action. They demonstrate that CQR strains have regulatory mechanisms that remain unclear. Furthermore, this thesis delivers evidence for a pivotal role of PfMDR1 residue 1042 in substrate transport. This work will contribute to a better understanding of CQ resistance in *P. falciparum* and lead to the development of new strategies for effective malaria treatment.

— Chapter 1 —

Literature Review

1.1 General Overview

1.1.1 History and prevalence of malaria

Malaria remains the most significant parasitic disease and threat to the human population worldwide. It claims the lives of more children than any other infectious disease and kills more than 600,000 people each year [5]. Although the disease was eliminated in North America and most parts of Europe in the past century, malaria is still endemic in over 100 countries. Approximately 3.4 billion people live in malaria risk areas, which represents half of the world's population [5]. It is estimated that about 300 million people worldwide are infected with malaria. In general, all people in a high-transmission area are infected with at least one species of *Plasmodium* parasites that are likely to be below PCR detection limits [6].

Research on the malaria parasite started approximately 140 years ago, when Alphonse Laveran first spotted a microgametocyte exflagellating in a blood sample [7]. The parasitic life cycle was described by Ronald Ross in 1897, when he discovered the *Plasmodium* vector to be the *Anopheles* mosquito [8]. Four *Plasmodium* species commonly infect humans: *P. falciparum*, *P. vivax*, *P. malariae*, and *P. ovale*. The latter is further subdivided into the two subspecies *P. ovale curtisi* and *P. ovale wallikeri* that are sympatric but are non-recombining [9]. *P. vivax* causes the majority of infections due to its wide distribution. It can be found throughout the tropics, subtropics, and temperate zones, whereas the most fatal species, *P. falciparum*, is generally confined to the tropics. *P. malariae* is widespread throughout sub-Saharan Africa, Asia and South America, but has only low prevalence and mild clinical manifestations. *P. ovale* infections are mainly limited to West Africa, Southeast Asia and some South Pacific islands. *P. malariae* and *P. ovale* combined are responsible for only 5% of worldwide malaria infections. Interestingly, data from 2004 suggest that a fifth malaria parasite, *P. knowlesi*, which usually infects macaque monkeys can also infect humans. Cases have been confirmed from Malaysia, Thailand, Myanmar and the Philippines [10]. Although it has been known for over 50 years that some monkey malaria strains could infect humans under laboratory conditions, it is now well established that *P. knowlesi* is an emerging zoonotic human pathogen.

Among all *Plasmodium* spp. that infect humans, *P. falciparum* causes the highest fatality rates. The mortality associated with falciparum malaria is approximately 0.1%, if effective drugs are readily available. In other cases, uncontrolled parasite multiplication leads to heavy parasite burdens, which result in vital-organ dysfunction, acidosis and severe anemia. Jaundice, pulmonary edema, and acute renal failure are commonly seen in adults. In these cases, the mortality rises, despite treatment, to 15-20% [6]. Death in severe malaria cases usually occurs within 48 hours of presentation, which correlates with one erythrocytic life cycle.

1.1.2 Life cycle of Plasmodium spp.

P. falciparum is transmitted to humans by female mosquitoes of the *Anopheles* genus, which are mainly found in warm climate zones around the world. An infected mosquito harbors the sporozoite stage of *Plasmodium* parasites in its salivary glands and injects the sporozoites together with the saliva into the skin of a human host (Figure 1.1). While sexual reproduction of the parasites takes place in the mosquito, two asexual propagation cycles occur in an infected human. Within the first hour, the injected sporozoites are transported via the blood stream to liver cells. After one week of exo-erythrocytic schizogony, each infected hepatocyte liberates approximately 30,000 merozoites [6]. The released liver-merozoites then infect RBCs. During the 48-hour erythrocytic cycle, the parasites undergo three different stages with distinct characteristics. After RBC invasion, the merozoite converts into a ring-shaped parasite for 24 hours. Within the following 12 hours, the ring stages develop into trophozoites. This stage contains the replication of DNA, which begins 26 h post invasion (p.i.) and ends approx. 37 h p.i. [11]. From 36 to 48 hours p.i., the trophozoites develop into schizonts. Depending on the parasite strain, each schizont harbors an average of 16 to 24 merozoites [12, 13]. Each host cell harbors large numbers of mature merozoites that are synchronously released and immediately capable of invading new RBCs. The burst of huge numbers of RBCs and release of merozoites with their toxic by-products are the major factors for high fever attacks. Severe pathogenesis of the disease is usually attributed to parasite burden and sequestration of mature forms in the vascular bed of several organs, including brain and lungs. This asexual erythrocytic cycle is the main target of currently used antimalarial drugs. They either

interfere with the cell metabolism and, therefore, reduce the parasite's growth, or they inhibit the detoxification of heme, which, in turn, kills the parasite. However, the mechanism of action of most antimalarials remains controversial.

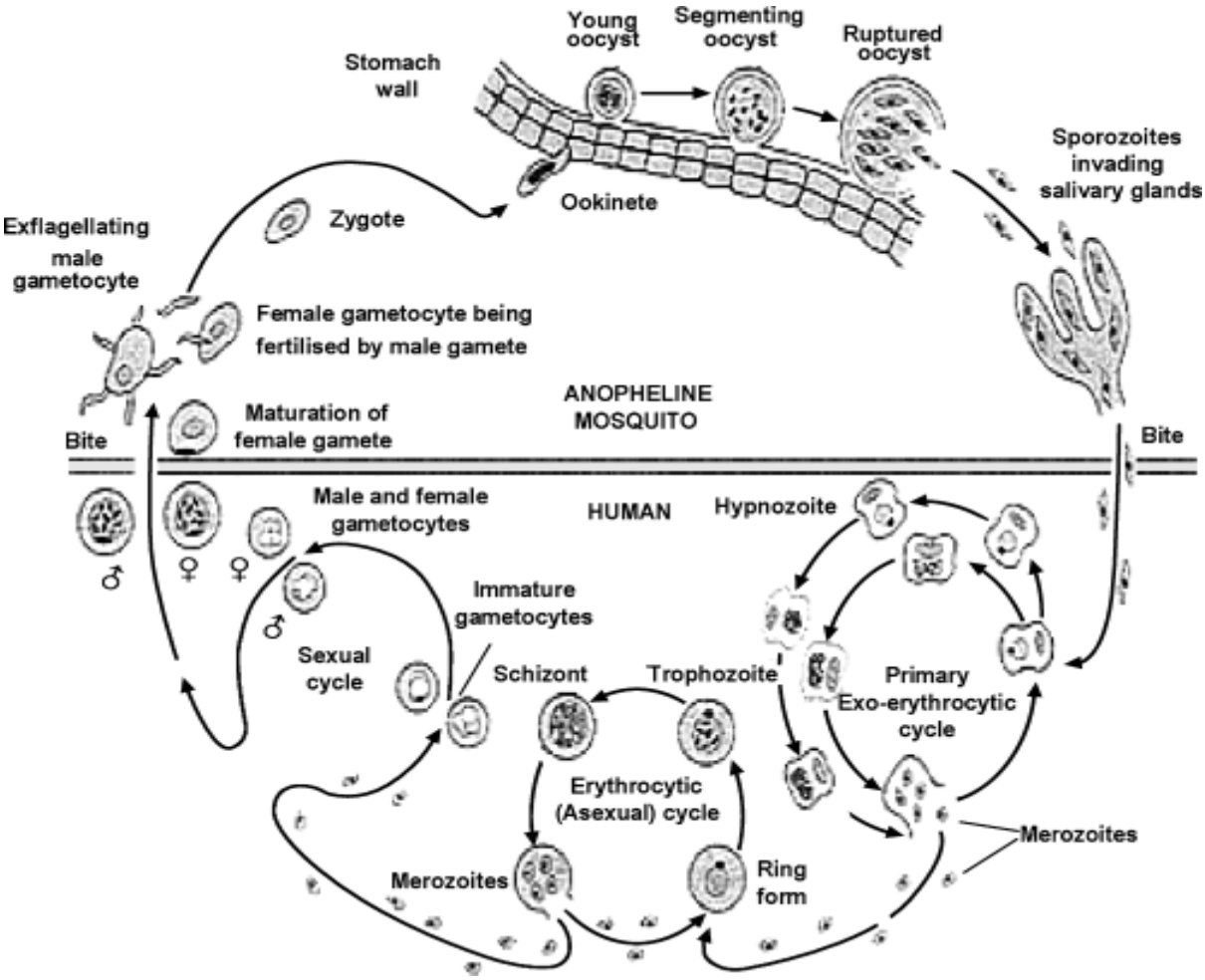

Figure 1.1 *P. falciparum* life cycle. An infected female mosquito transmits sporozoites into the human host, which migrate to the liver and undergo schizogony during the hepatocyte stage. The released merozoites then infect red blood cells (RBCs) and transform within 48 hours from ring stages into trophozoites and finally schizonts. The RBCs release new merozoites, which start another erythrocytic replication cycle. Eventually, some blood stage parasites differentiate into male or female gametocytes. Once a naive female mosquito takes a blood meal from the infected human host, the gametes mature in the mosquito's gut, where the male microgametocytes undergo nuclear division by a process called exflagellation and mate with the female macrogametes. New genetic recombination takes place in the motile zygote, now called the ookinete. It migrates to the mosquito midgut and grows into the oocyst, which extends to the insect's hemocoel. Depending on climate conditions such as humidity and temperature, the oocyst matures in 10-21 days and produces hundreds of sporozoites that finally cause the oocyst to rupture. The released sporozoites disperse throughout the insect's body and reach the salivary glands. When the mosquito takes its next blood meal, the sporozoites are injected with the saliva into the new mammalian host. (from [14])

If the RBC infection is only partially controlled by the immune system or drug treatment, the residing parasites will continue proliferating and subsequently result in the re-appearance of clinical symptoms, termed recrudescence. All *Plasmodium* spp. cause recrudescence, while only *P. vivax* and *P. ovale* harbor the property to cause a recurrence or true relapse from dormant liver stage hypnozoites that can be released months or years after the first round of erythrocytic infection is resolved.

1.1.3 Emergence of drug resistance

Most drugs used in antimalarial treatment are active against the erythrocytic stages. These drugs include chloroquine (Resochin®), artemether-lumefantrine (Coartem®), Sulfadoxine-pyrimethamine (Fansidar®), mefloquine (Lariam®), quinine, quinidine, doxycycline used in combination with quinine, clindamycin used in combination with quinine, and artesunate. In addition, primaquine is active against hypnozoites and prevents relapses but should not be used by pregnant women or people with glucose-6-phosphate dehydrogenase deficiency. A list of region-specific recommended treatment for uncomplicated or severe *P. falciparum* malaria is available through the World Health Organization, based on local resistance patterns of *P. falciparum* parasites. CQ in combination with primaquine is recommended in the Americas, while artemisinin-based combination therapies (ACT) are recommended for uncomplicated malaria in the African, Eastern Mediterranean and South-East Asian regions.

P. falciparum parasites have evolved resistance to almost all available antimalarial drugs, including mefloquine (MQ), halofantrine (HF), lumefantrine (LF), pyrimethamine, chloroquine, sulfonamides, and artemisinin (ART) and derivatives [6]. CQ resistance occurs in most malaria-affected areas, and resistance to sulphadoxine-pyrimethamine is spreading rapidly. Resistance to MQ is mainly confined to areas where it has been used extensively, such as Thailand, Cambodia and Vietnam, and arose within six years of systematic deployment [15]. Cases of resistance to ACTs have been reported for regions of the Thai-Myanmar and Thai-Cambodian border [16, 17], raising concerns of further spread of resistance to this treatment since this is the last antimalarial treatment currently on the market without widespread resistance. Recently, mutations in the kelch propeller

domain were identified as a molecular marker for artemisinin resistance [18]. This will provide a useful tool in monitoring the spread of artemisinin resistance worldwide.

Low cost of antimalarial treatment is crucial in most malaria-affected countries, where annually less than US$10 per person are available for healthcare and malaria treatment should not cost more than 50 cents. Therefore, treatment that is highly effective, safe, and affordable is of major importance. CQ has been the drug of choice for decades and has saved the lives of more people than any other antimalarial drug. If the mechanism for CQ resistance is known, treatment failure could be circumvented and CQ administration re-established in countries with emerging ACT resistance.

1.2 Chloroquine

CQ was effective for decades before resistance emerged. CQ treatment was used extensively in Africa during the 1980s, with an estimated distribution of nearly 200 tons of CQ base in 1988 alone [19]. Although CQ resistance in *P. falciparum* is now found worldwide, it still has high efficacy against *P. vivax* [20]. Two main advantages of CQ compared to other antimalarials are its low production costs, which makes it affordable to people with low income, and its good tolerability. In addition, removal of CQ as treatment of choice in regions where resistance is common can reverse CQ-resistant (CQR) parasite populations back to CQ-sensitivity, making CQ treatment once again effective.

Efficacy of CQ is stage-specific

CQ is most effective on trophozoite stage parasites [21]. At this stage, hemoglobin degradation is a major factor in the parasite's development. CQ uptake of the parasites is divided into two phases: a rapid saturable uptake phase and a slower non-saturable phase. CQ uptake within the parasite reaches a maximum level within 1 hour of exposure rather than continuing indefinitely [20]. Discrepancies have been reported for the parasite stage that is most vulnerable to CQ exposure. One study suggested that ring stage parasites are more sensitive to CQ than trophozoites or

schizonts, with an IC_{50} in trophozoites that was determined to be 6-fold higher compared to rings [22]. Furthermore, therapeutic concentrations of CQ only prevent the transformation of rings to trophozoites but did not affect the development from trophozoites to schizonts or from schizonts to new rings. Other researchers showed that trophozoites were the most sensitive to CQ exposure [21, 23, 24].

1.2.1 Effect of CQ in the digestive vacuole of malaria parasites

CQ accumulates in the parasite's digestive vacuole based on a pH gradient. The parasite cytosol has a pH of ~7.2, whereas the DV has a pH of ~5.2 [25]. Due to its intrinsic weak base properties, CQ is suggested to accumulate in the DV in its diprotonated form [3, 26-30]. It is debated whether intrinsic pH of the parasite cytosol and DV differ between CQS and CQR parasites, thereby influencing CQ uptake [31-33]. Using radiolabeled CQ, its uptake into the parasite was found to be dependent on the external CQ concentration and ranged from >1000-fold accumulation at low CQ external concentrations to 100-fold accumulation at high external CQ concentrations [3, 4, 34-39]. Furthermore, CQ accumulation was reduced by half in CQR compared to CQS strains [35, 40]. However, these studies could not differentiate between CQ accumulation in the parasite cytosol and the DV. Only CQ concentrations in the whole host-parasite system were determined.

An *in silico* approach based on a physical compartmental model of a cell can be used to calculate CQ accumulation in the cytosol and DV, compared to external CQ concentration. Cellular traffic can be described with a set of coupled differential equations, accounting for substrate diffusion and active transport across membranes [41, 42]. CQ can reach concentrations in the DV that are >2000-fold higher than in the parasite cytosol at physiological pH (Figure 1.2). Since CQ, being a weak base, moderately raises the pH of the DV, CQ accumulation was calculated for increasing digestive vacuolar pH (pH_{DV}) with decreasing cytosolic pH (pH_{cyt}). At an estimated pH_{DV} of 6.0 and pH_{cyt} of 7.0, CQ concentrations are still 60-fold higher in the DV compared to the cytosol. Therefore, relatively small changes in pH of the DV that are thought to distinguish CQS and CQR strains should have little effect on CQ accumulation in the DV.

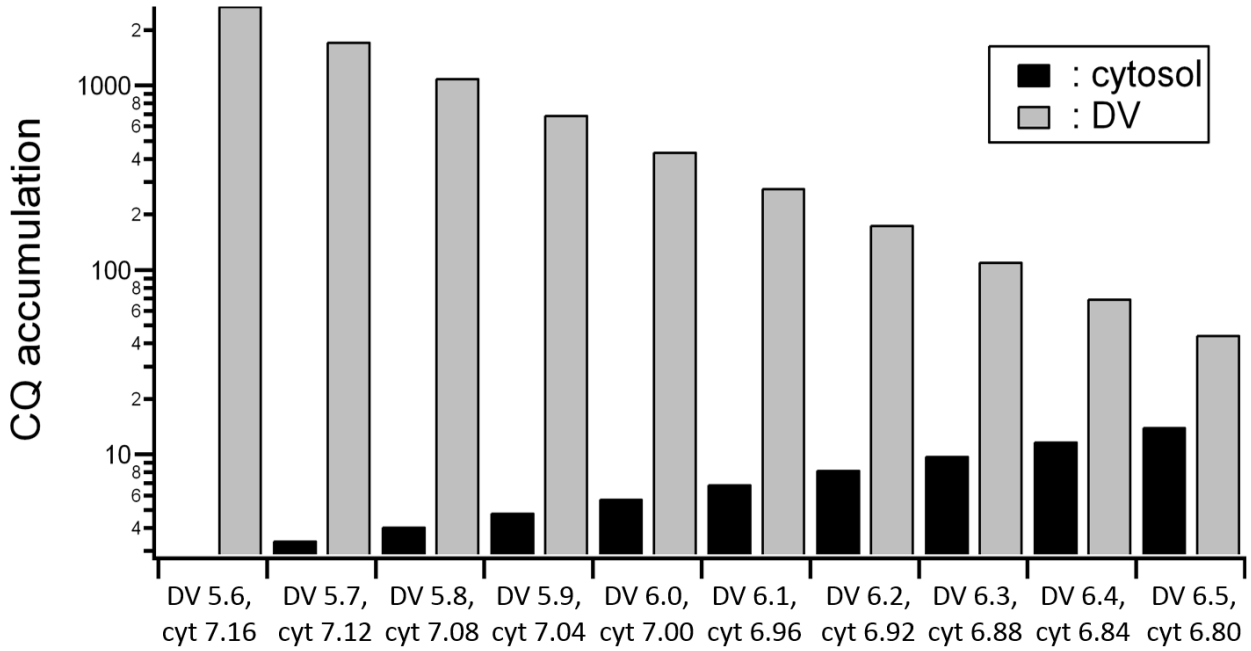

Figure 1.2 Accumulation of CQ in the parasite cytosol and DV. Calculations based on substrate diffusion and membrane trafficking show the fold accumulation of CQ in the parasite cytosol and DV at increasing pH_{DV} with decreasing pH_{cyt}. (personal communication)

The first electron microscopy (EM) images of CQ-treated infected RBCs were taken in the late 1980s [43]. The images showed swelling of the DV after 24 h CQ exposure in CQS strains but not CQR strains. Using a customized Nipkow spinning disk confocal microscope (SDCM), Gligorijevic and colleagues showed that CQR strains had significantly increased DV volumes compared to CQS strains, even in the absence of CQ exposure [44].

The hypothesis that a higher digestive vacuolar pH will lead to inefficient hydrolase activity and subsequent dysfunction of this organelle was originally proposed by Homewood and colleagues [45]. However, they assumed that the pH gradient is the only force that drives CQ to accumulate in the DV, while affinity of CQ for any molecules, either in the DV or in the cytosol, was neglected. Furthermore, it was observed that the alkalinizing effect of CQ in the DV was only achieved at concentrations of 1-2 orders of magnitude greater than the CQ IC_{50} [27]. This suggests that DV alkalinization does not primarily kill the parasites but may be a side effect of quinoline antimalarials. This was supported by findings of Geary and coworkers [3], who measured the uptake of radiolabeled CQ in CQR and CQS strains. They showed that the difference in alkalinization between CQS and CQR strains was not significant. Using the pH sensitive fluorescent dye acridine orange,

one study showed that intrinsic digestive vacuolar pH is significantly different between a CQS and a CQR strain [46]. However, later studies using various fluorescent pH indicators revealed that there is no significant difference in the resting pH_{DV} between CQS and CQR strains, and CQ uptake was not influenced by induced changes in the pH_{DV} of a CQS strain [31]. Thus, the influence of digestive vacuolar pH on CQ sensitivity or resistance remains unclear.

1.2.2 Effect of CQ in the cytosol of malaria parasites

Exposure of susceptible *Plasmodium* parasites to CQ not only alters the environment in the DV, but has also crucial effects on cytosolic pathways. The influence of CQ on cytosolic proteins or pathways is not known. While hemoglobin endocytosis is undisrupted, the processing of endocytic vesicles is impaired [47-53]. This leads to accumulation of vesicles containing undigested hemoglobin [48, 53, 54] and the formation of vacuoles [48, 49, 51]. Furthermore, monomeric hematin (ferriprotoporphyrin IX; FPIX) accumulates in the parasites [54-56], presumably through denaturation of hemoglobin [57, 58], while nucleation of FPIX into hemozoin crystals is inhibited [59, 60]. *In vitro* experiments were supported by studies using *P. berghei* in the malaria mouse model [59].

CQ binds to FPIX. The primary effect caused by the CQ-FPIX complex is probably membrane impairment, which interferes with the docking of mature hemoglobin-laden endocytic vesicles [61]. Yayon and colleagues have proposed that CQ prevents fusion of hemoglobin-laden vesicles with the DV membrane [29], which might play a crucial role in the lethal effect of CQ.

It is unclear whether the accumulation of vesicles containing undigested hemoglobin is caused directly by the CQ-FPIX complex or indirectly by altering a signaling pathway that triggers vesicle docking. Although accumulation of free FPIX is suggested to result in lysis of membranes after several hours of CQ exposure, intercalation of the CQ-FPIX complex into lipid bilayers may increase membrane fluidity [62] and cation permeability [63] long before the concentration of the complex is high enough to cause lysis.

1.2.3 Binding of CQ to FPIX

CQ binds to FPIX in a covalent complex [30, 64-67]. Direct binding of CQ to hemozoin crystals and subsequent inhibition of crystal growth seems to be less important for its antimalarial properties, since it was demonstrated that CQ only binds with low affinity to β-hematin stored in hemozoin [49, 68]. FPIX is a toxic byproduct of hemoglobin digestion and either converted into hemozoin crystals in the DV or degraded in the cytosol through glutathione (GSH) [69-71]. Even if CQ fully inhibits the polymerization of FPIX this would only increase the FPIX load on detoxification through GSH by 50%, which should not overwhelm the system [20].

Furthermore, FPIX was described to form a complex with lipids, which promotes FPIX dimerization [59, 72, 73]. The size of hemozoin crystals found in *P. falciparum* infected RBCs is determined by the lipid composition and structure of the DV membrane [73]. In addition to lipids, histidine-rich proteins are suggested to facilitate hemozoin formation by binding to FPIX molecules, thereby promoting dimer formation [74]. Subsequently, lipids may shield the hydrogen bonds of FPIX side chains from competitive binding with water, stabilize the structures and, therefore, facilitate long chain formation of FPIX molecules held together by hydrogen bonds [74, 75]. Usually about 40% of these lipids are masked; this percentage increased significantly to 90% when CQ was added [59]. It is suggested that a neutral aminopeptidase is involved in unmasking lipids that promote FPIX dimerization [48]. Upon CQ treatment, neutral aminopeptidase activity is no longer associated with endocytic vesicles, which in turn results in the failure to unmask lipids, thereby reducing FPIX dimerization [48, 59]. This aminopeptidase is probably required in the initial step of hemoglobin digestion by initiating degradation of the inner membrane of hemoglobin-laden endocytic vesicles. QN and MQ are thought to prevent or reverse these CQ-induced effects [48, 54, 55], suggesting they play an opposing role.

Molecular dynamics simulations suggest that CQ binds to FPIX in a 1:2 or 2:4 (CQ:FPIX) ratio and retains this ratio even at high CQ concentrations [76, 77]. Three important CQ-FPIX interactions were identified: i) a hydrogen bond between the oxide bridge of the μ-oxo form of FPIX and the protonated quinolinium nitrogen atom of CQ, ii) π-stacking between the quinolone ring of CQ and the porphyrin rings, and iii) electrostatic interactions between the 7-chloro substituent of CQ and the porphyrin methyl hydrogen atoms [77]. These data were observed in aqueous solution at pH 7.4 [76, 77]. High field NMR experiments showed that the complex formation of the μ-oxo form of

FPIX, which is mainly found in aqueous solutions, changes significantly upon protonation of CQ [66]. Interestingly, the binding of the neutral CQ complex appeared to be more stable than binding of monoprotonated or diprotonated CQ. Thus, although the dibasic character of CQ is important for its accumulation in the DV, it is not necessarily important for high-affinity binding to μ-oxo dimer FPIX [66].

CQ was found to inhibit the degradation of FPIX by GSH [20, 70]. This is supported by findings that i) mercaptoethanol and dithitreitol, which also degrade FPIX, inhibit FPIX-induced lysis of RBC membranes [63], and ii) CQ enhances FPIX-dependent lysis of normal RBCs [78]. Ginsburg and coworkers strongly believe that the principal toxic effect of CQ lies outside the DV and is linked to the ability of CQ to bind to FPIX [79]. This was further supported by Combrinck and colleagues, who showed using transmission electron microscopy (TEM) techniques that CQ induced the redistribution of FPIX from the DV to the parasite cytoplasm [80]. Other researchers propose that CQ's main target lies within the DV [81].

Non-polymerized FPIX can easily escape the DV and is rapidly degraded by GSH. In the presence of CQ, GSH gradually accumulates in the membranes and provides binding sites for the drug [20, 70]. As much as 70% of the FPIX generated through hemoglobin digestion was found to be detoxified by cytosolic glutathione [21]. It was demonstrated that reducing intracellular levels of GSH resulted in increased sensitivity to CQ, while increasing cellular levels of GSH resulted in CQ resistance. Furthermore, there is evidence that CQR strains contain higher GSH levels than sensitive strains [79]. This potential target site can be regulated by the parasite. Therefore, resistance through GSH regulation seems plausible. In addition, it was demonstrated that the inhibitory effect of CQ on GSH-dependent degradation of FPIX is competitive, and higher concentrations of CQ are needed for inhibition of FPIX degradation when GSH levels are increased [21].

High levels of FPIX may also increase the permeability of membranes to cations, which can lead to lysis of organelles and cells [63]. In the parasite, the DV membrane remains intact after CQ exposure and subsequent increases in FPIX [82]. Binding of CQ to FPIX enhances the solubility of FPIX in membranes [70], suggesting that it facilitates the release of FPIX from the DV. Treatment of *P. falciparum*-infected RBCs resulted in drug-induced binding of FPIX to parasite glycolytic enzymes in the cytosol, significantly reducing the activity of 6-phosphogluconate dehydrogenase

[83]. Controversies among researchers about the importance of CQ in the parasite cytosol reveal that CQ's role in this compartment needs to be further elucidated.

FPIX is also suggested to play a major role in saturable CQ uptake [36], while nonsaturable uptake may be associated with low affinity CQ binding to various cytosolic proteins [64, 84]. The saturable phase of CQ uptake correlates with the availability of FPIX, and inhibition of FPIX generation was shown to decrease the uptake of CQ [36]. This suggests that not only does pH play a role in CQ uptake, but also the binding/affinity of CQ to its target molecule. Furthermore, it was shown that, even though resistant and sensitive parasite strains have equal amounts of CQ binding sites, the apparent affinity for CQ binding to FPIX is reduced in CQR strains [36]. For this reason, CQ binding to FPIX cannot be attributed to proton trapping or active transport alone.

1.2.4 CQ resistance

CQR parasites accumulate less drug than susceptible parasites [2, 3, 34, 36, 85-89]. This was mainly demonstrated using [^{3}H]CQ as a substrate. More recent publications have used fluorescently tagged CQ to assess its intracellular distribution, as well as its uptake and efflux in CQS compared to CQR strains [4, 90-92].

Three hypotheses could explain reduced CQ accumulation. The first hypothesis assumes that the cytosol-DV pH gradient is smaller in CQR parasites [29, 32, 45]. The second hypothesis proposes that the FPIX complex has a reduced affinity for CQ and, therefore, fewer toxic CQ-FPIX complexes accumulate. The third hypothesis suggests that the *P. falciparum* chloroquine resistance transporter (PfCRT) carrying the K76T mutation in CQR parasites causes CQ to be transported out of the DV and reduces the amount of CQ available to bind to its digestive vacuolar target. While the first hypothesis could not be convincingly demonstrated, multiple studies support the latter two [2, 34, 36, 39, 93-95].

PfCRT was the first malaria transporter in which a single amino acid mutation was linked to drug resistance. This was identified through the analysis of a genetic cross between a CQS and CQR parasite strain. PfCRT is a 45 kDa protein located on the DV membrane, transporting substrates out of the DV. A single amino acid mutation from lysine (K) to threonine (T) at residue 76 was found

to be the main player in CQ resistance, which can be reversed by the addition of verapamil [2]. These results are largely consistent with *in vivo* findings that indicated an association between the K76T mutation and CQ treatment failure, which has resulted in its widespread use as a molecular marker of CQ resistance [96].

The K76T amino acid substitution itself cannot fully explain the mechanism of resistance. CQR strains that were incubated with increasing CQ concentrations had to accumulate higher internal CQ concentrations compared to CQS strains to obtain the same efficacy in parasite killing [3, 4, 36, 90, 97]. Furthermore, inconsistencies were found between the occurrence of the K76T mutation and resistance to CQ both *in vitro* and *in vivo* [98-102]. In addition, mutant PfCRT was found to be important in the IC_{50} shift between CQS and CQR strains but only responsible for 10-20% of the LD_{50} in CQR parasites [103]. This indicates that, even though the same CQ concentration is reached within the DV, CQR strains require a second mechanism that prevents CQ from efficiently binding to its target to cause lethal effects [97]. Reduced affinity of CQ for FPIX, the second hypothesis, is a plausible candidate.

Co-expression network analysis of *pfcrt* and *pfcrt*-interacting genes in CQS and CQR recombinant progeny clones revealed functional and regulatory relationships that were either conserved (such as hemoglobin metabolism) or have diverged (DNA repair and histone acetylation) between CQS and CQR parasites [104]. Regulatory networks can affect multiple target genes, and their dysregulation remains undetected by genome sequencing. Thus, CQS and CQR strains may harbor more differences than previously thought.

Resistance to CQ is partially reversible with the addition of verapamil (VP). It was suggested that VP prevents CQ efflux from the DV via PfCRT, thereby enhancing CQ's antimalarial effect on the DV target [94, 105, 106]. Another possibility suggested by Bray and coworkers is that VP reverses CQ resistance by increasing the affinity of CQ for its target, not through altered PfCRT transport [36]. Furthermore, they proposed that altered affinity for CQ binding through chemosensitizers is likely due to an indirect effect that is dependent on the parasite's membrane integrity. VP interacts with phospholipids of RBCs, likely due to differential expansion of the membrane bilayer [107]. Finally,

the increase in intracellular CQ concentrations after addition of VP is not enough to simply explain resistance reversal by inhibition of rapid CQ efflux.

1.2.5 CQ and autophagy

CQ has not only been used for malaria treatment, but was also studied for its effect on cancer cells. Elucidating CQ's target site in cancer cells may help malaria researchers to find additional pathways that may be involved in CQ resistance of *Plasmodium* parasites. It has been reported that exposure of cancer cells to CQ resulted in cell death. Although CQ was shown to induce apoptotic cell death-related proteins such as p53, it was not dependent on classical regulators of apoptosis [108-111]. In addition, CQ disrupted lysosomal functions by preventing the fusion of endosomes or autophagosomes with lysosomes, thereby inhibiting lysosomal protein degradation [112]. CQ-induced death of tumor cells could only be reduced when both apoptosis and autophagy were inhibited [110]. Maclean and coworkers suggested that alterations in lysosomal functions trigger a p53-dependent cell death response [110]. On the other hand, Geng and coworkers suggested a p53-independent pathway through autophagic vacuole accumulation [113]. Although CQ-treated cells showed cleavage of apoptosis-related caspase-3 and caspase-9 as well as a caspase substrate, a broad-spectrum caspase inhibitor (Z-VAD-fmk) was unable to inhibit CQ-induced cell death [110, 113]. However, caspase-independent programmed cell death (PCD) pathways such as programmed necrosis were not investigated in more detail.

Autophagy can be determined by the effects of CQ on LC3, which is necessary for the formation of autophagosomes [110], and is modified into LC3-I and LC3-II. Rapid accumulation of LC3-II was detected in CQ-treated cells [110, 113], as well as cells treated with the caspase inhibitor Z-VAD-fmk [114], indicating that both CQ and Z-VAD-fmk induce autophagy. The lysosome inhibitor bafilomycin-A1 (Baf-A1) also triggered autophagic cell death similar to CQ [115]. Baf-A1 inhibits vacuolar type H^+-ATPases (V-ATPases) and prevents the acidification of organelles, such as lysosomes and endosomes, after an extended period of time (usually 12-24 hours of treatment with 100 nM Baf-A1). Short term treatment simply disrupted the acidification process of these organelles [116]. Furthermore, other agents that disrupt the acidification process also blocked

autophagosome-lysosome fusion. These include CQ diphosphate, nigericin, and ammonium chloride [116].

Recently, researchers started to investigate cell death pathways in *Plasmodium* parasites. Programmed cell death (PCD) in unicellular organisms seems paradoxical at first. However, there is now evidence for PCD in unicellular eukaryotes, including parasitic protozoa [117-119]. To date, non-apoptotic pathways, such as autophagic mechanisms that would enhance survival under ambient physiological conditions, have been included on the list of PCD pathways [120]. However, a considerable amount of crosstalk between apoptosis, necrosis and autophagic pathways is reported, suggesting that autophagy itself is not sufficient for cell killing but activates PCD pathways if survival mechanisms fail [121, 122].

Apoptotic cell death after CQ exposure of malaria parasites was excluded for several reasons. A central component of the apoptotic machinery are caspases. A protease family closely related to caspases, called metacaspases, was found in *Plasmodium* parasites [123, 124]. However, the caspase inhibitor Z-VAD-fmk was unable to prevent parasite death after CQ exposure [125]. Furthermore, other apoptotic features, such as chromatin condensation, DNA fragmentation, disruption of the plasma membrane and nucleus dissolution, were not observed [125-127].

Most researchers suggest an autophagic-like PCD in *Plasmodium* parasites upon CQ exposure [125, 128]. This is in agreement with the observation that CQ interferes with hemoglobin digestion, which effectively leads to starvation of the parasite. Although autophagy is a strategic mechanism for cell survival, it can also lead to the death of the organism when rescue attempts are not effective. Autophagic vacole formation after CQ exposure of *Plasmodium* parasites was noted as early as 1967 [49, 51, 129]. Cytoplasmic vacuolization similar to autophagy was confirmed by electron microscopy [125]. However, cytoplasmic vacuolization does not only occur during autophagy but is also characteristic for other PCD pathways such as methuosis or necroptosis [130, 131]. In plants, a vacuolar PCD was described that critically requires autophagy and its upstream regulator, a metacaspase [132]. The slow vacuolar death executed by metacaspase-dependent autophagy leads to self-disassembly of dying cells and the formation of functional structures outside of the cell corpses [133]. Thus, studying PCD in plants may provide further insight into various cell death mechanisms that could also be activated in protozoan parasites.

LD_{50}-directed quantitative trait loci analysis in CQS versus CQR strains revealed differences in loci that encode proteins linked to autophagy pathways but no genes that are involved in apoptosis [103]. A set of genes involved in the induction of phagophore-formation are named *ATG* (autophagy-related genes). A *Plasmodium* homologue called PfATG8 was linked to autophagy and, more importantly, the autophagy cascade was altered in CQR parasites [103]. Researchers have only recently set out to elucidate the role of autophagy in CQ-induced programmed cell death. This is a promising field for the better understanding of CQ's antimalarial mode of action and may reveal additional resistance mechanisms that have evolved in CQR parasites.

1.3 The *P. falciparum* multidrug resistance-1 transporter, PfMDR1

Several *Plasmodium* transporters are involved in antimalarial drug resistance. Most, including the *Plasmodium falciparum* multidrug resistance (MDR) transporter 1 (PfMDR1), belong to the superfamily of ATP-binding cassette (ABC) transporters. Another transporter that plays a major role in CQ efflux from the DV into the cytosol is PfCRT, which belongs to its own family of CQ resistance transporters [134]. The CRT protein family will not be discussed here.

1.3.1 ABC Transporters

ATP-binding cassette (ABC) transporters are widely distributed in eukaryotes and transport a wide variety of endogenous metabolites, such as sugars, amino acids, ions, phospholipids, proteins, and other small molecules, across intra- and extracellular membranes [135]. Some of these transporters export waste products or toxic compounds out of the cell, including drugs administered as cancer treatment. This has led to intensive research on the role of ABC transporters in anticancer therapy.

48 ABC transporter genes are described in humans [136]. The alignment of amino acid residues in the nucleotide binding domain (NBD), the specific protein topology and drug specificity divide the ABC transporters into two main groups: i) the multidrug resistance associate proteins (MRP), and

ii) P-glycoprotein (Pgp) transporters, to which PfMDR1 belongs. Both MRP and Pgp transporters are widely distributed and are found in humans as well as *Saccharomyces cerevisiae* and various pathogens such as *Entamoeba histolytica*, *Cryptosporidium parvum*, *Leishmania* spp., *Plasmodium* spp. and *Toxoplasma gondii* [137]. *Plasmodium* parasites have several members of the ABC transporter family, which are thought to play a role in antimalarial drug resistance.

Structure, function and diversity of ABC transporters

The members of the ABC transporter superfamily typically have two homologous halves, each containing six transmembrane domains (TMDs) and a conserved cytosolic NBD, located in the cytosol. ATP hydrolysis occurs in alternating fashion between the two ATP binding sites but both are required for transport function [138]. It is assumed that the two NBDs act in concert as a single step rather than driving different steps in the substrate translocation cycle. Substrate binding enhances binding of ATP to the NBDs, thereby lowering the activation energy for a conformational change [139]. ATP binding was shown to provide sufficient energy to induce the key conformational changes involved in substrate transport [140]. Moreover, ATP binding can induce changes in the substrate binding properties of the TMDs in the absence of hydrolysis, where the substrate binding affinity is reduced while the affinity for a modulator at an allosteric site is not affected [141-143].

The NBD is a conserved region that contains an aromatic residue, the Walker A and B sites that are separated by a conserved signature motif, the D-loop and the H-loop [144]. The TMDs of different ABC transporter sub-families often consist of varying numbers of transmembrane alpha-helices and share little sequence identity. The TMD subunits form an enclosed aqueous pore in the membrane that appears open at the extracellular face and is closed intracellularly. The pore that is formed by the TMDs contains one or more substrate binding sites [145]. Detailed pharmacological studies have identified three interacting substrate binding sites for Pgp in mammalian cells [141, 142, 146]. Two drug molecules can bind simultaneously, and one substrate can stimulate the transport of the other [147-149].

MDR transporters in cancer

Cancer cells proliferate in an uncontrolled manner and, in some cases, metastasize. In humans, there are more than 100 types of cancer, typically named for the organs or tissue from which they originate, e.g., lung cancer or skin cancer. Tumors also have abnormal cell growth, called neoplasm, and are further subdivided into two groups. Malignant and invasive tumors are considered cancer, while benign tumors are not. The progression from normal cells to cancer cells involves multiple steps, known as malignant progression. This includes self-sufficiency in growth signals, evasion of PCD, limitless replicative potential, sustained angiogenesis, tissue invasion and metastasis [150].

Some cancers can be treated successfully using chemotherapy, while others exhibit resistance to treatment. Resistance can be further subdivided into intrinsic resistance and acquired resistance. Multidrug resistance (MDR) is a form of acquired resistance and can be mediated by Pgp or MRP transporters. They transport chemotherapeutic drugs out of the cell, leading to reduced accumulation of the drug within the cell and subsequently drug resistance. Although MRPs are similar to Pgps in terms of substrate specificity and action, they only share 15% amino acid homology [151]. Six isoforms of MRP were identified in humans, termed MRP1-6. It is known that MRP1 and MRP2 require drug conjugation with glutathione or glucuronic acid prior to efflux across the plasma membrane [152]. For Pgp, three isoforms are known: class I, II and III. Classes I and II confer multidrug resistance when transfected into sensitive cells, while class III Pgps are not associated with drug resistance [153]. Pgps play an important role in processes involved in cell homeostasis and are expressed in a large variety of tissues, such as the liver, kidney, colon, small intestine, pancreas, uterus, and in specialized capillary endothelial cells in the brain [151]. Pgp was shown to be capable of direct substrate transport [154].

1.3.2 Structure of PfMDR1

The *P. falciparum* ABC family consists of 16 transporters that are categorized in eight subfamilies (B to I; A is missing in all Apicomplexa), according to the phylogenetic relationships of primary and secondary structures of the conserved NBDs [155, 156]. The largest subfamily is ABC B, which contains seven members, including PfMDR1 (PfABCB1). PfMRP1, PfMRP2 and PfMDR5 are localized

in the plasma membrane of all asexual parasite life stages [155]. While PfMDR2 and PfMDR5 were recently identified to influence antimalarial drug resistance, their effect was only marginal and their impact will have to be further assessed [157]. Other putative drug transporters of the ABC family are PfABCC1, PfABCC2, PfABCG2 and PfABCI3. Their exact functions remain to be determined.

PfMDR1 has a size of ~162 kDa and is associated with the DV membrane throughout the asexual cycle of the parasite, with the ATP binding domain localized in the cytosol [145, 158]. PfMDR1 mediates solute import into the DV rather than regulating solute efflux out of this compartment [159]. It remains unclear if PfMDR1 is also localized in the plasma membrane, although to a lesser extent when compared to the DV membrane. PfMDR1 contains five main amino acid mutation sites at residues 86, 184, 1042, 1034 and 1246. These mutation sites have been reported to influence resistance or sensitivity to various antimalarial drugs such as QN, MQ, CQ, LF, ART, HF, and amodiaquine (AQ) [160-167].

PfMDR1 has two symmetric halves, each containing a TMD with three external loops (EL) and two internal helices (IH) that link six transmembrane regions with a NBD (Figure 1.3). Two hinges allow for different conformations of the transporter. One hinge is found in EL2 (residue 189-194) and EL3 (residue 311-315), and the other one in EL5 (residue 929-933) and EL6 (residue 1055-1059) [168]. The internal helices mediate communication between TMDs and NBDs. The intertwined interface between the two halves of the transporter interlock NBD1 with TM10/TM11/IH4 and NBD2 with TM4/TM5/IH2 [168]. This structural feature was shown to transmit a conformational change to the transmembrane domains, resulting in an outward-facing conformation and thereby activating substrate transport [169, 170].

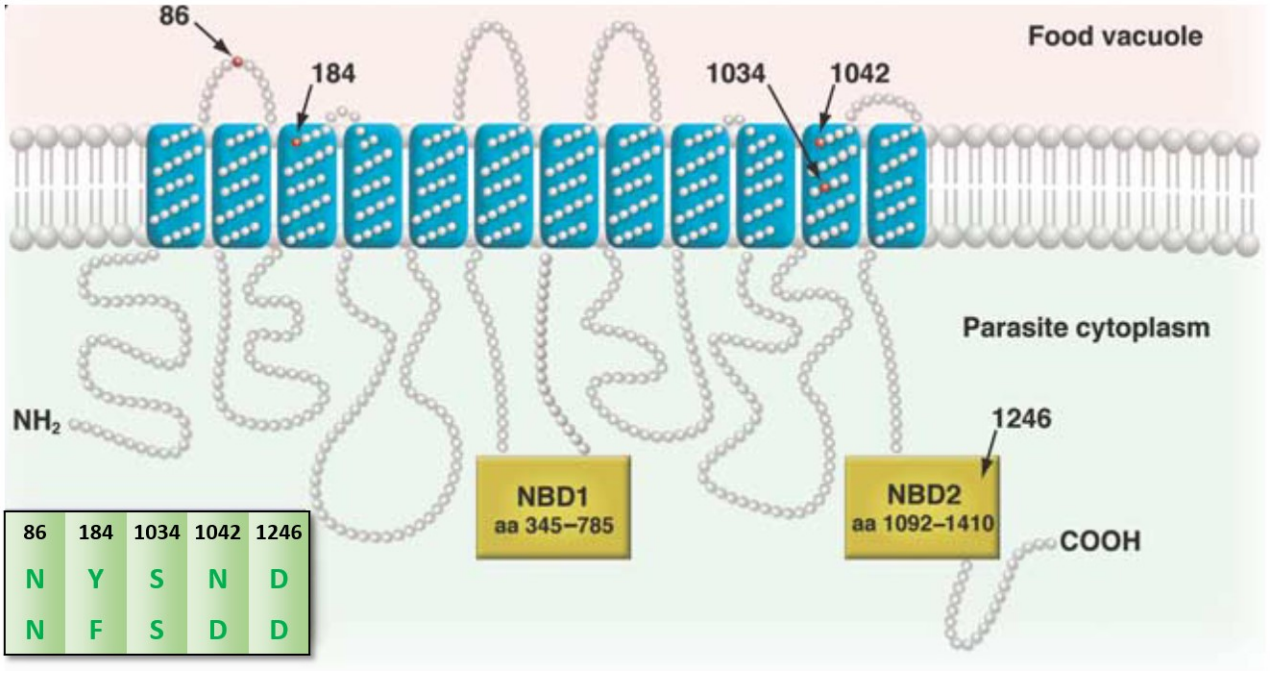

Figure 1.3 Predicted topology of PfMDR1. Polymorphisms of two drug sensitive parasites strains are indicated (top, 3D7; bottom, HB3). NBD, nucleotide-binding domain. (modified after [159])

Apart from the suggested involvement in drug resistance, the endogenous function of PfMDR1 is not known. Its human homologue, MDR1, exports hydrophobic compounds and steroids and is associated with multidrug resistance in cancer cells by increasing the efflux of drugs [156]. It is currently unclear which physiological substances are transported by PfMDR1. Unlike other ABC proteins, MDR1 shows a high basal level of ATPase activity in the absence of drugs, which may be caused by physiological transporter functions. In general, MDR1 transporters hydrolyze ATP and transport only large, hydrophobic, uncharged or slightly positively charged molecules [171]. Antimalarial drugs bind directly to PfMDR1, which transports them into the DV [172].

1.3.3 PfMDR1 polymorphisms

Differences in *pfmdr1* functions can either occur as an increase in gene copy number or single nucleotide polymorphisms (SNPs). Changes in at least one of these two parameters have been associated with decreased susceptibility to a variety of antimalarial drugs, including QN, MQ, CQ, and ART. Altered amino acids at residues 86, 184, 1034, 1042, and 1246 have been reported to

play a role in drug resistance [161, 173-176]. The wild-type amino acids at these residues are N86, Y148, S1034, N1042, and D1246. For a better overview, these five mutation sites will be shortened to amino acid abbreviations only in the subsequent order of residues, e.g. N86, Y148, S1034, N1042, and D1246 will be shortened to NYSND, where applicable. To date, the N86Y mutation has been investigated in more than 40 publications and is likely involved in CQ, AQ, and LF resistance [162, 172]. The N1042D substitution was found to contribute mainly to low-level QN resistance [163]. Exposure of *P. falciparum* laboratory strains to MQ resulted in the amplification of the *pfmdr1* gene and a simultaneous increase in resistance to MQ, QN, and HF [173]. However, in the absence of drug pressure, the parasites with multiple gene copies showed decreased survival fitness [177].

Changes in gene copy number alter the expression profile of *trans*-regulated genes and may fundamentally alter the parasite's transcriptional network [178]. Using selection experiments on laboratory parasite strains, it is estimated that *pfmdr1* duplications arise once in 10^8 parasites, and further amplification from two to three copies occurred in one in 10^3 parasites [177]. Worldwide, there are about 3×10^{16} malaria parasites in asymptomatic carriers, while symptomatic carriers contain between 5×10^{16} and 5×10^{17} malaria parasites [179]. Therefore, it is likely that gene modifications occur naturally in the field. Increased *pfmdr1* gene copy numbers are supported by long monomeric A/T tracts or microsatellite repeat sequences on chromosome 5 that are prone to chromosome breakage [180]. A clinical study in Thailand showed that the transition from one to two *pfmdr1* gene copy numbers resulted in the highest risk of treatment failure to MQ, as well as the largest shift in IC_{50} values in the sampled parasite populations [161]. However, further increase in gene copy numbers, e.g., from two to three *pfmdr1* copies, showed no further *pfmdr1* expression or treatment failure [181].

The population structure of *Plasmodium* spp. depends on local epidemiological and demographic situations, such as the incidence of infected people, the vector transmission intensity, and inhabitant migration [182]. In addition, all drug-related mutations in a parasite population are based on previous treatment policies that vary between different countries. Therefore, resistant populations can affect adjacent malaria endemic regions. This led to the independent evolution of several mutation patterns in Asia, sub-Saharan Africa and South America (Figure 1.4). A brief

overview of the history of drug policies, treatment failures, and emergence of resistances is required before going into more detail about the variant *pfmdr1* mutation patterns on these continents.

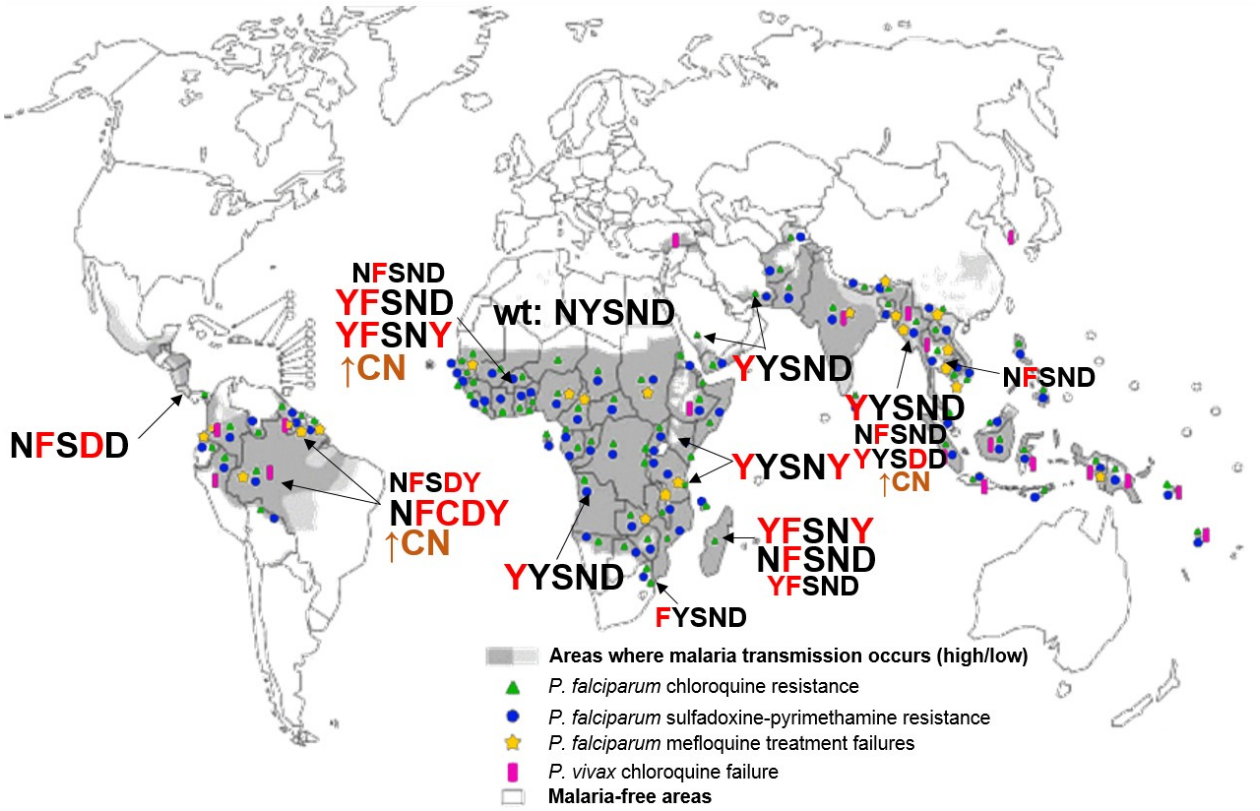

Figure 1.4 PfMDR1 mutation patterns worldwide. The letters refer to the amino acids at positions 86, 148, 1034, 1042, and 1246. The wild-type is NYSND, while all letters in red indicate the amino acid mutations at the given position. Smaller fonts depict minor mutation variations in this area. ↑CN, increase of *pfmdr1* gene copy number. (modified from [183])

Mutation patterns in Southeast Asia

In a long-term study by Mungthin and coworkers, *pfmdr1* mutation patterns were investigated in field isolates from Thailand during a 15-year period [184]. Antimalarial treatment policies were revised periodically in Thailand due to the rapid spread of multidrug resistance in *P. falciparum*. Although considered to be a low transmission area, the genetic diversity of *Plasmodium* is relatively high [182]. CQ was introduced in 1965, and was partially replaced by sulfadoxine-pyrimethamine

in 1974. Subsequently, QN and MQ were the treatment of choice between 1980-1986 and 1986-1995, respectively [185]. The introduction of a 3-day artesunate-mefloquine combination therapy in 1995 was expected to stabilize the multidrug-resistance problem in Thailand. However, emerging resistance to ACTs has been reported for the Thai-Myanmar and Thai-Cambodian borders [16, 17].

The prominent pattern for *pfmdr1* polymorphisms in Thailand at residues 86, 184, 1034, 1042, and 1246 was found to be NFSND instead of the wild-type pattern that harbors a tyrosine at amino acid position 184 (NYSND), with a drastic prevalence increase from 40% to 95% from 1988 to 2003 [184]. In addition, increased *pfmdr1* copy numbers were observed. A study of Thai patients from 1995 to 2002 revealed selection for the N86Y polymorphism (YYSND) after treatment with artemether-lumefantrine [186]. Patient samples from 2003 to 2008 showed N86Y as the major point mutation, with a prevalence of 18%, which was associated with increased susceptibility to MQ and QN. At the same time, increased *pfmdr1* gene copy numbers resulted in higher resistance to MQ, QN and ART [161, 187, 188]. The diversity of mutations in PfMDR1 resulting in drug resistance emphasizes the necessity to monitor the evolution of drug-resistant *Plasmodium* spp. in Asia. Moreover, declining endemicity could lead to a more fragmented parasite population structure with greater genetic isolation between endemic foci. This will reduce gene flow and spread of resistances between the populations, but also enhance the rate of evolution of multiple resistant phenotypes [189]. Previously, increased gene copy numbers were only reported for field isolates in Thailand and Cambodia but not elsewhere [190]. Increasing gene copy numbers provide a simple way for the parasite to increase gene expression without requiring a functional change in the nucleotide sequence.

Mutation patterns in South America

Most malaria cases in South America are reported from the Amazon region, where migrant populations, great distances, and poor access to diagnosis and treatment are major barriers for malaria control [191]. In the past ten years, malaria prevalence in Brazil alone has increased 3-fold, to nearly half a million cases each year. *P. falciparum* drug resistance has spread quickly for CQ,

sulfadoxine-pyrimethamine and to some extent QN [192]. As vector control is not a realistic approach in this area, early diagnosis and effective treatment are essential tools for control strategies. In the 1990s, nearly 100% of patient samples were resistant to CQ, and 3% to QN. In addition, there was evidence of decreasing sensitivity to MQ and HF [191].

Interestingly, the *pfmdr1* mutant alleles S1034C, N1042D and D1246Y, mainly in combination with Y184F (NFCDY), are especially prevalent in South America and rarely found in isolates from other continents. In contrast to parasite populations from other malaria endemic areas, the majority of drug resistant parasites in South America carries multiple SNPs. A study conducted in Venezuela found the pattern NFSDY and NFCDY at frequencies of 37% and 63%, respectively, with wild-type amino acid asparagine at position 86 in all samples [193]. The NFCDY pattern was found in 97% of field samples from a Brazilian study [194]. In addition, increases up to four *pfmdr1* gene copies were detected in 12% of the samples from Venezuela [193].

Mutation patterns in sub-Saharan Africa

While the combination of artesunate and MQ has been used with success in Southeast Asia, most countries in sub-Saharan Africa have preferred either artemether-lumefantrine or artesunate-amodiaquine for first line therapy. Two African clinical trial reports provided evidence for the selection of distinct *pfmdr1* alleles after artemether-lumefantrine treatment [162, 195].

In Zanzibar, post-treatment prevalence of N86 was significantly increased, a finding supported by similar evidence from Uganda, where parasites were selected for the NFSND haplotype [162]. No increase in *pfmdr1* gene copies was found, suggesting that gene amplification is less important in African parasite populations. In Tanzania, AQ monotherapy selected for the YFSNY haplotype, whereas artemether-lumefantrine retained the wild-type (NYSND) haplotype [195]. Here, too, no increase in *pfmdr1* gene copy number was reported. This suggests that the N86Y mutation has an indirect fitness disadvantage in parasite populations not under drug pressure. Although this mutation could result in increased survival of parasites in the drug-treated human host, molecular analysis of the transmission potential demonstrated that parasites harboring the N86Y mutation

have up to 4-fold impaired transmission to *Anopheles* mosquitoes [196] and, therefore, a remarkable fitness loss compared to unaffected parasite populations.

Up to 80% of field isolates from Burkina Faso carry the YYSND or YFSND mutations [197]. Mutation pattern YFSND was detected in 30% of Ghanaian isolates and wild-type NFSND in 42% of the samples [198]. In Madagascar, the most prevalent PfMDR1 mutation patterns were YFSNY (28%), wild-type NFSND (23%), YFSND (18%) and YYSND (15%). Interestingly, isolates from Madagascar showed a significant association of CQ resistance with the PfMDR1 N86Y mutation in parasites that carry wild-type PfCRT [199].

1.3.4 PfMDR1 amino acid polymorphisms and their influence on substrate binding

PfMDR1 mutation sites show distinct features involved in drug resistance. An amino acid mutation at position 86 was suggested to increase resistance to CQ and LF but enhance sensitivity to MQ, ART and QN. While asparagine at position 86 in the wild-type transporter may be glycosylated, replacement with tyrosine (N86Y) abolishes the potential glycosylation site. However, the importance of glycosylation in *P. falciparum* remains to be determined, as the parasite's ability for N-glycosylation is low [200]. An alternative explanation is that the N86Y mutation in PfMDR1 brings the tyrosine side chain in TM1 closer to residue K1054 in TM11. These two TMDs are crucial for correct positioning of the transmembrane domains in human Pgp and change the transporter's affinity in a drug-specific manner [169, 201]. Similar observations were made for the N86Y mutation in PfMDR1, resulting in a significant change in drug affinity [202].

Allelic exchange in *pfmdr1* shows a critical role for residue 184 in PfMDR1 transport kinetics, while drug specificity appears to be unaffected [160, 202]. This amino acid mutation is located in TM3 and is weakly associated with antimalarial drug resistance in field studies [161, 203-205].

The amino acid residue 86 in EL1, and residues 1034 and 1042 in TM11, are located in the putative drug binding pocket of PfMDR1. Spatial analysis revealed that residues 1034 and 1042 alternate between facing the cytosol in the open state conformation and the DV in the closed state conformation [168]. Interactions with residue N1042 are described for MQ, QN and CQ. While CQ

was found to have electrostatic interactions with residue 1042, the single H-bond donor in its substrate binding pocket was unable to establish a H-bond with the functional residues. On the other hand, CQ displayed extensive van der Waals interactions with polar amino acids in the drug binding pocket [166]. MQ was the only tested drug that showed differences in its ability to form H-bonds between wild-type N1042 and mutant N1042D. The replacement of asparagine with aspartic acid at position 1042 abolished the ability of mefloquine to form a H-bond with this residue [166].

Residue 1246 is located in NBD2, which is essential for ABC transporter function. However, mutation from aspartic acid to tyrosine (D1246Y) by itself was not found to inhibit PfMDR1 ATPase activity but only in conjunction with serine at residue 1034 (1034S) or aspartic acid at residue 1042 (1042D) [206]. Moreover, a functional impact on substrate transport was suggested to be substrate specific and dependent on their ability to bind to residues at TM11 in the drug binding pocket [202].

1.3.5 Involvement of PfMDR1 in drug resistance and sensitivity

Research focusing on *pfmdr1* mutations and their role in drug resistance remains controversial (Table 1.1). While some studies suggest that mutations or amplification of this gene are associated with increased CQ resistance [207], others propose that mutations or polymorphisms are associated with CQ sensitivity [207-209]. There is a general agreement that mutations in *pfmdr1* are associated with altered sensitivity to MQ and ART derivates *in vitro*, although the exact role of gene polymorphisms is still under debate [160, 204].

Table 1.1 Single nucleotide polymorphisms in PfMDR1

amino acid mutation	increased sensitivity	increased resistance
N86Y	CQ, LF	MQ, ART, QN
Y184F	LF	—
S1034C	—	MQ
N1042D	—	MQ, ART, CQ
D1246Y	CQ	MQ

CQ, chloroquine. LF, lumefantrine. MQ, mefloquine. ART, artemisinin. QN, quinine.

The PfMDR1 N86Y mutation is suggested to be favorable for resistance to both CQ and the related drug AQ but is concomitantly associated with increased sensitivity to MQ and HF. In addition, increased resistance to QN and increased sensitivity to MQ was found to be related to *pfmdr1* gene mutation N1042D alone, or the combination of mutations S1034C, N1042D, D1246Y [172]. Most studies are limited to single geographical areas, where specific polymorphisms can be isolated events. Thus, to obtain a global picture about *pfmdr1* polymorphisms and drug resistance, multiple samples from various regions and continents would need to be analyzed.

1.4 Conclusion

This literature review provides insight into the current understanding of CQ's mode of action. Furthermore, controversies that have been reported were discussed. Although some properties of CQ have been characterized, CQ's mechanism(s) in *P. falciparum* parasites that lead to irreversible cell damage remain unclear. The following chapters describe new findings observed between CQS and CQR parasites, which will advance our understanding of CQ resistance in *P. falciparum*.

Furthermore, this literature review summarizes the current view for the role of PfMDR1 in drug resistance. While several PfMDR1 mutations have been reported to play a role in drug resistance, these findings were mainly reported from patient isolates. Chapter 2 of this thesis describes a molecular tool to study PfMDR1 mutations. Live cell imaging techniques allow in-depth studies of antimalarial drug transport by PfMDR1 in *P. falciparum* strains of different genetic background, thereby providing insight into the altered transport properties of drug-sensitive and –resistant parasites.

— Chapter 2 —

Manuscript I

Monitoring PfMDR1 transport in *Plasmodium falciparum*

S.J. Reiling[1] and P. Rohrbach[1]

[1] Institute of Parasitology, McGill University, Ste. Anne de Bellevue (Montreal), Quebec, Canada

Malaria Journal 2015. 14(1): 270

2.1 Abstract

Background: The *Plasmodium falciparum* multidrug resistance 1 transporter, PfMDR1, contains five amino acid polymorphisms that are suggested to be involved in altered drug transport from the parasite's cytosol into the digestive vacuole (DV). Transport of a substrate into another intracellular compartment influences the drug availability at its site of action, therefore making the parasite more susceptible or resistant to a drug. Fluo-4 is a known fluorescent substrate that can be used as a molecular tool to investigate transport dynamics of PfMDR1 in many parasite strains.

Methods: Six *P. falciparum* strains with varying PfMDR1 mutations were loaded with Fluo-4 AM. Accumulation of the fluorophore in the DV was measured using confocal microscopy. The role of a key amino acid mutation was verified using selected parasite clones harboring point mutations at PfMDR1 amino acid position 1042. Equal expression of PfMDR1 was confirmed by Western blot.

Results: Fluo-4 was transported by PfMDR1 into the DV of most drug-sensitive and -resistant parasites. Asparagine at PfMDR1 position 1042 was crucial for Fluo-4 transport, while the N1042D substitution abolished Fluo-4 transport. Competition studies of Fluo-4 with chloroquine, quinine and mefloquine were performed on parasites harboring asparagine at PfMDR1 position 1042. A distinct Fluo-4 transport inhibition pattern for each tested antimalarial drug was observed in parasite strains of different genetic background.

Conclusion: This study demonstrates that Fluo-4 can be used to investigate PfMDR1 transport dynamics in both drug-sensitive and -resistant parasites. Furthermore, direct evidence of altered substrate transport in PfMDR1 was linked to a single amino acid mutation in the substrate binding pocket. This system offers a great tool to investigate the role of substrate transport by PfMDR1 and the mutations necessary to support transport, which would lead to new insights for the development of novel antimalarial drugs.

2.2 Introduction

Emerging resistance to commonly used antimalarial drugs is a major setback in the fight against malaria worldwide [210]. Understanding the molecular mechanisms behind drug resistance is of high importance in ongoing efforts to control this disease.

Early on, researchers found a correlation between antimalarial resistance and the *Plasmodium falciparum* multidrug resistance 1 transporter (PfMDR1) [160, 209]. PfMDR1 is a P-glycoprotein homologue (Pgh1) and belongs to the ATP binding cassette (ABC) transporter superfamily. It is a 162 kDa protein with two nucleotide binding domains (NBD) and twelve transmembrane domains (TMDs), with a putative substrate binding pocket in TMD11 [202]. The transporter is located in the membrane of the digestive vacuole (DV) [158], transporting substrates from the parasite's cytoplasm into the DV [159].

Two factors have been suggested to play a role in altered drug susceptibility to specific antimalarial drugs: PfMDR1 polymorphisms and *pfmdr1* gene duplications. Resistance has been associated with one or more variations at five amino acid positions in the PfMDR1 transporter, with wild-type PfMDR1 containing the amino acids N86, Y184, S1034, N1042, D1246. Increased *pfmdr1* copy numbers have been linked to mefloquine (MQ), lumefantrine (LF), halofantrine (HF), quinine (QN) and artemisinin (ART) resistance [161, 175, 211], while PfMDR1 amino acid mutations S1034C, N1042D, D1246Y were found to enhance parasite susceptibility to MQ, HF and ART, independent of gene copy number [160, 163].

Additional evidence for altered drug transport in wild-type *versus* mutant PfMDR1 was shown through expression of different *pfmdr1* variants in *Xenopus laevis* oocytes. Wild-type PfMDR1 transported chloroquine (CQ) and QN but not HF, while mutant PfMDR1 transported HF but not QN or CQ [202]. Furthermore, residue 184 altered transport kinetics independent of drug binding specificity [212].

Computational models of PfMDR1 describe a substrate binding pocket that includes residues 86, 1034 and 1042 [166, 168]. The binding of several antimalarial drugs was investigated using docking simulations within the PfMDR1 substrate binding pocket. Among the tested drugs, MQ was the

only candidate whose ability to form a H-bond with residue 1042 was completely abolished through the N1042D substitution [166].

Apart from antimalarial drug transport, it was shown that several PfMDR1 variants could transport the fluorescent substrate Fluo-4 into the DV of the parasite [159]. In contrast, Fluo-4 transport was abolished in drug-sensitive HB3 parasites harboring the PfMDR1 variant N86, F184, S1034, D1042, D1246. In a follow-up paper, the pump rate of PfMDR1 (F/Y86, Y184, S1034, N1042, D1246) was determined for Dd2 parasites using live cell imaging of intact infected erythrocytes [213].

In this study, drug-sensitive and -resistant *P. falciparum* strains of different genetic background and varying PfMDR1 polymorphisms were used to investigate the mutation(s) required for Fluo-4 transport. In addition, *P. falciparum* clones of different genetic background that harbor a single PfMDR1 amino acid mutation at position 1042 were analyzed. Aspartic acid (D) at position 1042 was found to abolish Fluo-4 transport into the DV. This could be restored by replacing aspartic acid at position 1042 with asparagine (N). Furthermore, the N1042D substitution resulted in increased sensitivity to MQ. Using Fluo-4 as a competitive substrate offers a powerful tool to investigate the role of PfMDR1 in transport of currently used antimalarial drugs for both drug-sensitive and -resistant parasites.

2.3 Material and Methods

2.3.1 Parasite strains and culture conditions

Three CQS (3D7, D10, HB3) and three CQR (Dd2, FCR3, FCB) *P. falciparum* strains, as well as stably transfected *P. falciparum* clones, derived from the parental lines GC03 and 3BA6, were used in this study. Strains GC03 and 3BA6 are progeny of the HB3 x Dd2 genetic cross [214] and harbor the PfMDR1 variant from HB3 but differ in their PfCRT phenotype and genotype (Table 2.1). PfMDR1 mutants derived from GC03 and 3BA6 were produced by Sidhu and colleagues through partial *pfmdr1* gene replacement that substituted aspartic acid (D) at position 1042 with asparagine (N) while leaving amino acids at residues 1034 and 1246 unchanged. The resulting clones were SND^{GC03} (S1034, N1042, D1246 in a GC03 genetic background), SND^{3BA6} (S1034, N1042, D1246 in a 3BA6

genetic background) as well as the recombinant controls SDD^{GC03} and SDD^{3BA6} [163]. All strains were cultured continuously, as described by Trager and Jensen [215], with modifications. Briefly, parasites were propagated at 5% hematocrit in culture medium containing RPMI 1640 (Life Technologies, Burlington, ON, Canada) supplemented with 25 mM HEPES, 2 mM L-glutamine, gentamicin (20 µg/ml) (Life Technologies, Burlington, ON, Canada), 100 µM hypoxanthine (Sigma-Aldrich, Oakville, ON, Canada), 0.5% AlbuMAX I (Life Technologies, Burlington, ON, Canada). Parasites were maintained at 37°C with an atmosphere of 5% CO_2, 3% O_2 and 92% N_2. A^+ red blood cells were obtained from the Interstate Blood Bank (Memphis, TN, USA). Giemsa-stained blood smears were prepared daily to monitor parasite growth. For synchronization, parasites were treated with 5% D-sorbitol (BioShop Canada, Burlington, ON, Canada) for 10 min at 37°C; sorbitol was removed and parasites were washed once before putting them back into culture. To obtain highly synchronous parasite cultures, this treatment was repeated after 6-8 h.

2.3.2 DNA isolation and sequence analysis

The full length sequence of *pfmdr1* and partial sequence of *pfcrt* was verified for all strains. Parasite strains were grown to ≥5% parasitemia and DNA was extracted using the QIAamp DNA Blood Mini Kit (Qiagen, Toronto, ON, Canada) according to manufacturer's instructions. DNA was amplified in overlapping PCR fractions using HotStarTaq DNA polymerase (Qiagen, Toronto, ON, Canada). To account for the AT-rich nucleotide content in the *P. falciparum* genome, dNTPs (Invitrogen Canada, Burlington, ON, Canada) were mixed at 75% AT and 25% GC. For PCR, 2 mM $MgCl_2$, 300 µM dNTPs and 300 nM primers were used. For each reaction mix, 20 ng genomic DNA was used. PCR reactions consisted of an initial activation step of 94°C for 3 min, followed by 35 cycles of 94°C for 60 sec, 49–61°C (adjusted for each primer pair) for 30 sec, and 72°C for 1 min. Primers used for *pfmdr1* gene sequencing are described in [213]. Primers used for sequencing of the *pfcrt* gene region containing the main mutation sites were: *pfcrt_F*: 5'-GGAGGTTCTTGTCTTGGTAAATG, *pfcrt_R*: 5'-TGGTAGGTGGAATAGATTCTCTTATAAA. Samples were sent for sequencing to Genome Quebec, Canada and analyzed using the BioEdit software [216].

2.3.3 Protein expression

To determine PfMDR1 protein levels, 20 µg whole cell protein lysate were loaded in each lane of an 8% acrylamide gel containing SDS. The proteins were transferred onto a PVDF membrane, which was then blocked O/N at 4°C with 5% milk (w/v) and 0.05% Tween-20 (ACP Chemicals, St-Leonard, QC, Canada) in phosphate buffered saline (PBS). The membrane was further incubated with a 1:2,000 dilution of primary anti-PfMDR1 (kindly provided by Prof. Cowman, Walter and Eliza Hall Institute, Victoria, Australia) or anti-PfHSP70 antibody (GenWay Biotech, San Diego, CA, USA) (1:2,000) in PBS-T + 5% milk for 1 h (RT), then washed and incubated with HRP-conjugated anti-rabbit IgG secondary antibody (Abcam, Toronto, ON, Canada) (1:20,000) for 1 h (RT). Immunoreactive bands were detected with ImmunStar WesternC Chemiluminescent Kit (Bio-Rad Laboratories, Mississauga, ON, Canada) using a myECL Imager (Thermo Scientific, Burlington, ON, Canada). To confirm equal protein loading, chemiluminescence intensities of PfMDR1 were calculated for each parasite clone relative to the respective PfHSP70 chemiluminescence using ImageJ 1.47q (National Institutes of Health, USA).

2.3.4 Growth inhibition assay

All drugs were obtained from Sigma-Aldrich Canada (Oakville, ON, Canada) and dissolved in dH_2O, except for DHA, which was dissolved in DMSO. Growth inhibition assays were performed as described previously [217], with modifications. Briefly, synchronized ring stage parasites were diluted to final parasitemia of 0.5% and hematocrit of 2%. A total of 100 µl culture medium per well was prepared in a 96-well plate assay, with a drug dilution series of 1:3, ranging from 1 µM to 0.15 nM. Plates were incubated at 37°C, 5% CO_2, 3% O_2 and 92% N_2 for 72 h, then frozen and stored at -80°C. Plates were thawed at room temperature and 100 µl 2x lysis buffer (20 mM Tris pH 7.5, 5 mM EDTA, 0.008% saponin, 0.08% Triton X-100, 0.2 µl SYBR Green I/ml) was added to each well. Plates were incubated in the dark for at least 1 h. Fluorescence intensity was determined using a Synergy H4 plate reader (Fisher Scientific, Nepean, ON, Canada) with 485 nm excitation and 520 nm emission wavelengths. IC_{50} values were determined by fitting concentration response curves with a custom-made procedure for IGOR Pro 6.2 based on an R script kindly provided by Le Nagard and used as described [218, 219].

2.3.5 Live cell imaging

Synchronized trophozoite stage parasites were loaded with 5 µM Fluo-4 AM (Life Technologies, Burlington, ON, Canada) in Ringer's solution (122.5 mM NaCl, 5.4 mM KCl, 1.2 mM $CaCl_2$, 0.8 mM $MgCl_2$, 11 mM D-glucose, 10 mM HEPES, 1 mM NaH_2PO_4, pH 7.4) for 50 min at 37°C. If treated with tariquidar (TQ) (MedKoo Biosciences, Chapel Hill, NC, USA) parasites were pre-incubated at 37°C with 100 nM TQ for 10 min before adding 5 µM Fluo-4 AM as described. Cells were then washed twice with Ringer's solution and transferred to a microscope chamber. Parasites were kept at 37°C during microscopy using a stage-top incubator (Tokai Hit, Shizuoka-ken, Japan). A series of four images per parasite was taken using a Zeiss LSM710 confocal microscope (Carl Zeiss, Oberkochen, Germany) equipped with a water-corrected objective (C-apochromat 63x/1.20 W Korr M27) and a 488 nm laser (12.5 mW, 2% intensity). The range of emitted fluorescence was measured from 493-622 nm. Images were analyzed using ImageJ 1.47q (National Institutes of Health, USA).

2.4 Results and Discussion

2.4.1 PfMDR1 transports Fluo-4 into the digestive vacuole.

A genetic linkage between Fluo-4 accumulation in the DV and the PfMDR1 transporter was previously described [159]. Although variations in Fluo-4 accumulation were observed between parasite strains harboring different PfMDR1 mutations, the crucial amino acid mutation(s) responsible for Fluo-4 transport remained to be determined. To identify PfMDR1 mutation(s) crucial for Fluo-4 transport, several drug-sensitive and -resistant *P. falciparum* strains of different genetic backgrounds were tested for accumulation of Fluo-4 in the DV. Three CQ-sensitive (CQS) and three CQ-resistant (CQR) strains harboring different PfMDR1 mutations were selected for these experiments (Table 2.1). While PfMDR1 has been suggested to play a role in CQ resistance, the key genetic indicator for CQS *versus* CQR parasites is attributed to the amino acid mutation K76T in the *P. falciparum* chloroquine resistance transporter (PfCRT) [94]. This was taken into

consideration in this study and the relevance of PfMDR1 polymorphisms is discussed for strains harboring either lysine (K76) or threonine (K76T) in PfCRT.

Table 2.1 Main PfCRT and PfMDR1 mutations of *P. falciparum* parasites used in this study

	PfCRT	PfMDR1				
	76	86	184	1034	1042	1246
strains						
HB3	K	N	F	S	D	D
3D7	K	N	Y	S	N	D
D10	K	N	Y	S	N	D
Dd2	T	Y/F	Y	S	N	D
FCR3	T	Y	Y	S	N	D
FCB	T	Y	Y	S	N	D
clones						
GC03	K	N	F	S	D	D
SDD^{GC03}	K	N	F	S	D	D
SND^{GC03}	K	N	F	S	N	D
3BA6	T	N	F	S	D	D
SDD^{3BA6}	T	N	F	S	D	D
SND^{3BA6}	T	N	F	S	N	D

Of the five mutation sites in PfMDR1 known to play a role in drug resistance, the parasite strains used for these experiments contained mutations at amino acid positions 86, 184 and 1042, which are mainly found in African and Asian isolates [175, 204, 220, 221]. To determine if mutations at these residues influence transport of Fluo-4 by PfMDR1, accumulation of Fluo-4 in the DV was measured in live parasites using confocal microscopy. All parasite strains, except HB3, showed high accumulation of Fluo-4 in the DV (Figure 2.1A+B). Fluo-4 accumulation in the DV was impeded by pre-incubation of the parasites with tariquidar (TQ), a specific inhibitor of Pgp transporters [222], including PfMDR1 (Figure 2.1B). Importantly, Fluo-4 accumulation in the DV was shown to be independent of the PfCRT K76T mutation, suggesting that the PfCRT mutation alone has no effect on Fluo-4 accumulation.

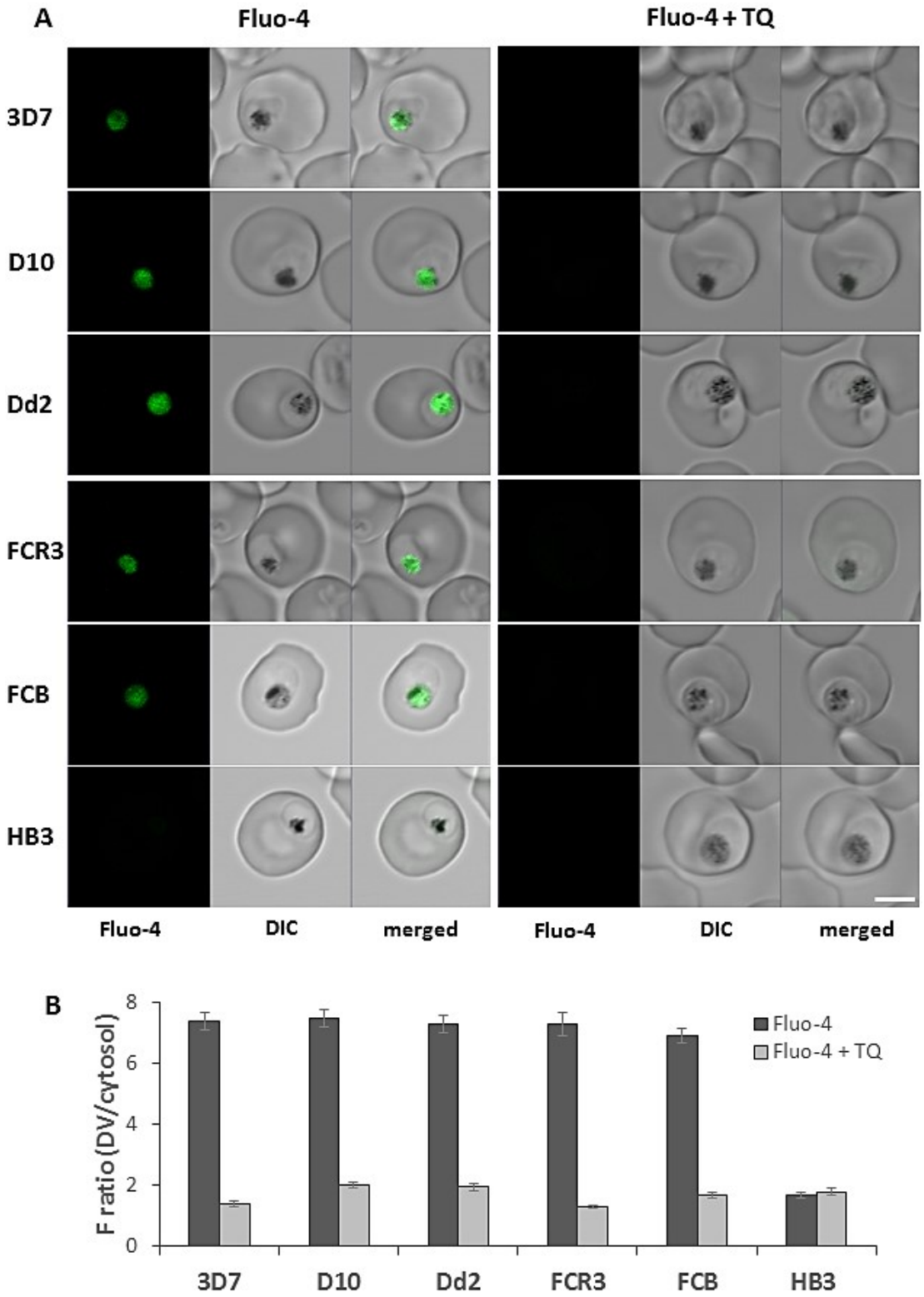

Figure 2.1 Fluo-4 fluorescence in *P. falciparum* parasites. Parasites were incubated with 5 µM Fluo-4. **A**, Representative images of *P. falciparum*-infected erythrocytes. Scale bar, 5 µm. **B**, Mean Fluo-4 fluorescence ratio (DV/cytosol) ± SEM. When treated with the Pgp inhibitor tariquidar (TQ), fluorescence ratio was reduced, indicating that Fluo-4 transport occurred exclusively through PfMDR1. Total n ≥ 67 for each strain, done in three independent experiments.

2.4.2 Fluo-4 transport is associated with PfMDR1 N1042.

Strain HB3, which does not accumulate Fluo-4 in the DV, harbors two PfMDR1 amino acid mutations, Y184F and N1042D, which are not found in the other tested *P. falciparum* strains (Table 2.1), suggesting that one of these two residues is responsible for the altered Fluo-4 transport seen in HB3 parasites. It has previously been demonstrated for the human homolog of PfMDR1 that the Y184F mutation does not influence drug specificity [212]. Furthermore, this residue only mildly increased drug resistance in comparison to other PfMDR1 mutation sites [168]. In contrast, amino acid position 1042 is thought to be part of the transporter binding pocket and forms electrostatic interactions with amodiaquine (AQ), CQ, MQ (only in the presence of asparagine), HF, vinblastine and vincristine [163, 166, 168]. Therefore, the role of PfMDR1 mutations at position 1042 were investigated in more detail.

To analyze the influence of PfCRT on Fluo-4 transport, existing parasite clones containing either lysine (K) or threonine (T) at residue 76 in PfCRT were selected and compared. For this, stably transfected *P. falciparum* clones derived from the parental lines GC03 and 3BA6 were used, where GC03 harbors the K76 PfCRT genotype and is CQ sensitive, and 3BA6 contains the PfCRT K76T mutation that confers CQ resistance (Table 2.1). Both GC03 and 3BA6 contain the PfMDR1 sequence N86, Y184F, S1034, N1042D, D1246, identical to the HB3 strain. Experiments verified that neither GC03 nor 3BA6 were able to accumulate Fluo-4 in the DV, as expected. As a control, clones SDD^{GC03} and SDD^{3BA6}, harboring the same mutations as GC03 and 3BA6, revealed that the PfMDR1 N1042D mutation did not transport Fluo-4 into the DV (Figure 2.2A+B). Fluo-4 transport was only established with the introduction of asparagine at residue 1042 for both clones (SND^{GC03} and SND^{3BA6}). Transport was independent of the PfCRT K76T mutation, since Fluo-4 transport was equally impaired in GC03 and 3BA6 parental lines as well as the SDD^{GC03} and SDD^{3BA6} controls, and only seen in the clones SND^{GC03} and SND^{3BA6}. Transport specificity for PfMDR1 in clones SND^{GC03} and SND^{3BA6} was confirmed through pre-incubation of the samples with the Pgp inhibitor TQ (Figure 2.2B + Suppl. Figure S2.5). These results indicate a pivotal role for asparagine at PfMDR1 residue 1042 in Fluo-4 transport, independent of PfCRT.

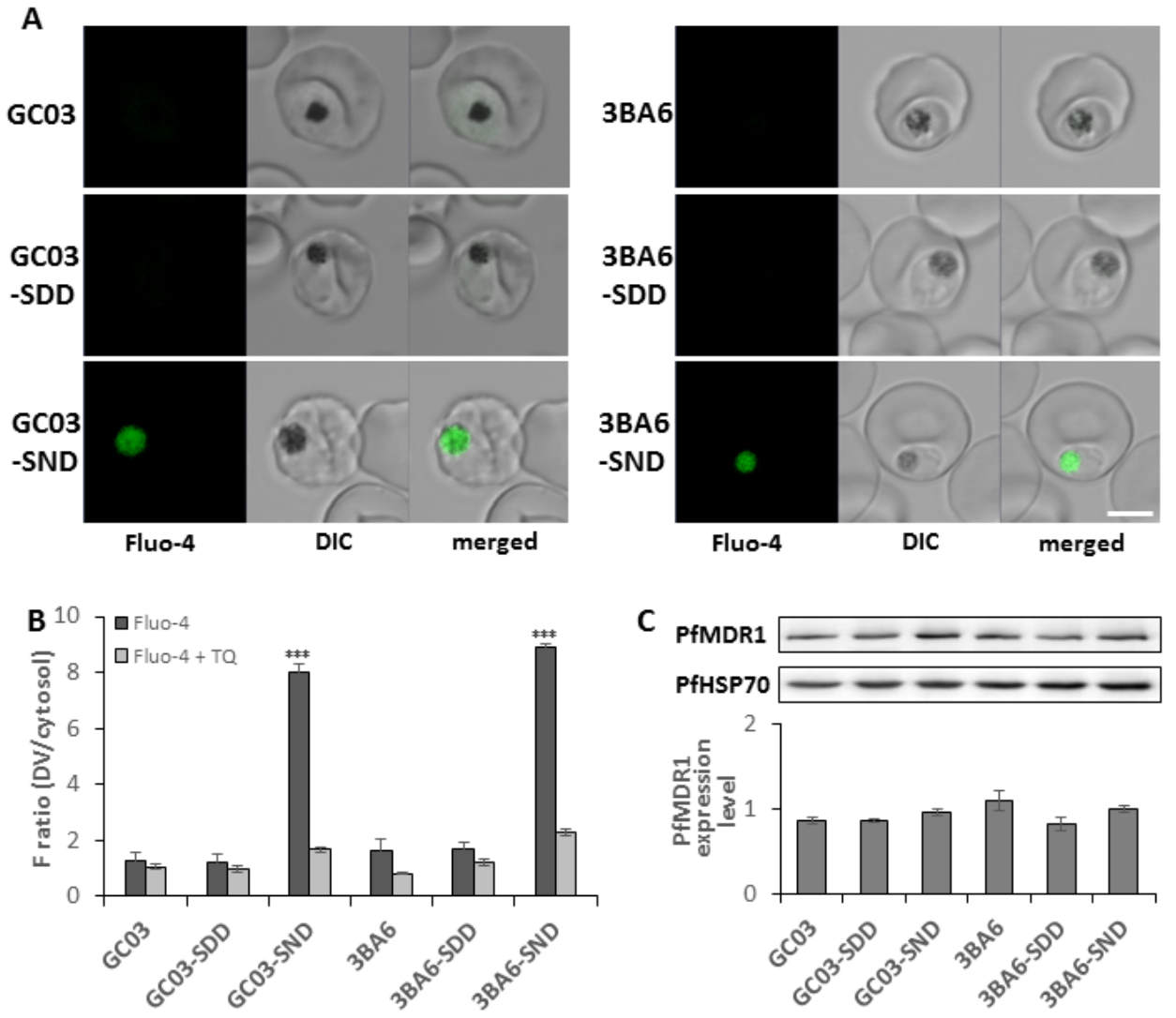

Figure 2.2 Fluo-4 fluorescence in *P. falciparum* clones with different PfMDR1 and PfCRT mutations. Parasites were incubated with 5 µM Fluo-4 AM in Ringer's solution for 50 min at 37°C, then washed with Ringer's solution and transferred onto a microscope chamber. **A**, Single images of different P. falciparum clones. Scale bar, 5 µM. **B**, Mean Fluo-4 ratio of the digestive vacuole (DV) compared to the cytosol. When treated with tariquidar (TQ), parasites were pre-incubated with 100 nM TQ for 10 min at 37°C before adding Fluo-4 AM for 50 min. Total n ≥80 for each strain, done in three independent experiments on different days. Error bars represent SEM. ***, p <0.0001. **C**, Western blot of synchronized trophozoite stage parasites using anti-PfMDR1 antibodies. Anti-PfHSP70 was used as a loading control. PfMDR1 protein expression levels were normalized to PfHSP70 and measured in triplicate ± SEM.

In addition to PfMDR1 polymorphisms, increased *pfmdr1* gene copy numbers and PfMDR1 expression levels have also been suggested to play a role in drug resistance or susceptibility [161, 211, 223]. To verify that Fluo-4 accumulation in the DV of the clones SND^{GC03} and SND^{3BA6} was not linked to increased PfMDR1 expression, PfMDR1 protein levels were analyzed for these parasite

clones (Figure 2.2C). No significant increase in PfMDR1 expression was detected for the GC03 and 3BA6 parental lines or their clones harboring the D1042N substitution ($p > 0.05$). Therefore, Fluo-4 accumulation in the DV of these clones was only associated with the mutation at PfMDR1 residue 1042.

2.4.3 Effect of N1042D polymorphism on drug susceptibility.

Since transport of Fluo-4 was dependent on specific PfMDR1 polymorphisms, it follows that the N1042D substitution in the PfMDR1 substrate binding pocket may not only alter the binding and transport of Fluo-4, but also influence other substrates, such as antimalarial drugs. To determine if the amino acid substitution at residue 1042 resulted in altered drug sensitivity or resistance of the parasite clones, growth inhibition assays were performed. A change in a given drug's IC_{50} would indicate a role for PfMDR1 amino acid position 1042 in its transport. CQ IC_{50} values for the CQS clones were found to be 47 ± 2.6 nM for GC03, 46 ± 2.2 nM for SDD^{GC03} and 49 ± 2.8 nM for SND^{GC03}, while CQ IC_{50} values for CQR clones were 262 ± 5.7 nM for 3BA6, 204 ± 9.4 nM for SDD^{3BA6} and 274 ± 5.6 nM for SND^{3BA6} (Table 2.2). This suggests that an amino acid mutation at PfMDR1 residue 1042 does not affect susceptibility or resistance to CQ. CQ resistance could be reversed in CQR strains through the addition of 1 µM verapamil, while no significant difference in CQS strains was observed ($p > 0.05$), as expected. Similarly, CQS clones were more susceptible to quinacrine (QC) with IC_{50} values of 11 ± 0.3 nM for GC03, 13 ± 0.3 nM for SDD^{GC03} and 14 ± 0.4 nM for SND^{GC03} compared to the higher QC IC_{50} values of 43 ± 3.4 nM for 3BA6, 41 ± 1.0 nM for SDD^{3BA6} and 42 ± 2.3 nM for SND^{3BA6}. Here again, as for CQ, an amino acid mutation at PfMDR1 residue 1042 did not affect susceptibility or resistance to QC. The same was found for dihydroartemisinin (DHA). CQS clones were four-fold less sensitive than CQR clones (4 ± 0.1 nM *versus* 1 ± 0.1 nM) and this resistance was not reversible by the addition 1 µM verapamil. Therefore, the PfMDR1 N1042D mutation alone does not appear to be a major determinant for altered CQ, QC or DHA susceptibility in these parasites (Table 2.2).

Interestingly, the N1042D mutation did provide changes in drug susceptibility for the antimalarial drugs QN and MQ. A significant decrease in QN IC_{50} values was observed in the GC03 and 3BA6-

derived clones SND^{GC03} and SND^{3BA6} compared to the parental lines GC03 and 3BA6 or their recombinant controls SDD^{GC03} and SDD^{3BA6} ($p < 0.005$) (Table 2.2), which is in agreement with previous findings [163]. The opposite effect was observed for MQ. For the clones SND^{GC03} and SND^{3BA6}, the D1042N substitution led to an approx. three-fold increase in resistance to MQ (Table 2.2). MQ IC_{50} values increased from 6 ± 0.9 nM in GC03 to 19 ± 0.6 nM in SND^{GC03}, and from 5 ± 0.3 nM in 3BA6 to 14 ± 0.5 nM in SND^{3BA6}. This was a significant increase in MQ IC_{50} values for the clones SND^{GC03} and SND^{3BA6} compared to the parental lines ($p = 0.0003$ for GC03 *vs* SND^{GC03}; $p = 0.0001$ for 3BA6 *vs* SND^{3BA6}). Similar increases in MQ resistance (approx. 3-fold) have been found in field isolates from Africa and Asia [224, 225]. A three-fold increase in MQ resistance was also confirmed *in vitro* through allelic exchange of *pfmdr1* [160]. Therefore, the PfMDR1 mutation crucial for MQ resistance *in vitro* is likely to play a role in increased MQ resistance in the field. Nevertheless, growth inhibition experiments do not fully elucidate the altered transport of MQ by PfMDR1. For this reason, co-incubation antimalarial drugs with Fluo-4 can provide additional insight into PfMDR1 transport properties.

Table 2.2 IC_{50} values of *P. falciparum* parasites used in this study

	CQ	CQ + VP	DHA	DHA + VP	QC	QC+ VP	QN	MQ
3D7	24 ± 5.6	17 ± 1.2	n.d.	n.d.	n.d.	n.d.	14 ± 2.7	8 ± 1.2
Dd2	169 ± 3.9	53 ± 6.5	n.d.	n.d.	n.d.	n.d.	31 ± 6.4	27 ± 4.0
GC03	47 ± 2.6	46 ± 2.1	4 ± 0.1	4 ± 0.1	11 ± 0.3	18 ± 0.4	55 ± 7.3	6 ± 0.9
SDD^{GC03}	46 ± 2.2	47 ± 0.6	4 ± 0.1	3 ± 0.2	13 ± 0.3	15 ± 0.7	54 ± 5.1	7 ± 0.6
SND^{GC03}	49 ± 2.8	47 ± 2.2	4 ± 0.1	3 ± 0.1	14 ± 0.4	17 ± 0.3	54 ± 1.6	19 ± 0.6
3BA6	262 ± 5.7	41 ± 1.8	1 ± 0.1	1 ± 0.1	43 ± 3.4	47 ± 2.2	48 ± 3.2	5 ± 0.3
SDD^{3BA6}	204 ± 9.4	63 ± 1.5	1 ± 0.0	1 ± 0.1	41 ± 1.0	39 ± 0.5	51 ± 1.6	6 ± 0.7
SND^{3BA6}	274 ± 5.6	69 ± 5.6	1 ± 0.1	1 ± 0.0	42 ± 2.3	39 ± 0.4	55 ± 5.2	14 ± 0.5

All values are given in nM. CQ = chloroquine; VP = verapamil; DHA = dihydroartemisinin; QC = quinacrine; QN = quinine; MQ = mefloquine; n.d. = not determined. Values were determined from at least three independent experiments, carried out on three separate days.

2.4.4 Substrate competition of antimalarial drugs with Fluo-4 to determine drug transport by PfMDR1.

PfMDR1 is involved in the transport of substrates, including various antimalarial drugs, from the cytosol into the DV [163, 202], but the role of PfMDR1 polymorphisms in drug resistance is not fully understood. Mutations at residue 86 have been suggested to allosterically influence the TMD11 drug binding site [202], while PfMDR1 residues 1034 and 1042 are located in a proposed binding pocket. Electrostatic interactions with both asparagine and aspartic acid at position 1042 have been demonstrated *in silico* for CQ, QN and MQ [166, 168]. While CQ was unable to form a hydrogen (H)-bond with either asparagine or aspartic acid at residue 1042, asparagine at residue 1042 was able to form a H-bond with MQ [166]. No information is available on H-bond formation of QN with residue 1042.

Further insight into the importance of PfMDR1 in drug transport can be achieved through competition studies using two potentially competitive substrates, e.g., fixed amounts of Fluo-4 and increasing drug concentrations. For this purpose, two parasite strains were chosen to evaluate potential differences in antimalarial drug transport in sensitive (3D7) and resistant (Dd2) parasites. 3D7 is sensitive to CQ, QN and MQ (Table 2.2), while Dd2 is resistant to these drugs. HB3 was not used, since it does not transport Fluo-4 into the DV. The measured changes of Fluo-4 accumulation in the DV in the presence of antimalarial drugs were compared for 3D7 and Dd2 parasites.

For 3D7 parasites, increasing CQ concentration led to a strong decrease in Fluo-4 accumulation in the DV (Figure 2.3A). While TQ is a noncompetitive inhibitor of MDR1 through inhibition of the ATPase activity [226], CQ is thought to bind to the transporter's substrate binding pocket and is likely a competitive inhibitor of Fluo-4. Pre-incubation of 3D7 parasites with 250 nM CQ resulted in decreased Fluo-4 accumulation in the DV, where only 5% ± 1.0% of the Fluo-4 fluorescence in the absence of drug was measured. In Dd2 parasites, pre-incubation with 250 nM CQ reduced Fluo-4 fluorescence in the DV by half (48% ± 3.0%).

MQ reduced Fluo-4 transport into the DV to 45% ± 2.0% in 3D7 parasites and only 82% ± 6.0% in Dd2 parasites (Figure 2.3A). For MQ, decreased Fluo-4 transport in 3D7 compared to Dd2 cannot be attributed to a PfMDR1 amino acid mutation at position 1042 alone since both strains harbor

wild-type N1042. However, Dd2 parasites harbor an amino acid mutation at PfMDR1 residue 86, which was described to influence MQ sensitivity in African field isolates [207, 221, 227] and, therefore, may alter MQ transport through PfMDR1 as seen in the experiments presented here.

QN was less effective than CQ or MQ and only decreased Fluo-4 fluorescence in the DV to 59% ± 2.9% in 3D7 parasites and not significantly in Dd2 parasites (92% ± 3.4%) (Figure 2.3A). The differences between 3D7 and Dd2 parasites at the level of Fluo-4 reduction may be linked to PfMDR1 residue 86, which is suggested to influence CQ susceptibility [228]. It is conceivable that N86Y can allosterically influence the drug binding site at TMD11, as suggested in {Ferreira, 2011 #1044}. In this study, residue 86 was not examined in detail.

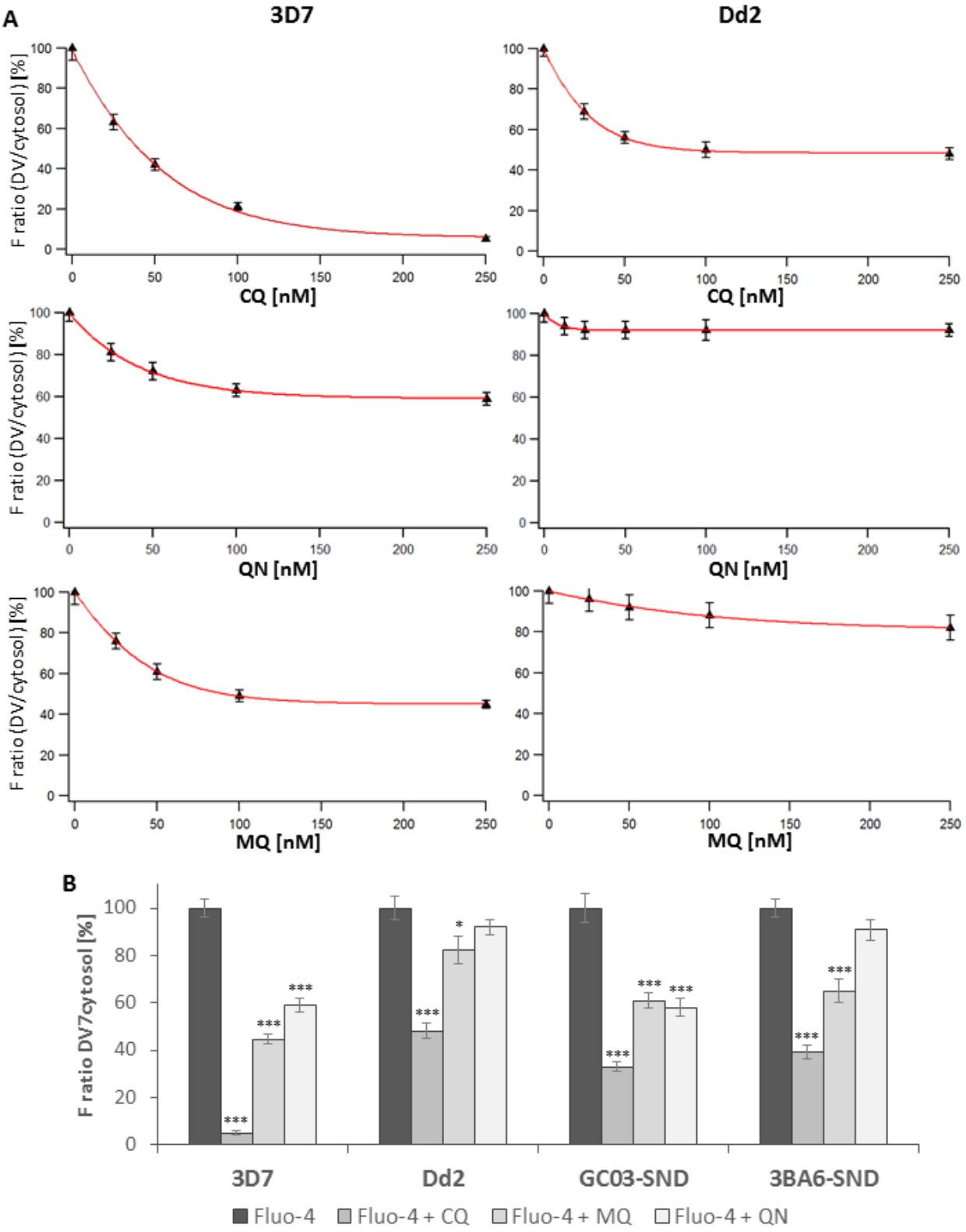

Figure 2.3 Competition of Fluo-4 transport with antimalarial drugs. A, Parasites were pre-incubated with different concentrations of chloroquine (CQ), mefloquine (MQ) or quinine (QN), or left untreated before adding Fluo-4. **B**, Parasites were pre-incubated as described with 250 nM of CQ, MQ or QN. Experiments were done in triplicate in independent experiments. Error bars represent SEM. *, $P < 0.05$; ***, $P < 0.0001$.

Fluo-4 competition with antimalarial drugs was also tested on the parasite clones SND^{GC03} and SND^{3BA6}. Using a single drug concentration of 250 nM, Fluo-4 accumulation was decreased in the DV of SND^{GC03} and SND^{3BA6} parasites to 33% ± 1.9% and to 39% ± 3.0% for CQ, to 61% ± 3.1% and to 65% ± 4.8% for MQ, and to 58% ± 3.9% and to 91% ± 4.4% for QN, respectively. Almost all tested antimalarial drugs decreased Fluo-4 accumulation in the DV in both SND^{GC03} and SND^{3BA6} clones, except QN (Figure 2.3B). This again suggests that the influence of antimalarial drugs on substrate transport by PfMDR1 is not only dependent on PfMDR1 polymorphisms but also on the varying genetic background of the parasite strain.

The influence of the N1042D substitution on Fluo-4 transport is explained in a proposed model (Figure 2.4). Fluo-4 is intrinsically negatively charged and, therefore, replacement of a neutral asparagine at residue 1042 with a negatively charged aspartic acid alters the local environment, making it less favorable to Fluo-4. TQ does not influence Fluo-4 affinity for the substrate binding pocket but prevents adenosine triphosphate (ATP) hydrolysis of PfMDR1. Since both NBDs act in concert [229], complete inhibition of ATPase activity is already achieved when one nucleotide binding site is blocked.

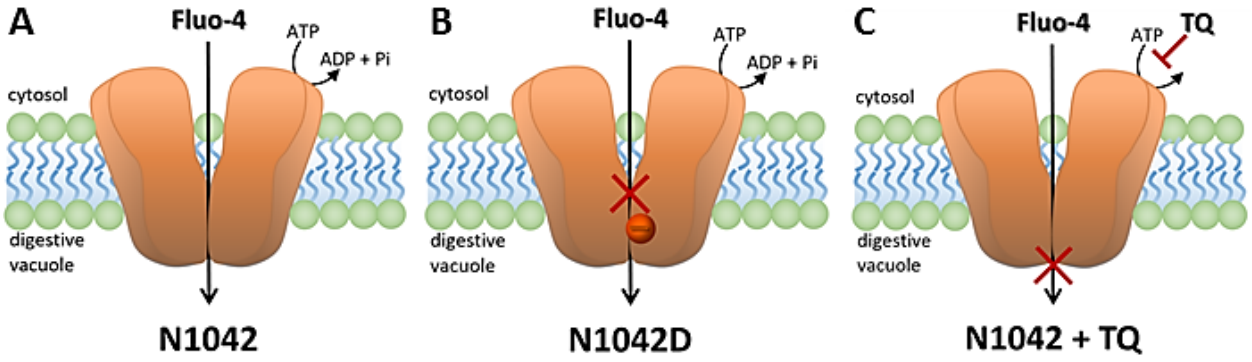

Figure 2.4 Model of Fluo-4 transport. The docking of substrates in the PfMDR1 binding pocket is influenced by the size, charge and polarity of local amino acids. Asparagine (N) and aspartic acid (D) are both polar, hydrophilic and small in volume. While N is an amide and uncharged, D is acidic and negatively charged. **A**, for parasites containing the PfMDR1 N1042 polymorphism, the intrinsically negatively charged Fluo-4 gets transported from the cytoplasm into the digestive vacuole (DV) where it accumulates. **B**, in the presence of PfMDR1 N1042D, which adds a negative charge to the binding pocket, Fluo-4 does not get transported by PfMDR1 and no Fluo-4 accumulation is detected in the DV. **C**, Fluo-4 transport is abolished through the addition of the Pgp inhibitor tariquidar (TQ), which does not alter the substrate binding but prevents ATP hydrolysis and therefore the conformational change that is necessary for substrate dislocation.

Detailed transport kinetics for parasite strains of different origin will provide additional information on substrate transport by PfMDR1. Using Fluo-4 as a competitive substrate circumvents the issue of direct labeling of antimalarial drugs with a fluorescent tag that may alter their transport properties. Therefore, Fluo-4 is a powerful tool to selectively study transport kinetics of PfMDR1 in intact *P. falciparum*-infected erythrocytes.

2.5 Conclusion

This study provides direct evidence for reduced PfMDR1-driven substrate transport through the single amino acid mutation N1042D, located in the substrate binding pocket. The relevance of this amino acid mutation may have been underestimated and needs further investigation. Furthermore, it is now possible to test additional mutations within the binding pocket of PfMDR1 to verify their potential role in drug transport. Accordingly, using Fluo-4 in a drug competition assay is a powerful tool to better examine drug transport kinetics via PfMDR1. This newly acquired information can help elucidate the role of PfMDR1 in drug transport, which has remained controversial for decades. For example, while earlier investigations have suggested a link between MQ resistance and asparagine at PfMDR1 amino acid position 86 in isolates from Thailand and West Africa [205, 207], others have associated wild-type PfMDR1 and increased gene copy numbers with MQ resistance [209, 230]. More recent publications have found strong evidence for a role for N1042 in MQ resistance in Thai isolates [99, 231], suggesting that the importance of this mutation has been underestimated in previous field studies. The importance of N1042 for MQ resistance was similarly demonstrated *in vitro* through combined amino acid substitutions that generated a parasite strain harboring the mutations S1024C, N1042D, D1246Y [160]. This newly generated strain was approx. three-fold more susceptible to MQ exposure compared to the parental strain [160]. The results presented here support a potential role of PfMDR1 N1042 in parasite resistance to MQ. Further investigations will help elucidate the significance of this polymorphism on substrate transport.

2.6 Chapter-related Acknowledgements

This study was supported in part by fellowships from the German Academic exchange Service (DAAD) (SJR) and the Centre for Host-Parasite Interaction (FRQNT) (SJR), and grants from the Natural Sciences and Engineering Research Council (NSERC) Discovery Grant (PR) and the Canada Foundation for Innovation (CFI) Leaders Opportunity Fund (PR).

2.7 Chapter-related Supporting Information

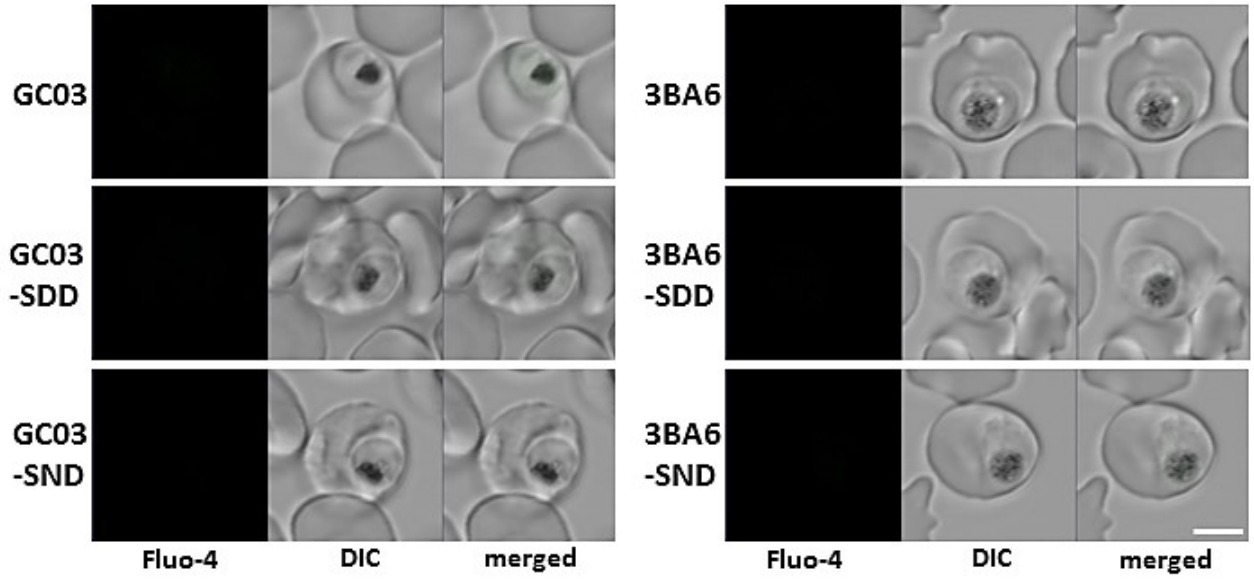

Suppl. Figure S2.5 Inhibition of Fluo-4 transport through tariquidar. *P. falciparum* clones were pre-incubated with 100 nM tariquidar for 10 min at 37°C, then 5 µM Fluo-4 AM was added for 50 min. Fluo-4 accumulation in the digestive vacuole was abolished. Experiments were done in triplicate. These images are supplementary to the data obtained for Figure 2.3B. Scale bar, 5 µm.

Connecting Statement I

In the first manuscript, a pivotal role of PfMDR1 residue 1042, located in the substrate binding pocket, was demonstrated for Fluo-4 transport. Furthermore, the N1042D mutation was shown to increase parasite susceptibility to MQ but not CQ or QN. In addition, competition studies of Fluo-4 with MQ, CQ and QN revealed distinct inhibition patters for parasite strains of drug-sensitive or -resistant background. Highest changes in Fluo-4 transport inhibition between a drug-sensitive and -resistant strain were seen with increasing CQ concentrations.

In the following chapter, differences between CQS and CQR strains will be further elucidated. The exact mechanism of CQ resistance is not understood. The importance of various factors, such as the role of the PfCRT K76T mutation, polymorphisms in the PfMDR1 transporter, or altered CQ affinity to FPIX are discussed. Researchers agree that CQR strains accumulate less CQ than CQS strains. In addition, some studies suggest that CQR strains tolerate higher intracellular CQ concentrations than CQS strains. Therefore, molecular and phenotypic differences between CQS and CQR strains will be investigated using CQ concentrations that are equivalent to the IC_{50} values of each strain.

— Chapter 3 —

Manuscript II

Chloroquine induces formation of cytosolic hemozoin-containing compartments in chloroquine-sensitive *Plasmodium falciparum* parasites

S.J. Reiling[1], G. Tadeus[1,2], G. Krohne[3], and P. Rohrbach[1]

[1] Institute of Parasitology, McGill University, Ste. Anne de Bellevue (Montreal), Quebec, Canada

[2] Institute of Chemistry and Biochemistry, Free University Berlin, Berlin, Germany

[3] Division of Electron Microscopy, Biocenter, University of Würzburg, Würzburg, Germany

3.1 Abstract

Chloroquine (CQ) treatment failure in *Plasmodium falciparum* parasites has been documented for decades. The exact mechanism of parasite killing in CQ-sensitive (CQS) versus CQ-resistant (CQR) parasites is not fully understood. In this study, we analyze the onset of cellular responses in synchronized CQS and CQR parasite strains when exposed to CQ concentrations equivalent to their respective IC_{50} concentrations. We found that parasite survival is higher in CQR parasites when compared to CQS parasites in the initial 10 h of CQ exposure. Additionally, live cell imaging showed that dark cytosolic structures start to appear in CQS but not CQR parasites within 1 h of CQ exposure that were later confirmed as hemozoin (Hz) crystals. Electron microscopy (EM) revealed that the cytosolic Hz was always confined in compartments surrounded by a membrane bilayer and not found freely within the cytosol. Leakage of Hz crystals from the digestive vacuole (DV) was ruled out, since pre-incubation with Fluo-4 AM prior to CQ exposure showed that the DV membrane remained intact. To determine the origin of these compartments, CQS parasites were loaded with Fluo-4 AM, which accumulates in the DV. Subsequent treatment with CQ showed co-localization of Fluo-4 with Hz-containing cytosolic compartments, indicating that they originate from the DV. Our findings suggest that CQS but not CQR parasites form cytosolic Hz-containing compartments on exposure to CQ. CQR parasites tolerate higher levels of extracellular CQ and require prolonged CQ exposure before parasite killing events are triggered. We conclude that CQ resistance is not linked to reduced intracellular CQ concentration alone and additional regulatory mechanisms most likely play an important role for parasites coping with CQ exposure.

3.2 Author Summary

Malaria continues to be a major threat to humanity; more than 300 million people live in risk areas. Chloroquine (CQ) was the drug of choice to treat malaria for more than 30 years until resistance emerged. Since then, researchers have mainly focused on understanding the mechanisms of CQ resistance by studying genetic mutations. When the K76T mutation in the *P. falciparum* chloroquine resistance transporter (PfCRT) was found to be linked to CQ resistance, an important aspect of CQ resistance was revealed. However, recent findings suggest that additional mechanisms are most likely involved. Here, we show that CQ-sensitive (CQS) parasites display phenotypic features subsequent to drug exposure that are absent in CQ-resistant (CQR) parasites, even when CQR parasites are exposed to equally lethal CQ concentrations. While 61% of CQS parasites formed cytosolic hemozoin-containing compartments within 4 h after CQ exposure, only 9% of CQR parasites developed similar structures. The formation of cytosolic hemozoin-containing structures in CQS parasites after CQ exposure has not been previously described. Its absence in CQR parasites may be a key contributor to their increased survival.

3.3 Introduction

Reducing the worldwide malaria burden is a top priority of global health organizations. Although extensive malaria control measures have decreased the number of malaria cases worldwide [232], much remains unknown about drug resistance mechanisms, hampering control strategies to adequately contain this disease. Treatment failures with currently used antimalarial drugs due to resistance is the biggest concern, since a very limited number of new drug combinations is readily available. For this reason, it is imperative to understand the mechanisms of drug resistance to currently used antimalarials.

Chloroquine (CQ) belongs to one of the most effective, low-cost antimalarial drug classes available, and resistance to this drug required decades to evolve [233, 234]. CQ passes through biological membranes in its uncharged form and accumulates due to its weak base properties in the parasite's acidic digestive vacuole (DV) [3]. CQ has been shown to bind to ferriprotoporphyrin IX (FPIX), a product that is released during proteolysis of hemoglobin [235]. High concentrations of FPIX are potentially toxic to the parasite, since FPIX has the ability to permeabilize membranes, eventually leading to cell lysis [63, 78, 236]. To overcome this, the parasite biocrystalizes FPIX dimers into inert hemozoin (Hz) crystals [237]. Binding of CQ to FPIX inhibits hemozoin production [21, 53, 56, 79, 97, 238], resulting in an increase of toxic FPIX in the DV that is able to permeabilize the DV membrane and release DV content into the cytosol, thereby triggering parasite death.

Resistance to CQ has mainly been attributed to a point mutation in the *Plasmodium falciparum* chloroquine resistance transporter (PfCRT) at amino acid position 76 [2, 95, 239], although other PfCRT mutations may also play a role [240]. PfCRT containing the K76T mutation is able to transport CQ out of the DV, away from its site of action [90], limiting the concentration of CQ molecules available to bind to FPIX and consequently reducing cell damage. However, CQ-resistant (CQR) parasites have been shown to tolerate higher CQ levels in the DV, which cannot be explained by CQ concentration-dependent toxicity effects alone. When CQ-sensitive (CQS) and CQR parasites are exposed to varying concentrations of extracellular chloroquine to obtain equal CQ-concentrations found in the DV, CQR parasites still have higher IC_{50} values than CQS parasites [4].

Therefore, a more detailed understanding of the mechanism of CQ-triggered parasite death is of high importance.

In this study, we investigated phenotypic differences in CQS and CQR parasites after CQ exposure. Our work focused on alterations in CQS and CQR parasites when exposed to equally effective CQ concentrations based on their IC_{50} values. We found that, within hours of CQ exposure, multiple Hz-containing compartments were observed in the cytosol of CQS but not CQR parasites. These Hz-containing compartments originate from the DV and are independent from the disruption of the DV membrane, which most likely occurs at a later stage during CQ treatment. Our novel findings suggest that, when exposed to CQ, CQS and CQR parasites display different cellular responses during the same time frame.

3.4 Material and Methods

3.4.1 Parasite strains and culture conditions

CQS (3D7, HB3) and CQR (FCB, Dd2) parasite strains were cultured continuously, as described by Trager and Jensen [215], with modifications. Briefly, parasites at 5% hematocrit were propagated in RPMI 1640 (Life Technologies, Burlington, ON, Canada) supplemented with 25 mM HEPES, 2 mM L-glutamine, gentamicin (20 µg/ml) (Life Technologies, Burlington, ON, Canada), 100 µM hypoxanthine (Sigma-Aldrich, Oakville, ON, Canada), and 0.5% AlbuMAX I (Life Technologies, Burlington, ON, Canada). Parasites were maintained at 37°C under an atmosphere of 5% CO_2, 3% O_2 and 92% N_2. A^+ red blood cells were obtained from the Interstate Blood Bank (Memphis, TN, USA). Giemsa-stained blood smears were prepared daily to monitor parasite growth. For synchronization, parasites were exposed to 5% D-Sorbitol (BioShop Canada, Burlington, ON, Canada) for 10 min at 37°C; sorbitol was removed and parasites were washed once before being put back into culture. To obtain highly synchronous parasite cultures, this treatment was repeated 6-8 h later.

3.4.2 Growth inhibition assays

All drugs were obtained from Sigma-Aldrich Canada (Oakville, ON, Canada) and dissolved in dH_2O. Growth inhibition assays were performed as described previously [217], with modifications. Synchronized ring stage parasites were diluted to a final parasitemia of 0.5% and a hematocrit of 2%. A total of 100 µl culture medium per well was prepared in a 96-well plate assay, with a drug dilution series of 1:3, ranging from 1 µM to 0.15 nM. Plates were incubated at 37°C, 5% CO_2, 3% O_2 and 92% N_2 for 72hrs, then frozen and stored at -80°C. Plates were thawed at room temperature and 100 µl 2x lysis buffer (20 mM Tris pH 7.5, 5 mM EDTA, 0.008% saponin, 0.08% Triton X-100, 0.2 µl SYBR Green I/ml) was added to each well. Plates were incubated in the dark for at least 1 h. Fluorescence intensity was determined using a Synergy H4 plate reader (Fisher Scientific, Nepean, ON, Canada) with 485 nm excitation and 520 nm emission wavelengths. IC_{50} values were determined by fitting concentration response curves with a custom made procedure for IGOR Pro 6.2 based on an R script kindly provided by Le Nagard and used as described [218, 219].

3.4.3 Parasite killing

Synchronized ring stage parasites were prepared in triplicates at 1% parasitemia and 2% hematocrit in 100 µl culture medium in a 96-well plate. They were left untreated (control) or exposed to concentrations of CQ 10x, 20x or 30x their IC_{50} values (Table 3.1) and incubated for various lengths of time. After incubation, parasites were washed with cell culture medium (as described above) to remove CQ and resuspended in 100 µl culture medium. Parasites were incubated for 48 h at 37°C, 5% CO_2, 3% O_2 and 92% N_2, after which the plates were frozen at -80°C. Analysis was performed with SYBR Green I detection as described above.

3.4.4 Fluo-4 AM loading of parasites

For analysis of DV membrane integrity, synchronized early trophozoite stage parasites were loaded with 5 µM Fluo-4 AM (Life Technologies, Burlington, ON, Canada) in Ringer's solution (122.5 mM NaCl, 5.4 mM KCl, 1.2 mM $CaCl_2$, 0.8 mM $MgCl_2$, 11 mM D-glucose, 10 mM HEPES, 1 mM NaH_2PO_4,

pH 7.4) for 50 min at 37°C. Cells were then washed twice with Ringer's solution and transferred onto poly-L-lysine (Sigma-Aldrich, Oakville, ON, Canada) coated cover slips in a microscope chamber containing 10 µM CQ in Ringer's solution. Parasites were kept at 37°C in a stage-top incubator (Tokai Hit, Shizuoka-ken, Japan) for the entire experiment. Ringer's solution was replaced every 60 min with or without 10 µM CQ for treated and control groups, respectively. The same parasites were imaged every 15 min using a time series on a Zeiss LSM710 confocal microscope (Carl Zeiss, Oberkochen, Germany) equipped with a water-corrected objective (C-apochromat 63x/1.20 W Korr M27) and 488 nm laser (12.5 mW, 0.8%). Images were analyzed using ImageJ 1.47q (National Institutes of Health, USA).

To investigate whether the Hz-containing cytosolic vesicles are DV-derived, trophozoite stage 3D7 parasites were loaded with 5 µM Fluo-4 AM in Ringer's solution for 60 min at 37°C. To remove excess Fluo-4, parasites were washed twice with Ringer's solution. Parasites were subsequently incubated with 500 nM CQ in Ringer's for 3 h at 37°C to trigger the formation of cytosolic Hz-containing compartments. Cells were then transferred onto a microscope chamber containing 500 nM CQ in Ringer's solution. A constant temperature of 37°C was maintained during imaging using a stage-top incubator. Images were taken with the Zeiss LSM 710 confocal microscope and 488 nm laser (12.5 mW, 3.0%) and analyzed using the ZEN 2010 software (Carl Zeiss MicroImaging, Oberkochen, Germany).

3.4.5 Parasite enrichment

Synchronous parasite cultures with 5% parasitemia were harvested and trophozoite stage parasites purified using an Easycoll (Cedarlane Laboratories, Burlington, ON, Canada) density gradient. In a 15 ml tube, a gradient of 4 ml 80% Easycoll, 3 ml 70% Easycoll, 3 ml 60% Easycoll and 3 ml 40% Easycoll was prepared. The gradient percentage was adjusted using warm Ringer's solution. Approx. 500 µl parasite culture was resuspended in 2 ml Ringer's solution and layered on top of the gradient. Tubes were centrifuged at 5000 rpm (Thermo Fisher Scientific, Mississauga, ON, Canada) for 45 min at 24°C with low acceleration and decelerated without brake. Trophozoite

stage parasites accumulated at the interphase between 60% and 70%. The parasites isolated from this phase were washed twice with Ringer's solution and typically enriched to 62-93% parasitemia.

3.4.6 Electron microscopy

The enriched trophozoite pellet was resuspended in 500 µl fixation solution containing 50 mM cacodylic acid (Carl Roth, Karlsruhe, Germany), 1% paraformaldehyde (Applichem, Darmstadt, Germany), 2.5% glutaraldehyde (Merck KGaA, Darmstadt, Germany), 2.5 mM $MgCl_2$ and 50 mM KCl, pH 7.2. The sample was centrifuged at 3000 rpm for 20 min at 4°C, the supernatant aspirated and another 500 µl fixation solution was added overnight at 4°C. Fixation solution was removed and the pellet was washed three times with 50 mM cacodylic acid, pH 7.2. The samples were stained with 2% OsO_4 in 50 mM cacodylic acid, pH 7.2 at 4°C for 2 h, then washed with H_2O, stained with 0.5% aqueous uranyl acetate at 4°C overnight and washed with H_2O. Samples were dehydrated and embedded in epon 812 (Serva, Heidelberg, Germany). Ultrathin sections of 50-70 nm thickness were analyzed using a JEM-2100 TEM (JEOL, Eching, Germany) at 200 kV. Images were taken using a 4K camera from Tietz Video and Image Processing Systems (TVIPS, Gauting, Germany).

3.4.7 JC-1 activity assay

Synchronized 3D7 and Dd2 trophozoites were washed with Ringer's solution and incubated for 4 h with 480 nM CQ for 3D7 and 3.4 µM for Dd2 (corresponding to their respective 20x IC_{50} CQ concentrations) at 37°C in 500 µl Ringer's solution at 5% hematocrit. In the final 30 min of incubation, 4 µM JC-1 (Life Technologies, Burlington, ON, Canada) was added. Cells were washed with Ringer's solution and placed onto a microscope chamber. Fluorescence was measured using a Zeiss LSM 710 confocal microscope (Carl Zeiss, Oberkochen, Germany) and a 488 nm laser (12.5 mW, 0.8%). Two emission spectra were used to distinguish JC-1 monomers (530 nm) and aggregates (590 nm).

3.5 Results

3.5.1 IC_{50} determination of CQ for sensitive and resistant strains.

Effects of CQ on CQS and CQR parasites were evaluated on all strains used in this study. Since the IC_{50} of a drug can vary among laboratories due to slight alterations in culture conditions, parasite handling and methods used, we first determined the CQ IC_{50} for the strains used in this study (Table 3.1) by fitting concentration-response curves obtained with the SYBR Green I detection assay using a standardized method for data analysis [218]. The CQS strains 3D7 and HB3 had IC_{50} values of 24 ± 5.6 nM and 14 ± 1.2 nM, respectively. IC_{50} values for the CQR strains Dd2 and FCB were 169 ± 3.9 nM and 166 ± 8.6 nM, respectively. Resistance to CQ could be reversed in the CQR strains by the addition of 1 μM verapamil (VP), while no significant difference was observed with VP in CQS strains ($p > 0.05$), as expected. All IC_{50} values are in good agreement with those obtained by other groups [217, 241-244]. Subsequent experiments using CQ were based on these IC_{50} values.

Table 3.1 IC_{50} values of *P. falciparum* strains used in this study

Strain	CQ (nM)	CQ + VP (nM)
3D7	24 ± 5.6	17 ± 1.2
HB3	14 ± 1.2	19 ± 1.6
Dd2	169 ± 3.9	53 ± 6.5
FCB	166 ± 8.6	41 ± 6.5

Values obtained from three independent experiments ± SEM.
CQ, chloroquine; VP, verapamil.

3.5.2 Effect of CQ on CQS and CQR parasite morphology.

Synchronized early trophozoite stages of two CQS (3D7, HB3) and CQR (Dd2, FCB) strains were examined using differential interference contrast (DIC) microscopy to observe morphological changes 1-4 h after incubation with 500 nM CQ. In CQS strains, dark, rapidly moving structures appeared in the cytosol after CQ exposure, moving freely and non-directionally within the cytosol (Figure 3.1A). Parasites with dark cytosolic structures were detected using DIC microscopy shortly after CQ exposure and the number of these cytosolic structures steadily increased until it plateaued at approx. 3 h (Figure 3.1B). In CQR strains, very few of these cytosolic structures were observed (<10% after 4 h), even after the addition of high concentrations of CQ (30x CQ IC_{50}) (Figure 3.1A, Suppl. Figure S3.6).

To determine the rate of appearance of dark cytosolic structures in CQS and CQR parasites, 3D7 and Dd2 parasites were exposed to a 20x IC_{50} CQ concentration for up to 4.5 h. 22% of 3D7 parasites had dark cytosolic structures after 1 h of CQ exposure (Figure 3.1B), increasing to 43% after 2 h, 56% after 3 h and 61% after 4 h. At this point, the appearance of dark cytosolic structures seemed to abate, and further significant increases in these parasite structures were not observed. When the CQ concentration was lowered to 2x the IC_{50} value for 3D7 parasites, these structures still appeared but the number of cytosolic structures developing over time was reduced by about half (33% ± 0.9% after 4 h).

In contrast, very few Dd2 parasites were observed with dark cytosolic structures (Figure 3.1B). Only 2% of Dd2 parasites were found to have dark cytosolic structures after 1 h exposure to 20x IC_{50} CQ concentration. This increased to 6% after 2 h, 7% after 3 h and 9% after 4 h of CQ exposure. These values did not vary greatly when using a 2x IC_{50} CQ concentration. We conclude that the appearance of cytosolic structures is a feature specific to CQS parasites.

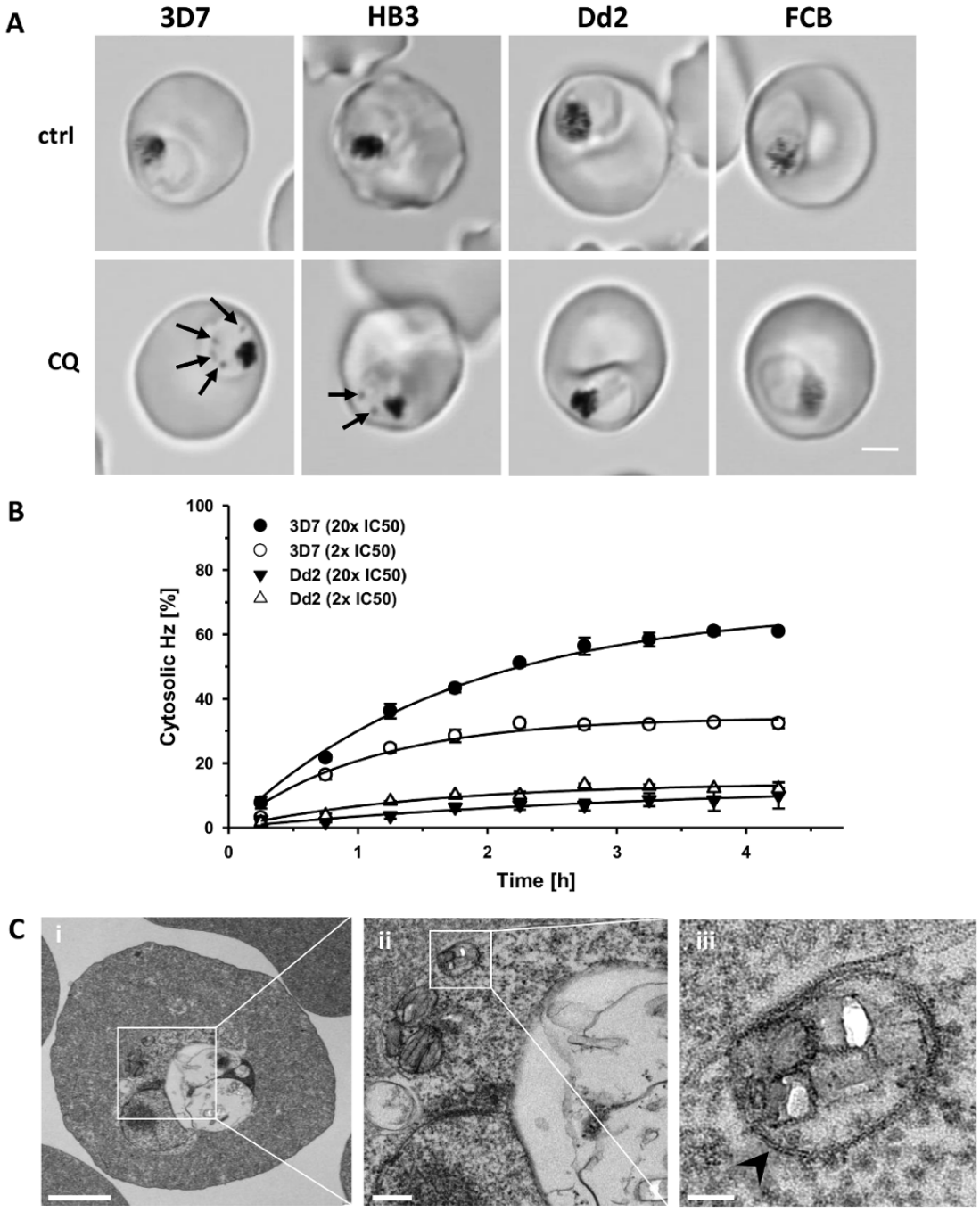

Figure 3.1 **Detection of dark cytosolic structures after CQ treatment.** Distinct dark structures appear in the cytosol of CQS *P. falciparum* parasites after CQ exposure. These structures were absent in CQR strains, even after high CQ concentration exposure. **A**, CQS (3D7, HB3) and CQR (Dd2, FCB) strains were incubated with 500 nM CQ or Ringer's solution only (control) for 3 h. Dark structures (arrows) were found in the cytosol of CQS strains. Scale bar, 2 µm. **B**, 3D7 and Dd2 parasites were incubated with various CQ concentrations and the percentage of parasites with dark cytoplasmic structures was determined at 30 min intervals. Results are from three independent experiments; total parasite numbers for 3D7, n = 4413; Dd2, n = 6135. Error bars represent SEM. **C**, electron microscopy (EM) images of Hz-containing cytoplasmic structures (15000 x magnification and digital zoom). 3D7 parasites were exposed to CQ for 3 h, fixed and prepared for EM. Hemozoin crystals were detected in a cytosolic compartment. Enlargements of the images show the intracellular localization of the structures and the surrounding membrane (arrowhead). Scale bars: i, 1 µm; ii, 200 nm; iii, 50 nm.

3.5.3 Ultrastructure analysis of CQ-exposed parasites.

To better understand the composition of the cytosolic structures, CQS and CQR parasites were prepared for electron microscopy (EM) imaging. 3D7 and Dd2 parasites were exposed to CQ for 3 h at 20x their IC_{50} concentration, or left unexposed as a control. Parasites were enriched using a Percoll gradient to allow for the structural preservation of the *P. falciparum*-infected erythrocyte. In addition, non-enriched treated and non-treated parasites were prepared to confirm that Percoll enrichment had no effect on the ultrastructure of the samples. No differences in parasite morphology due to sample preparation were observed (Suppl. Figure S3.7).

As seen in live cell imaging, multiple dark compartments were observed in the cytosol of 3D7 parasites using EM techniques (Figure 3.1C, Suppl. Figure S3.7). The EM images revealed compartments with a diameter of 150-200 nm that contained approx. 1-5 hemozoin crystals. This compartment was surrounded by a membrane bilayer, suggesting that it is an enclosed vesicular compartment. No Hz-containing compartments were observed in CQ-treated Dd2 parasites or in 3D7 and Dd2 non-treated parasites (Suppl. Figure S3.8).

3.5.4 The digestive vacuolar membranes of CQS and CQR parasites remain intact.

The disruption of the DV membrane and leakage of DV contents into the cytosol has been hypothesized to be the main contributors to parasite death after CQ treatment [245]. Therefore, we investigated if the cytosolic Hz-containing compartments were linked to the leakage of DV contents into the parasite cytosol. 3D7 and Dd2 parasites were loaded with Fluo-4 AM, a fluorophore that accumulates in the DV [159, 213] and requires the transport activity of PfMDR1 [246]. The loading of Dd2 and 3D7 parasites with Fluo-4 AM for 50 min prior to CQ exposure provided sufficient time for the fluorophore to accumulate in the DV. Since lengthy exposure time alone can lead to reduced fluorescence in the DV and increased fluorescence in the cytosol [246], leading to false interpretation of the results, the parasites used in our experiments were kept in the dark at 37°C and single images were taken every 15 min with low laser intensity (488 nm laser; 12.5 mW; 0.8% laser power). No leakage of Fluo-4 into the cytosol of non-treated parasites was shown to occur under these conditions (Figure 3.2).

To determine if high CQ concentrations damaged the integrity of the DV membrane, leading to leakage of DV content into the cytoplasm, 3D7 and Dd2 parasites were preloaded with Fluo-4 AM and exposed to 10 µM CQ for up to 4.5 h. The increase of Fluo-4 signal in the cytosol of the parasite is a good indication of DV membrane permeability. Possible leakage of Fluo-4 fluorescence into the parasite cytoplasm was monitored using confocal microscopy. No increase in cytoplasmic Fluo-4 fluorescence was seen in either CQS or CQR parasites, suggesting an intact membrane (Figure 3.2A+B, Suppl. Figure S3.9). While slight fluctuations of digestive vacuolar Fluo-4 fluorescence were seen over time for both 3D7 and Dd2 parasites exposed to CQ, these fluctuations were also observed in non-exposed parasites, suggesting that this is likely related to active transporters in the parasites and not due to DV leakage. Within the cytosol of the parasites, no increase in cytosolic Fluo-4 fluorescence indicative of DV leakage was observed during this time frame.

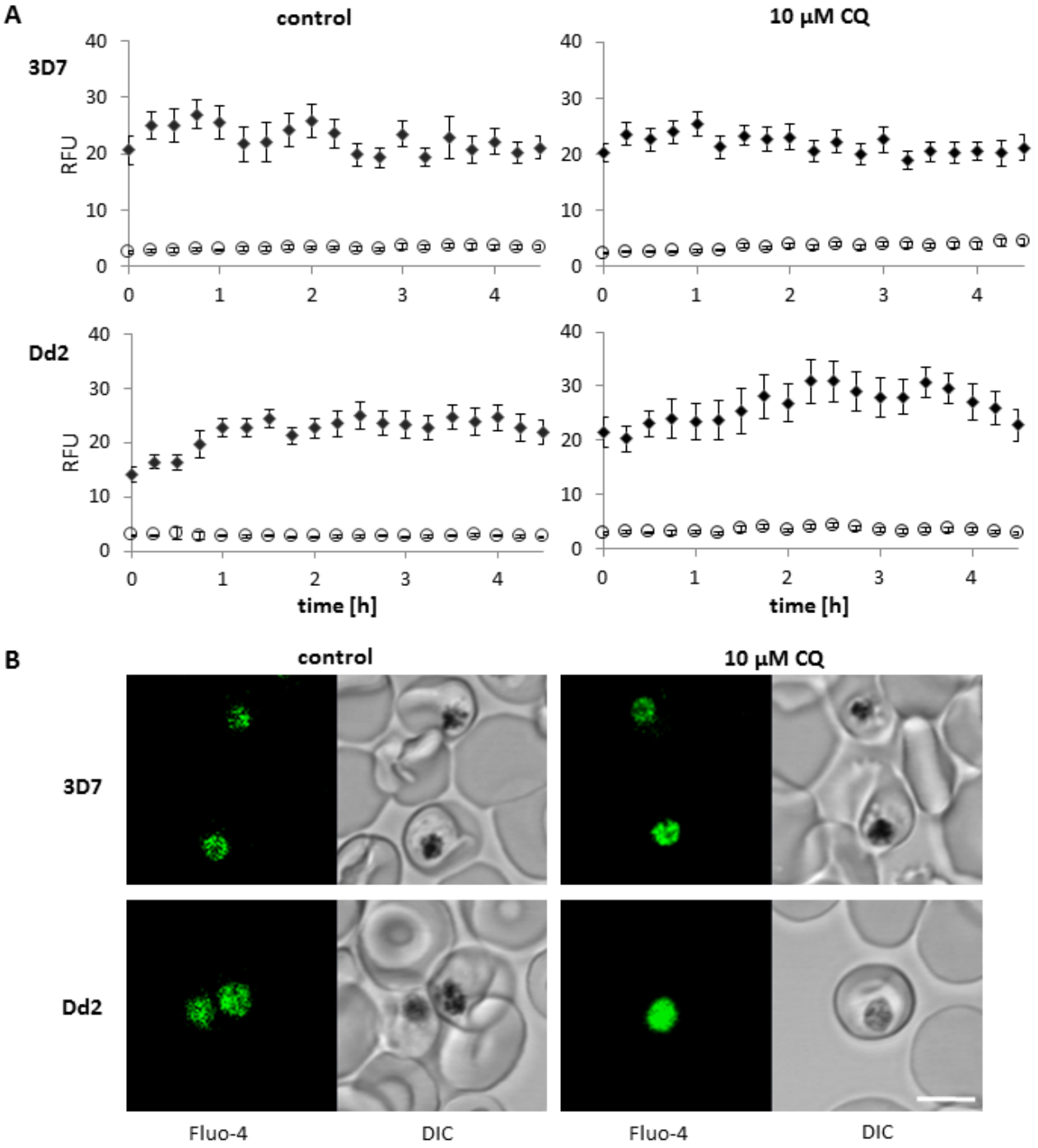

Figure 3.2 Analysis of DV membrane integrity. 3D7 and Dd2 parasites were pre-incubated with 5 µM Fluo-4 AM in Ringer's solution for 50 min and then placed in Ringer's solution only (control) or Ringer's solution containing 10 µM CQ. The same parasites were imaged in 15 min intervals. A, fluorescence intensity of Fluo-4 in the DV (diamonds) or cytosol (open circles) of the parasite. The ratio was calculated relative to background iRBC fluorescence. Results shown are from three independent experiments, total parasite numbers are: for 3D7, CQ treated n = 40, control n = 35; for Dd2, CQ treated n = 28, control n = 38. Error bars represent SEM. B, Fluo-4 fluorescence and DIC images of representative parasites are shown after 4 h CQ exposure. Scale bar, 5 µm.

3.5.5 Onset of parasite killing is delayed in CQR parasites.

Next, we investigated the time course of CQ killing in CQS and CQR parasites. 3D7 and Dd2 parasites were exposed for 1, 2, 4, 6, 24 or 48 h with their respective 10x, 20x and 30x IC_{50} concentrations of CQ, or left untreated, to provide equivalent killing rates for CQS and CQR parasites. After CQ incubation, parasites were washed with culture medium to remove CQ and placed back into culture for 48 h. To confirm that one wash step was sufficient to remove CQ from the medium, parasites from the 0 h treatment group were also incubated with their respective CQ concentration and washed immediately. No changes in parasite survival were observed in this group (Figure 3.3).

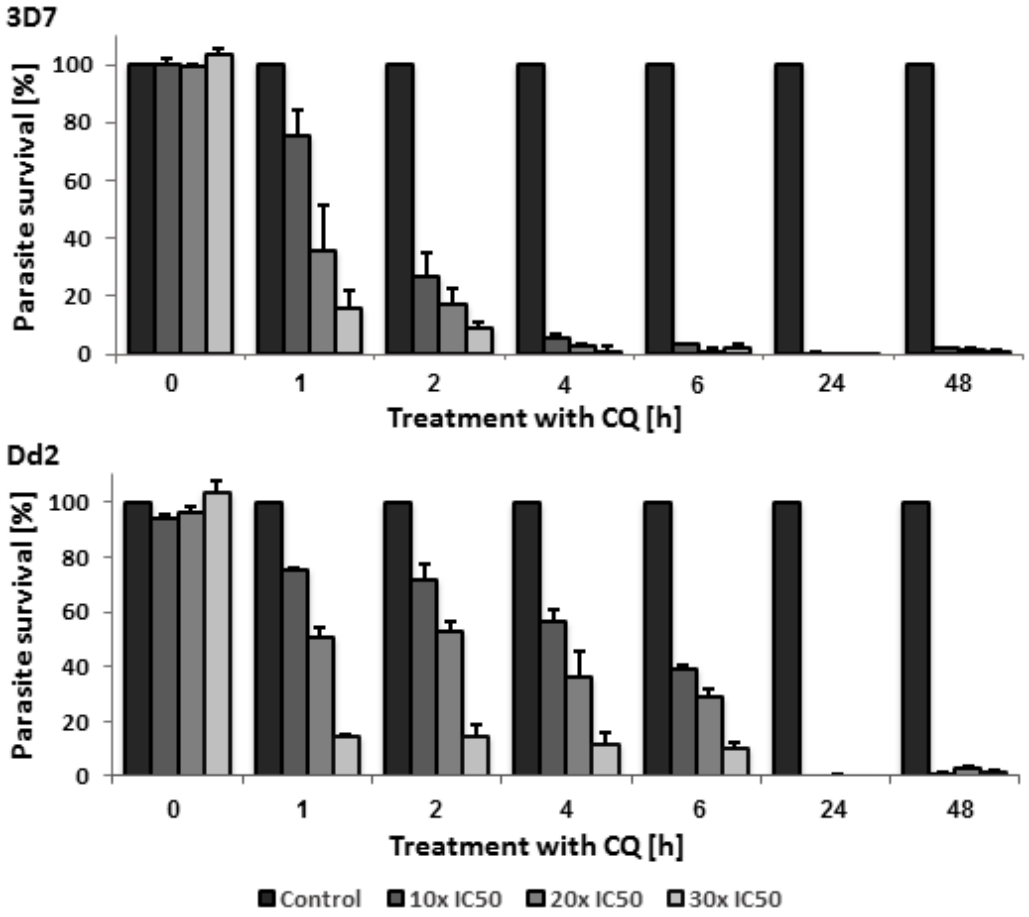

Figure 3.3 Parasite killing in CQS and CQR parasites. CQS (3D7) and CQR (Dd2) parasites were exposed to their respective 10x, 20x or 30x IC_{50} CQ concentrations for various lengths of time, or left untreated. Analysis was performed using the SYBR Green I detection assay. Percent survival relative to control was calculated for each time point. Results shown are from at least three independent experiments. Error bars represent SEM.

For all other time points, we show a decrease in parasite survival for all CQ concentrations used, albeit 3D7 killing occurred more rapidly than Dd2 killing. After 1 h of incubation, both 3D7 and Dd2 parasites showed similar survival rates for 10x IC_{50} CQ concentrations (75% vs. 76%, respectively), 20x IC_{50} CQ concentrations (36% vs. 51%, respectively), and 30x IC_{50} CQ concentrations (16% vs. 14%, respectively). At 2 h onwards, this similarity diverged, and a rapid decrease in parasite survival was observed in 3D7 parasites (<10% survived) for all CQ concentrations used. This lack of killing was only observed in Dd2 parasites after 10 h CQ exposure (Suppl. Figure S3.10). This result suggests that CQR parasites can tolerate high CQ concentrations for a longer time than CQS parasites.

3.5.6 Mitochondrial membrane potential in CQS and CQR parasites.

Apoptotic cell death is indicated by the loss of mitochondrial membrane potential (ψ_m). This has been shown in *P. falciparum*-infected erythrocytes using the fluorophore JC-1 [91, 247-249]. In the presence of a mitochondrial ψ_m, JC-1 aggregates and emits light at a longer wavelength (590 nm) compared to its monomer (530 nm). To investigate if the appearance of cytosolic Hz-containing compartments is linked to cell death, 3D7 and Dd2 parasites were incubated for 4 h in 20x IC_{50} CQ concentrations. JC-1 was added during the last 30 min of incubation and parasites were imaged using confocal microscopy. 3D7 and Dd2 parasites had a strong fluorescence signal for JC-1 aggregates at 590 nm (Figure 3.4A). In addition, an intact $\Delta\psi_m$ was also found in 3D7 parasites in the presence of cytosolic Hz-containing compartments. This result is consistent with our hypothesis that appearance of hemozoin-loaded compartments occurs prior to triggering classical cell death pathways.

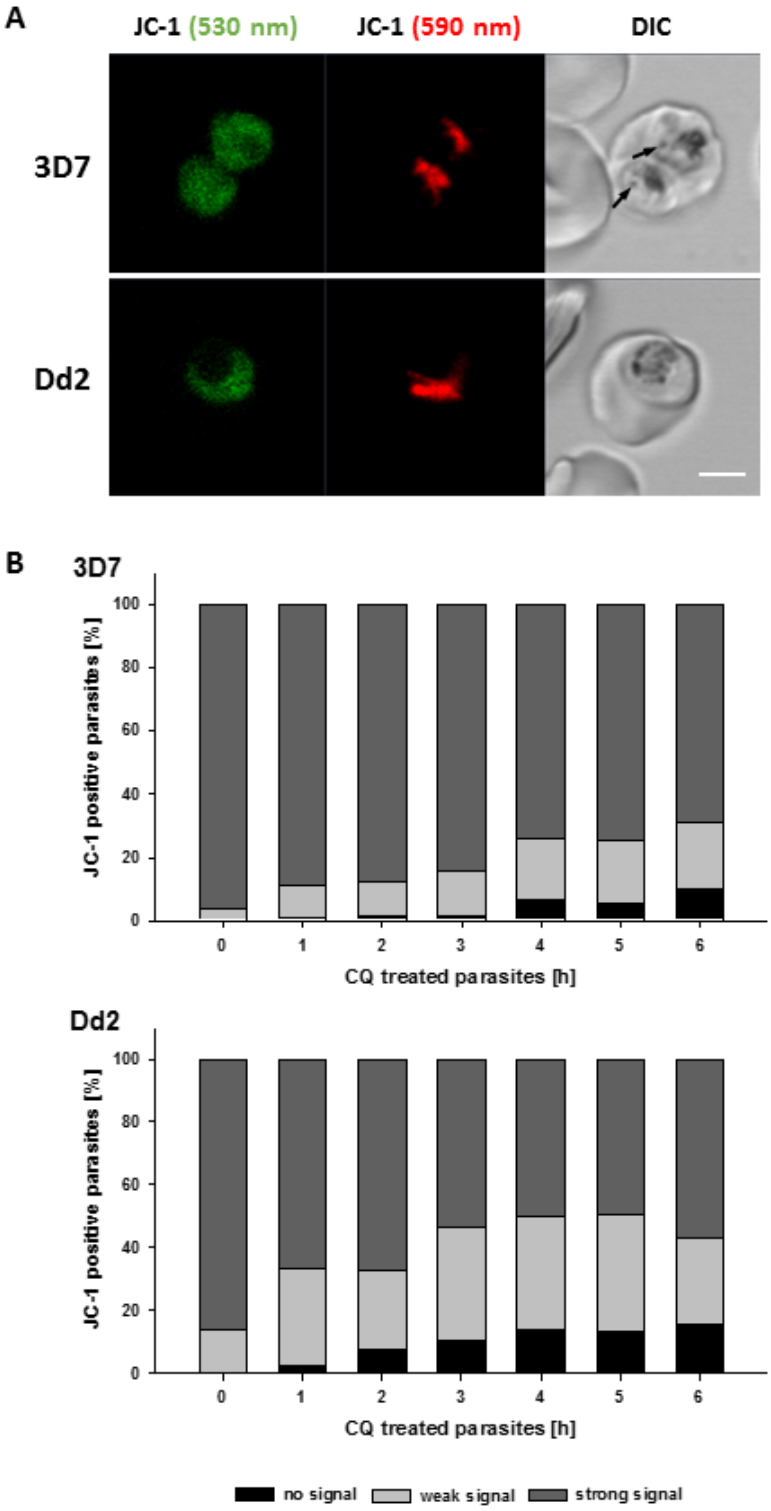

Figure 3.4 Measuring mitochondrial membrane potential after CQ treatment. A, JC-1 staining after 4 h of incubation with 20x IC_{50} CQ concentrations for 3D7 and Dd2 showed an intact mitochondrial membrane potential for both strains even when Hz-containing structures (arrows) were detected in the cytosol of 3D7 parasites. Scale bar, 5 µm. **B**, CQS 3D7 parasites and CQR Dd2 parasites were exposed to their respective 20x IC_{50} CQ concentrations. The percentage of parasites with strong (indicating an intact membrane potential), weak or no JC-1 fluorescence at 590 nm was analyzed. 3D7, n = 1939; Dd2, n = 2297.

3D7 and Dd2 parasites were also incubated with their respective 20x IC_{50} CQ concentrations for up to 6 h and the loss of mitochondrial ψ_m was monitored (Figure 3.4B). 3D7 parasites showed almost no loss of $\Delta\psi_m$ after 3 h of CQ treatment (98.3% ± 0.5% JC-1 positive parasites), which was slightly reduced to 93.5% ± 3.0% after 4 h of CQ treatment. CQ incubation of 3D7 parasites for 6 h led to further decrease of JC-1 positive parasites to 89.9% ± 2.6%. Considering that more than 90% of 3D7 parasites have an intact $\Delta\psi_m$ during the first 4 h of CQ treatment, a time point where more than 60% of the parasites had cytosolic Hz-containing compartments, these compartments appear to have formed before loss of $\Delta\psi_m$ is initiated.

Loss of $\Delta\psi_m$ was also detected in some Dd2 parasites after exposure to 20x IC_{50} CQ concentrations (Figure 3.4B). After 2 h, 92.3% ± 2.4% of Dd2 parasites had an intact $\Delta\psi_m$. This was decreased to 85.9% ± 4.8% after 4 h and to 84.3% ± 3.4% after 6 h of CQ incubation. Although a few more Dd2 parasites showed a loss of ψ_m compared to 3D7, both strains still had a high percentage of parasites with an intact $\Delta\psi_m$, providing further evidence that the loss of $\Delta\psi_m$ does not occur at an early stage after CQ exposure.

3.5.7 Origin of hemozoin-containing compartments.

To address the source of the Hz-containing compartments, we used the fluorescent substrate Fluo-4 AM that accumulates in the DV [159, 213]. CQS 3D7 parasites were initially loaded with 5 µM Fluo-4 AM for 50 - 60 min. The parasites were then washed twice to remove excess substrate and left untreated, or incubated with 500 nM CQ for 2 h, allowing ample time for the formation of Hz-containing compartments. If these compartments originate from the DV, we hypothesize that they will contain the fluorescent substrate. Indeed, live cell imaging of the parasites showed fluorescently stained compartments containing hemozoin in the cytosol of 3D7 parasites after CQ exposure but not in control parasites (Figure 3.5). These data strongly suggest that the Hz-containing compartments are derived from the DV.

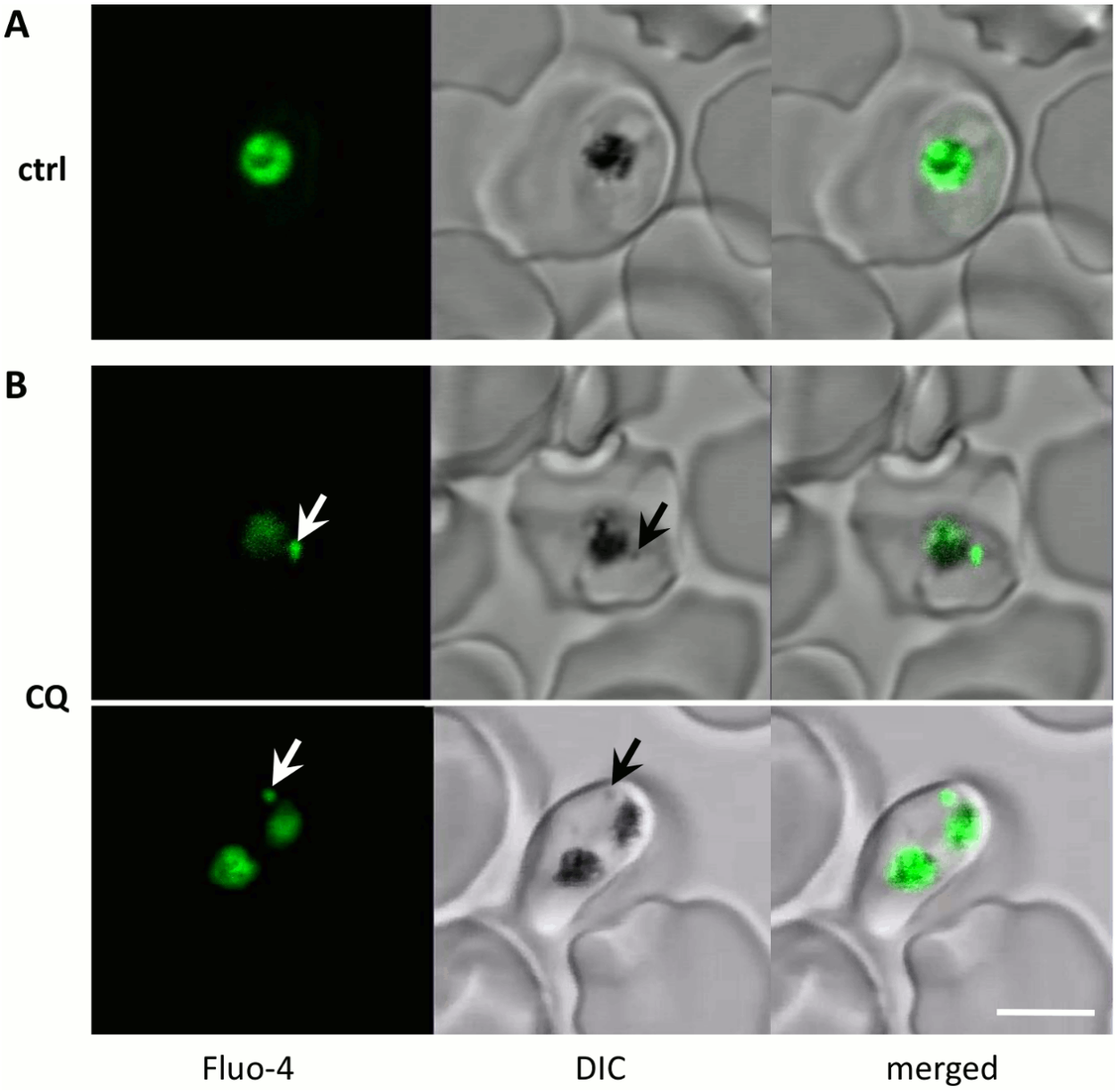

Figure 3.5 Origin of hemozoin-containing compartments. 3D7 parasites were loaded with 5 µM Fluo-4 AM for 50 - 60 min, then washed and left untreated (**A**), or incubated with 500 nM CQ for 2 h (**B**). Fluo-4 remained trapped in the DV of unexposed parasites for the duration of the experiment. CQ-treated parasites showed co-localization of the DV-derived Fluo-4 staining (white arrows) with cytoplasmic hemozoin (black arrows). Scale bars, 5 µM.

3.6 Discussion

We investigated responses of CQS and CQR parasites exposed to therapeutically relevant concentrations of CQ. Whole blood CQ concentrations of ≥500 nM are commonly attained in adults during prophylactic intake of 310 mg of CQ base/week [250]. While whole blood CQ concentrations of ≥100 nM are sufficient for clearance of *P. malariae* and *P. ovale* infections, a study revealed that more than 62% of Nigerian children with whole blood CQ concentrations of ≥500 nM were still harboring *P. falciparum* parasites [251].

We observed the appearance of Hz-containing compartments during CQ exposure in the cytosol of CQS parasites (exposed to 250 – 750 nM CQ) but not in CQR parasites (exposed to 1.7 – 5.1 µM CQ). This difference may be an indicator for an altered short-term drug response in drug-sensitive versus -resistant parasites. The cytosolic compartments in CQS parasites were readily visible with live cell imaging using differential interference contrast (DIC) microscopy. Giemsa-stained preparations could not resolve these structures, since the deep purple color of the staining solution did not provide sufficient contrast in the parasite cytosol to detect the small dark structures. When the samples were methanol-fixed but left unstained after CQ treatment, dark cytosolic structures were readily visible (Suppl. Figure S3.11).

To obtain more insight into the morphology of the dark cytosolic structures, EM was applied to CQ-treated and –untreated 3D7 and Dd2 parasites. The appearance of compartmentalized hemozoin crystals correlated with the dark structures observed in DIC images. To confirm that the Hz-containing compartments were not caused by Percoll enrichment of the parasites, non-enriched parasites were also examined. Hz-containing cytosolic compartments were detected in CQ-treated 3D7 parasites using both sample preparation techniques, indicating that parasite enrichment had no influence on the ultrastructure of the parasites.

Recent studies have suggested a model in which leakage of DV contents into the parasite cytosol is the causative agent of programmed cell death (PCD) [91, 245]. This was concluded from an experiment in which the fluorescent dye Fluo-4 was used to measure Ca^{2+} redistribution in CQ-treated versus non-treated 3D7 parasites. Although Fluo-4 is a widely accepted free Ca^{2+} indicator in eukaryotic cells [252-255], it cannot be used as a Ca^{2+} indicator in *P. falciparum* since it is actively

transported into the DV of the parasite by PfMDR1 [159, 246]. The sudden leakage of Fluo-4 from the DV into the cytosol described in [245] may have occurred due to phototoxicity of the dye, which has previously been reported [246]. Our experimental setup for live cell imaging was carefully monitored to assure reduced phototoxic effects when using the Fluo-4 fluorophore. To allow sufficient time for Fluo-4 transport into the DV, we loaded CQS and CQR parasites with Fluo-4 AM 50 min prior to CQ exposure. In addition, short exposure times and long recovery periods (15 min intervals) were used to reduce phototoxicity effects. No sudden redistribution of Fluo-4 from the DV into the cytosol was observed in either CQS or CQR parasites during the 4 h CQ treatment. Furthermore, high Fluo-4 accumulation in the DV was observed in parasites in the presence of dark cytosolic structures. This supports our hypothesis that Hz-containing compartments are not formed by leakage of DV contents into the cytosol. In addition, these results suggest that the cytosolic Hz-containing compartments are not part of a multilobular DV.

Delayed parasite killing in CQR parasites was shown by incubating trophozoite stage parasites with CQ for various lengths of time. Even when exposed to CQ concentrations corresponding to equivalent IC_{50} values, CQR parasites were viable longer than CQS parasites. It has been suggested that equal intraparasitic CQ concentrations alone are not sufficient to kill CQR parasites compared to CQS parasites [4]. Our results confirm a possible regulatory mechanism found in CQR parasites that allows CQ to be less toxic for these parasites. We propose that CQR parasites not only regulate intracellular CQ levels and reduce CQ concentrations in the DV but may also delay the initiation and progression of cell death.

It is still not fully understood how exposure to CQ leads to parasite killing, nor is anything known about differences in the cascade of events that may exist between CQS and CQR parasites. Furthermore, little is known about the regulation of cytosolic mediators that stabilize essential cellular pathways, which may also play a role in CQ resistance. To our knowledge, few papers have addressed cell death features after CQ exposure in *P. falciparum* [91, 125, 245, 256]. A major impediment is the lack of molecular tools available to study cell death in malaria parasites, e.g. *P. falciparum*-specific antibodies against regulatory proteins to such as caspase-3 to show the initiation of PCD. Another difficulty is the absence of typical apoptosis markers in the malaria genome, such as Apaf-1, Bax or other Bcl-2 proteins [91, 128, 257-259]. While other cell death

related features of CQ-exposed parasites have been described using EM images [48, 125, 245], there was no indication of the appearance of Hz-filled compartments within the cytosol of CQS parasites. Discovery of a novel feature that distinguishes CQS and CQR parasites may unravel new targets for drug development to reverse or circumvent CQ resistance.

A distinct characteristic of classical apoptosis is the activation of caspases and subsequent loss of mitochondrial membrane potential [91, 260]. We used the well described mitochondrial membrane potential probe JC-1 to monitor this parameter. Even though 4 h of exposure to CQ resulted in irreversible cell death in >95% of CQS parasites, no considerable reduction of $\Delta\psi_m$ was observed. Furthermore, no loss of $\Delta\psi_m$ was detected in parasites with cytosolic Hz-containing compartments. This is consistent with the findings of Ch'ng and coworkers, who reported only a slight reduction of JC-1 positive parasites after 4 h CQ exposure but more loss during longer incubations [91]. This would suggest that the appearance of cytosolic Hz-containing compartments observed in our study occurs prior to classical apoptosis events, opening the door for in-depth research of cellular mechanisms in malaria parasites that seem to be initiated after CQ exposure but occur prior to cell death cascade activation.

The specific accumulation of Fluo-4 in the DV allowed us to investigate whether the Hz-containing compartments are DV-derived. We used the fluorescent substrate Fluo-4 AM, which is actively transported into the DV by PfMDR1 [213] where it gets trapped and accumulates. Loading of CQS 3D7 parasites with Fluo-4 AM for 1 h allowed sufficient time for Fluo-4 to accumulate in the DV. Subsequent wash steps removed excess Fluo-4 from the culture before parasites were exposed to CQ. Thus, fluorescent staining of Hz-containing compartments can only occur if the compartments form at the DV and take up digestive vacuolar contents, including Fluo-4. Our results demonstrate colocalization of Fluo-4 fluorescence with dark cytosolic structures, suggesting that these structures arise from the DV.

Parasite resistance to CQ appears to be a complex biological mechanism that may not be attributed to one mutation alone. Discovery of the PfCRT K76T mutation [2, 94] has set a milestone to unraveling CQ resistance. However, studies have revealed that mutant *pfcrt* does not seem to be sufficient to confer CQR in all genetic backgrounds [243], and CQR must be determined by gene

loci other than *pfcrt* and *pfmdr1* [98]. Furthermore, it has been shown that reduced CQ concentrations in the DV are not necessarily linked to CQR [4]. Additionally, higher intracellular CQ concentrations were required to kill CQR parasites when compared to CQS parasites [3, 4], suggesting an intracellular effector as the mechanism of resistance. Other researchers have proposed that a cytosolic target for CQ may be a possible source for chloroquine's antimalarial mode of action [21]. Our results endorse the hypothesis of an existing intracellular resistance mechanism in addition to the PfCRT K76T mutation.

In conclusion, we have shown the appearance of hemozoin structures in the cytosol of CQS but not CQR parasites upon the addition of CQ. Further studies are underway to elucidate the role of cytosolic Hz-containing compartments in CQS parasites after CQ exposure and their absence in CQR parasite strains. Understanding programmed cell death in *Plasmodium* and obtaining insight into how CQR parasites maintain homeostasis even under drug pressure could reveal a unique mechanism in CQR parasites that could be exploited to reverse CQ resistance, opening new possibilities to overcome treatment failure in CQR parasites.

3.7 Chapter-related Acknowledgements

This study was supported in part by fellowships from the German Academic exchange Service (DAAD) (SJR) and the Centre for Host-Parasite Interaction (FRQNT) (SJR), and grants from the Natural Sciences and Engineering Research Council (NSERC) Discovery Grant (PR) and the Canada Foundation for Innovation (CFI) Leaders Opportunity Fund (PR). We thank Dr. Nina Simon (Institute of Medical Biotechnology, Friedrich-Alexander University of Erlangen-Nuremberg) for help with parasite cultures and Drs. Barbara Kappes and Oliver Friedrich (Institute of Medical Biotechnology, Friedrich-Alexander University of Erlangen-Nuremberg) for their comments. Very special thanks to Dr. Timothy G. Geary (Institute of Parasitology, McGill University) for fruitful discussions and reviewing the manuscript.

3.8 Chapter-related Supporting Information

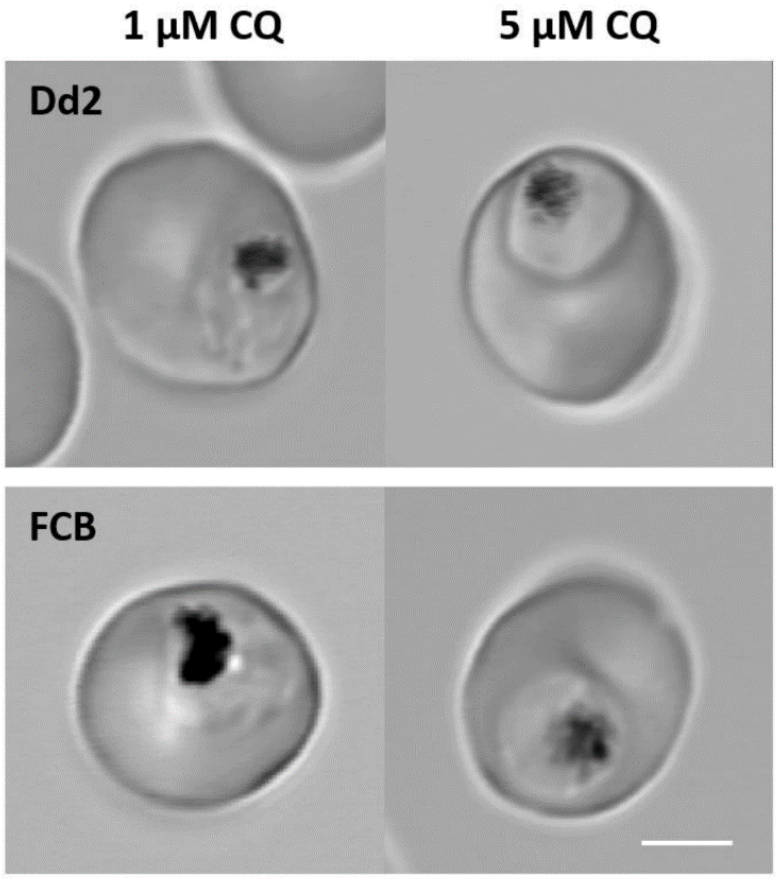

Suppl. Figure S3.6 No formation of cytosolic Hz-containing compartments in CQR parasites. CQR parasite strains Dd2 and FCB were exposed to 1 µM or 5 µM CQ for 4 h. No cytosolic Hz-containing compartments were observed. Scale bar, 5 µm. Experiments were done in triplicate on independent days.

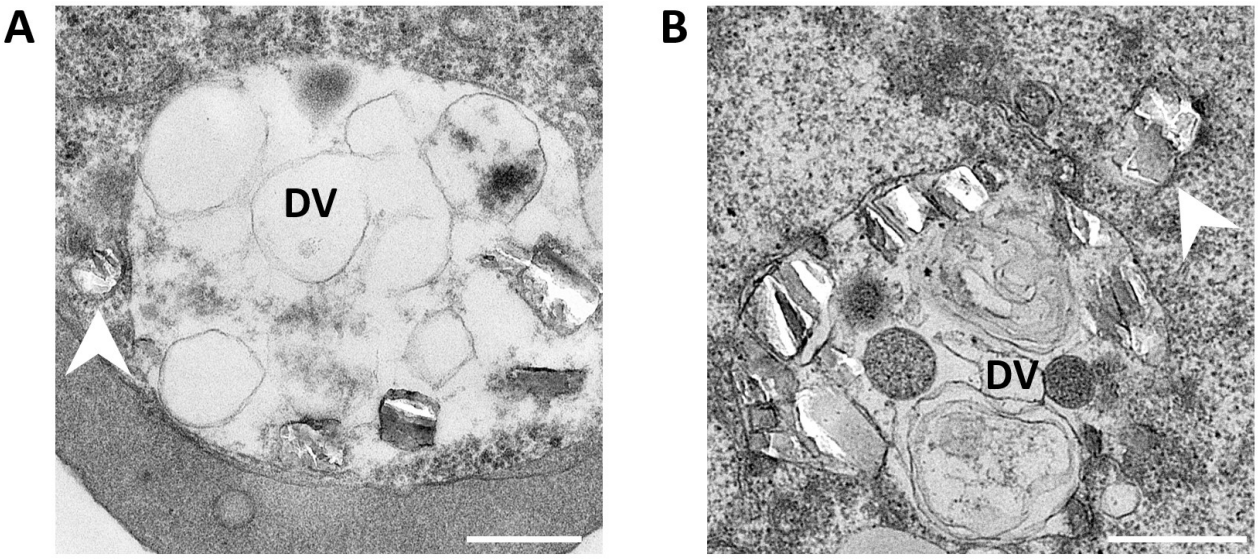

Suppl. Figure S3.7 No differences in sample preparation for EM imaging were observed. 3D7 parasites were incubated with 500 nM CQ for 3 h and then either left non-enriched (**A**) or enriched using a Percoll gradient (**B**). Hz-containing compartments (white arrowheads) were detected in the parasite cytosol for both preparation techniques. DV, digestive vacuole. Scale bar, 500 nm.

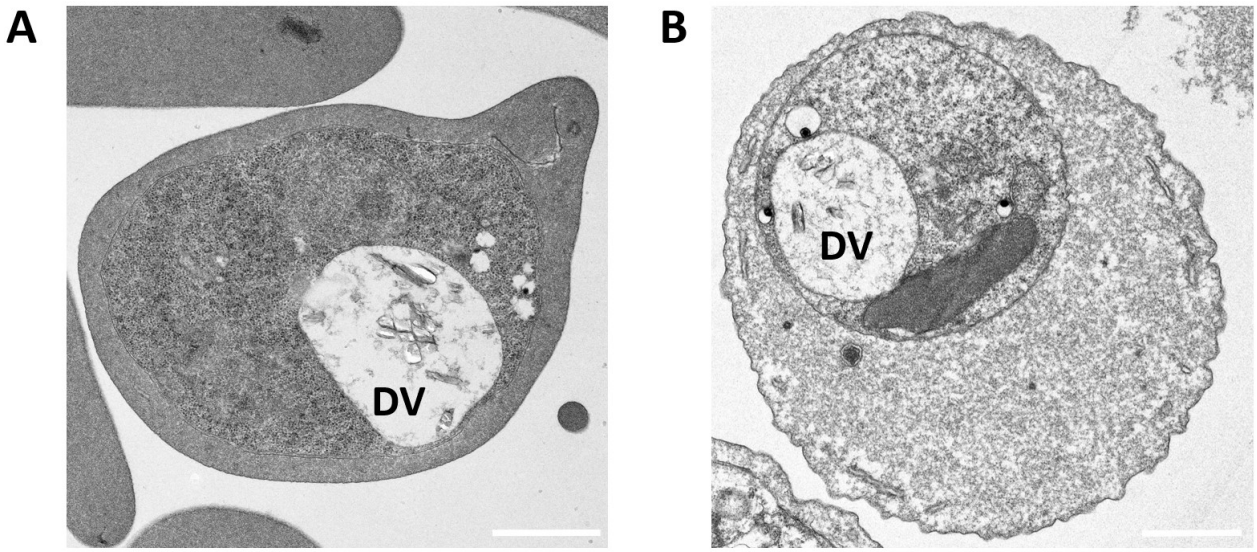

Suppl. Figure S3.8 No cytosolic Hz-containing compartments were observed in untreated parasites. 3D7 (**A**) and Dd2 (**B**) parasites were prepared for EM without CQ exposure (controls). DV, digestive vacuole. Scale bar, 1 µM.

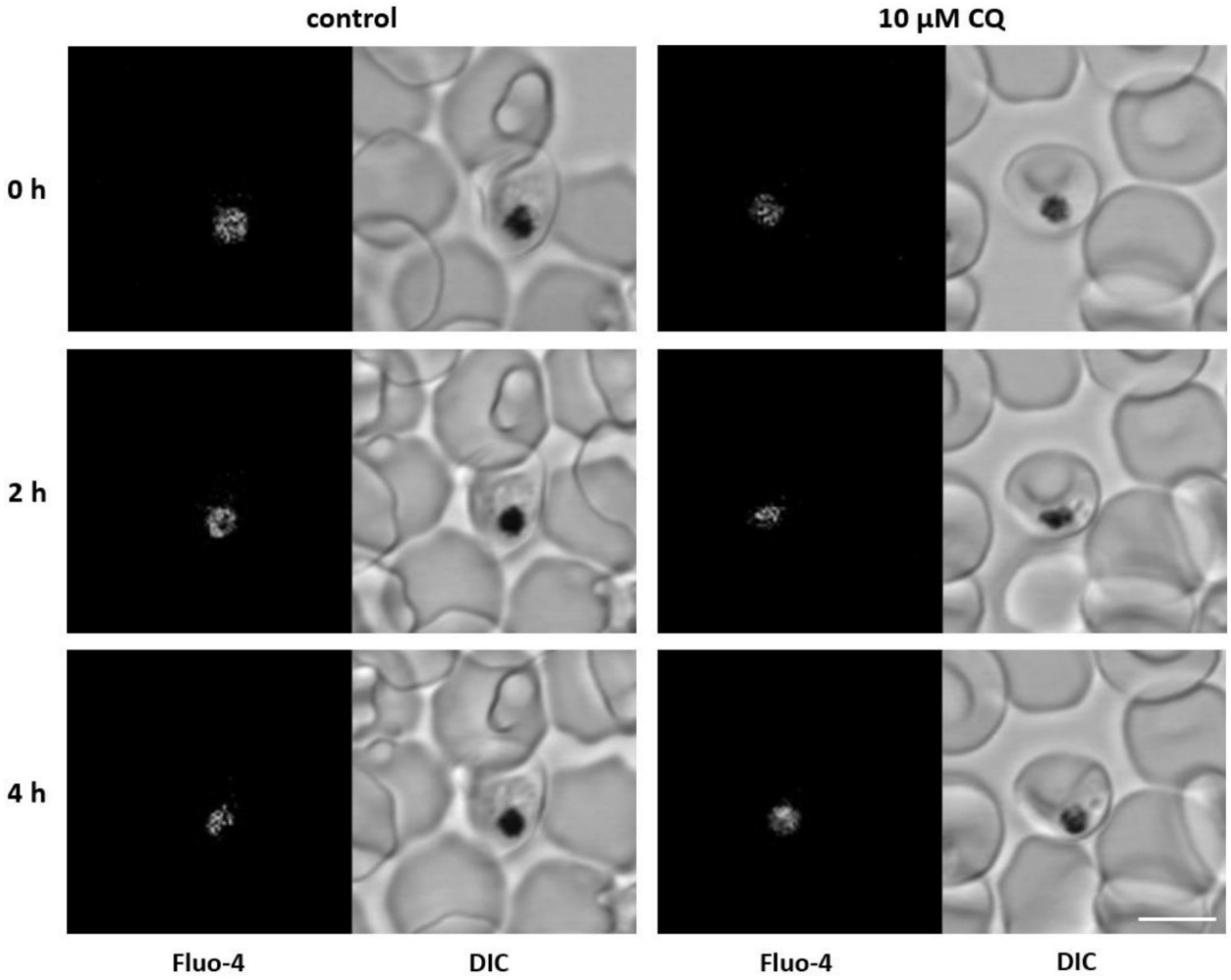

Suppl. Figure S3.9 No leakage of Fluo-4 into the cytosol within 4 h of CQ exposure. CQS 3D7 parasites were pre-incubated with 5 µM Fluo-4 AM in Ringer's solution for 50 min, then solution was replaced with Ringer's only (control) or Ringer's containing 10 µM CQ. The same parasites were imaged in 2 h intervals. No leakage of Fluo-4 into the parasite cytosol could be observed. Results are shown from three independent experiments. Scale bar, 5 µm.

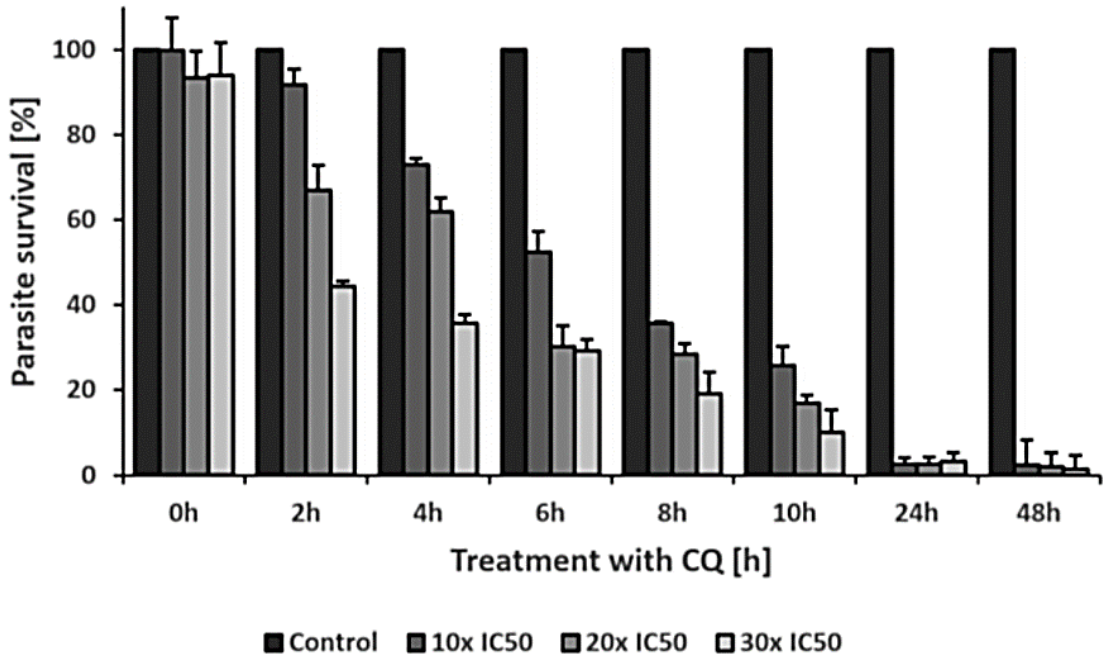

Suppl. Figure S3.10 Determining the onset of irreversible cell damage. CQR Dd2 parasites were exposed to their 10x, 20x or 30x IC_{50} CQ concentrations for the time indicated, or left untreated. Analysis was performed using the SYBR Green I detection assay. Percentage of survival relative to the control was calculated for each time point. Results are shown from three independent experiments. Error bars represent SEM.

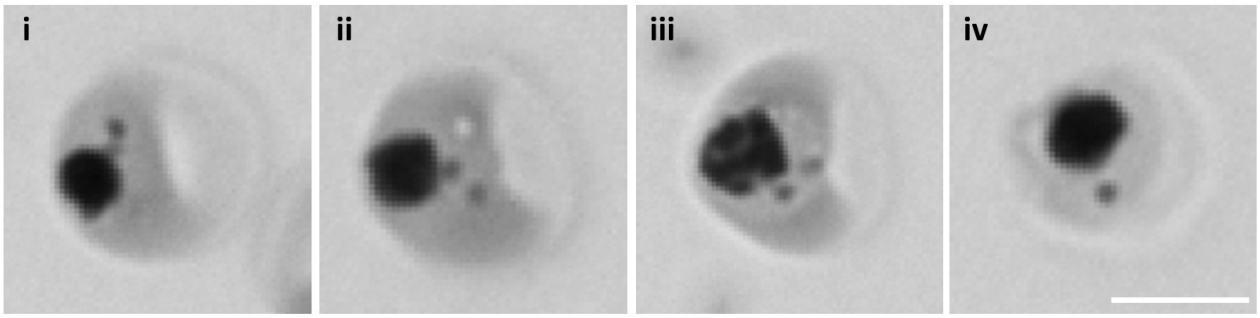

Suppl. Figure S3.11 Hz-containing cytosolic compartments are visible in methanol-fixed unstained parasites. 3D7 parasites were incubated with 500 nM CQ for 3 h and then fixed with methanol. Dark-stained Hz-containing compartments were easily observed in the parasite cytosol. i-iv, representative images. Scale bar, 5 µM.

Connecting Statement II

In the previous chapter, a novel phenotype was described for CQ-exposed sensitive *P. falciparum* strains that was absent in resistant strains. The formation of hemozoin-containing compartments in the cytosol of CQ-sensitive strains prior to rupture of the digestive vacuolar membrane and subsequent leakage of free hemozoin crystals into the cytosol indicates the presence of regulatory mechanisms that must play a role.

In the following chapter, a commercially available fluorescent tagged CQ analogue, LynxTag™-CQ_{GREEN} (CQ_{GREEN}), was investigated for its suitability for live cell imaging of intact *P. falciparum*–infected red blood cells. To date, only one study was published on CQ_{GREEN} and its effects on a *Plasmodium* protein [92]. This study focused on CQ_{GREEN} transport through PfCRT variants in microsomes derived from a yeast expression system. Therefore, a detailed analysis of CQ_{GREEN} and its intracellular localization in intact *P. falciparum*-infected RBCs will be described here.

— Chapter 4 —

Manuscript III

Fluorescently tagged chloroquine accumulates in the *Plasmodium falciparum* cytosol

S.J. Reiling[1] and P. Rohrbach[1]

[1] Institute of Parasitology, McGill University, Ste. Anne de Bellevue (Montreal), Quebec, Canada

4.1 Abstract

Background: Chloroquine (CQ) was the drug of choice for decades in the treatment of falciparum malaria until resistance emerged. CQ is suggested to accumulate in the parasite's digestive vacuole (DV), where it unfolds its antimalarial properties. However, discrepancies were observed between CQ accumulation in CQ-sensitive (CQS) and CQ-resistant (CQR) strains. Analysis of CQ transport and intracellular localization using a fluorescently tagged analogue could provide much needed information to distinguish susceptible from resistant parasite strains. Such a fluorescent tagged CQ analogue is commercially available and was assessed for its suitability.

Methods: IC_{50} values were determined for both CQ and LynxTag-CQ™$_{GREEN}$ (CQ_{GREEN}) in two CQ-sensitive and two CQ-resistant *P. falciparum* strains. Buffer solutions with varying pH were used to determine pH-dependent localization of CQ_{GREEN} in infected red blood cells. Furthermore, parasites were loaded with various concentrations of CQ_{GREEN} for up to 7 hours. Intracellular accumulation was investigated using live cell confocal microscopy. CQ_{GREEN} uptake rates were determined for the cytosol and DV in the presence or absence of verapamil.

Results: In CQS strains, twofold higher IC_{50} values were determined for CQ_{GREEN} compared to unmodified CQ. No significant differences in IC_{50} values were observed for these drugs in CQR strains. Live cell imaging revealed that CQ_{GREEN} accumulated in the cytosol but not in the DV of most parasites, independent of the concentration used. Longer incubation periods for up to 7 hours did not influence intracellular localization of CQ_{GREEN}. Nevertheless, CQ_{GREEN} uptake rates in CQR strains were reduced by 50% compared to CQS strains.

Conclusion: Accumulation of CQ_{GREEN} was mainly seen in the cytosol of parasites. However, IC_{50} assays showed similar efficacy of CQ_{GREEN} and CQ in parasite killing of CQS and CQR strains. Reduced uptake rates of CQ_{GREEN} in CQR strains compared to CQS strains indicate parasite-specific responses to CQ_{GREEN} exposure. The relevance of CQ_{GREEN} as a molecular tool to study CQ resistance in *P. falciparum* remains to be determined.

4.2 Introduction

For decades, chloroquine (CQ) was the safest, most affordable and effective drug against malaria, saving the lives of millions of people until resistance emerged [210]. To date, its mode of action is still not fully understood. To effectively use CQ as an antimalarial treatment in areas where CQ resistance has been reported, it is imperative to gain more insight into its mechanism of action. Some properties of CQ make it difficult to obtain valuable information. Its small size and uncharged form at neutral pH make it difficult to use for molecular biological experiments to determine its accumulation in intracellular compartments or its affinity to other proteins.

CQ transport studies have mainly been performed using radiolabeled CQ [102, 261, 262]. The great advantage of this method is that the intrinsic properties of CQ remain unaltered. On the other hand, it is not possible to study intracellular distribution and trafficking of radiolabeled CQ in intact parasites. Therefore, fluorescently labeled CQ analogues present a new tool to evaluate intracellular activity of this drug. Two fluorescently labeled CQ analogues are commercially available: LynxTag-CQ$^{TM}_{BLUE}$ and LynxTag-CQ$^{TM}_{GREEN}$ (BioLynx Technologies, Singapore). While CQ_{BLUE} was mainly found to be fluorescent in the parasite cytosol [91, 245, 263], only one study has been published with CQ_{GREEN}, showing its accumulation in the DV of CQ-sensitive (CQS) *P. falciparum* parasites and yeast-derived microsomes expressing the *P. falciparum* chloroquine resistance transporter (PfCRT) [92].

For this study, we compared CQ_{GREEN} with unmodified CQ and investigated whether the fluorescently tagged CQ analogue can be used to obtain insight into intracellular CQ trafficking and localization. A better knowledge of the differences in CQ accumulation, distribution, uptake and efflux between CQS and CQ-resistant (CQR) strains is imperative to understand drug resistance. Our findings show that, although CQ and CQ_{GREEN} have similar parasite killing, discrepancies were seen between CQ_{GREEN} and unmodified CQ in their expected intracellular localization. Accumulation of CQ_{GREEN} was mainly seen in the cytosol of CQS and CQR strains. Our findings suggest that affinity of CQ, or its analogues, to cytosolic molecules are underestimated.

4.3 Material and Methods

4.3.1 Parasite strains and culture conditions

Two CQS (3D7, HB3) and two CQR (FCB, Dd2) strains were used for all experiments. Parasites were cultured continuously, as described by Trager and Jensen [215], with modifications. Briefly, parasites at 5% hematocrit were propagated in culture medium containing RPMI 1640 (Life Technologies, Burlington, ON, Canada) supplemented with 25 mM HEPES, 2 mM L-glutamine, gentamicin (20 µg/ml) (Life Technologies, Burlington, ON, Canada), 100 µM hypoxanthine (Sigma-Aldrich, Oakville, ON, Canada), 0.5% AlbuMAX I (Life Technologies, Burlington, ON, Canada). Parasites were maintained at 37°C with an atmosphere of 5% CO_2, 3% O_2 and 92% N_2. A^+ RBCs were obtained from the Interstate Blood Bank (Memphis, TN, USA). Giemsa-stained blood smears were prepared daily to monitor parasite growth. For synchronization, parasites were treated with 5% D-sorbitol (BioShop Canada, Burlington, ON, Canada) for 10 min at 37°C; sorbitol was removed and parasites were washed once before adding them back into culture.

4.3.2 Growth inhibition assays

Growth inhibition assays were performed as described previously [217, 264], with modifications. Cultures of 0.5% parasitemia and 2% hematocrit were incubated in 100 µl culture medium per well in a 96-well plate assay. CQ was obtained from Sigma-Aldrich Canada (Oakville, ON, Canada) and dissolved in dH_2O. CQ_{GREEN} was obtained from BioLynx Technologies, Singapore. A drug dilution series of 1:3 was prepared, starting with 1 µM as highest substrate concentration. Plates were incubated at 37°C, 5% CO_2 and 3% O_2 for 72h, then frozen and stored at -80°C.

Readouts of the assay were performed using the SYBR Green I detection method. For this, plates were thawed at room temperature and 100 µl 2x lysis buffer (20 mM Tris pH 7.5, 5 mM EDTA, 0.008% saponin, 0.08% Triton X-100, 0.2 µl SYBR Green I/ml) was added to each well. Plates were incubated in the dark for at least 1 hour. Fluorescence intensity was determined using a Synergy H4 plate reader (Fisher Scientific, Nepean, ON, Canada) with 485 nm excitation and 520 nm emission wavelengths. IC_{50} values were determined by fitting concentration response curves with

a custom made procedure for IGOR Pro 6.2 based on a R script kindly provided by Le Nagard and used as described [218, 219].

4.3.3 Fluorescence of CQ_{GREEN} at varying pH

To determine if fluorescence intensity of CQ_{GREEN} is altered at varying pH, buffer solutions (122.5 mM NaCl, 5.4 mM KCl, 1.2 mM $CaCl_2$, 0.8 mM $MgCl_2$, 11 mM D-glucose) were prepared ranging from pH 5.0 – 8.0. Buffer solutions contained 10 mM HEPES for pH 7.0 - 8.0 or 10 mM MES for pH 5.0 - 6.5. In a 96-well plate, 100 µl buffer solutions of varying pH containing 1 µM CQ_{GREEN} were prepared in triplicate. Fluorescence intensity was measured at 37°C using the Synergy H4 fluorimeter (Bio-Tek, Winooski, VT, USA). Excitation spectra ranging from 400-520 nm were used with fixed emission at 540 nm, and emission spectra ranging from 500-630 nm were measured with fixed excitation at 488 nm. Quantification was done using Microsoft® Excel® 2013.

4.3.4 Live cell imaging

Intracellular CQ_{GREEN} accumulation at different concentration and pH was analyzed in intact parasitized RBCs. For this, 3D7 trophozoite stage parasites were incubated for 30 min at 37°C with 25, 50, 500 nM or 2.5 µM CQ_{GREEN} in Ringer's solution with pH 7.4 or buffer solutions with pH 7.2 or 5.2. Images were taken using a 488 nm argon laser (12.5 mW, 0.8%) on a Zeiss LSM 710 confocal microscope (Carl Zeiss, Oberkochen, Germany) equipped with a water-corrected objective (C-apochromat 63x/1.20 W Korr M27). Emission range was set to 500-600 nm. Localization of CQ_{GREEN} within the parasite under various pH conditions was determined using the ZEN 2010 software (Carl Zeiss MicroImaging, Oberkochen, Germany).

For long-term incubation with CQ_{GREEN}, early trophozoite stage 3D7 parasites were incubated with 100 nM, 300 nM and 500 nM CQ_{GREEN} for 7 h in culture medium at 37°C, 3% O_2, 5% CO_2. Parasites were then transferred onto a microscope chamber and imaged using a Zeiss LSM 710 confocal microscope (Carl Zeiss, Oberkochen, Germany), a 63x water corrected objective (C-apochromat

63x/1.20 W Korr M27) and a 488 nm laser (12.5 mW, 0.8%). Emission range was set to 500-600 nm. A constant temperature of 37°C was maintained during the measurements using a stage-top incubator (Tokai Hit, Shizuoka-ken, Japan). Images were analyzed with the ZEN 2010 software (Carl Zeiss MicroImaging, Oberkochen, Germany).

To analyze CQ_{GREEN} uptake of CQS and CQR strains, synchronized trophozoite stage parasites were washed in Ringer's solution and transferred onto a microscope chamber. Parasites were allowed to settle for 5 min, then the solution was aspirated and replaced with new Ringer's solution containing 500 nM CQ_{GREEN}. If verapamil (VP) (Life Technologies, Burlington, ON, Canada) was added, parasites were pre-incubated with 1 µM VP for 15 min at 37°C, then transferred onto a microscope chamber. For the time lapse measurement, 500 nM CQ_{GREEN} were added to the Ringer's solution with or without 1 µM VP. Images were taken every 3 seconds for a time span of 500 seconds using a Zeiss LSM 710 confocal microscope (Carl Zeiss, Oberkochen, Germany) and a 63x water corrected objective (C-apochromat 63x/1.20 W Korr M27). Excitation was done using a 488 nm laser (12.5 mW, 0.8%), and an emission range from 500-600 nm. Regions of interest (ROI) were set for the parasite cytosol, DV, infected RBC cytosol and uninfected RBC. Fluorescence of ROIs was determined for each time point using ImageJ 1.47q (National Institutes of Health, USA). Uptake rates were calculated for the cytosol and DV during the saturation phase and analyzed using IGOR Pro 6.2 by fitting influx to $f = y_0 + a(1 - e^{-bx})$ and initial rates (v_0) to $y = mx + b$, as described previously [90]. Graphs were created using IGOR Pro 6.2.

4.4 Results

4.4.1 IC_{50} determination of CQ and CQ_{GREEN} in CQS and CQR strains.

To evaluate the efficacy of the fluorescently tagged CQ analogue CQ_{GREEN}, the half maximal inhibitory concentrations (IC_{50}) were determined using the SYBR Green I detection assay and a standardized calculation method for data analysis in two CQS and two CQR *P. falciparum* strains (Table 4.1) [218]. The two CQS strains 3D7 and HB3 had a CQ IC_{50} of 24 ± 5.6 nM and 14 ± 1.2 nM,

respectively. The IC_{50} values were significantly higher in CQ_{GREEN} treated 3D7 (48 ± 2.8 nM) but not in HB3 (35 ± 7.9 nM). Treatment of the CQR strains FCB and Dd2 showed similar IC_{50} values for all tested drugs. IC_{50} values of 166 ± 8.6 nM for CQ, and 177 ± 43.0 nM for CQ_{GREEN} were determined in FCB. For Dd2, IC_{50} values of 169 ± 3.9 nM were obtained for CQ, and 174 ± 27.1 nM for CQ_{GREEN}. Resistance in CQR strains could be reversed with the addition of 1 µM VP, while no significant change was observed in CQS strains for treatment with CQ or CQ_{GREEN} in combination with verapamil.

Table 4.1 IC_{50} values of CQ and CQ_{GREEN} for *P. falciparum* strains used in this study

Strain	CQ	CQ + VP	CQ_{GREEN}	CQ_{GREEN} + VP	CQ *vs* CQ_{GREEN}	CQ + VP *vs* CQ_{GREEN} + VP
3D7	24 ± 5.6	17 ± 1.1	48 ± 2.8	50 ± 3.2	p = 0.02	p < 0.01
HB3	14 ± 1.2	19 ± 1.6	35 ± 7.9	36 ± 6.7	p = 0.06	p = 0.07
FCB	166 ± 8.6	41 ± 6.5	177 ± 43.0	35 ± 8.7	p = 0.81	p = 0.61
Dd2	169 ± 3.9	53 ± 6.5	174 ± 27.1	35 ± 6.2	p = 0.85	p = 0.12

All values are given in nM ± SEM and represent three independent experiments with or without 1 µM verapamil (VP).

4.4.2 Fluorescence intensity of CQ_{GREEN} is dependent on pH.

The fluorescence intensity and excitability of a protein often differs at varying pH [265]. While some fluorophores have stable emission at different pH, others are more pH sensitive [266, 267]. This must be taken into account when comparing fluorescence intensity of a fluorochrome in intracellular compartments with different pH. CQ_{GREEN} consists of a CQ analogue tagged with a BODIPY fluorophore, which is relatively insensitive to solvent polarity and pH [268]. To determine if this fluorescently tagged CQ is pH dependent, CQ_{GREEN} fluorescence was tested using buffer solutions containing HEPES or MES to obtain pH values ranging from 5.0 – 8.0. These buffer solutions were used to evaluate possible changes in fluorescence intensity seen in the parasite cytosol, having a physiological pH of 7.2, and the DV, maintaining a pH of 5.2 [25]. Excitation spectra for CQ_{GREEN} showed constant fluorescence intensity at a fixed emission of 540 nm (Figure 4.1A). The CQ_{GREEN} excitation peak was determined at 508 nm. Since live cell imaging will be performed

using a 488 nm laser for excitation, CQ_{GREEN} emission spectra were measured at different pH with a fixed excitation wavelength of 488 nm. CQ_{GREEN} emission intensity peaked at 522 nm and increased 1.6-fold from 13,698 RFU at pH 7.5 to 22,419 RFU at pH 5.5 (Figure 4.1B). Therefore, slightly higher CQ_{GREEN} fluorescence is recorded in acidic compartments compared to neutral compartments at equal intracellular CQ_{GREEN} concentrations.

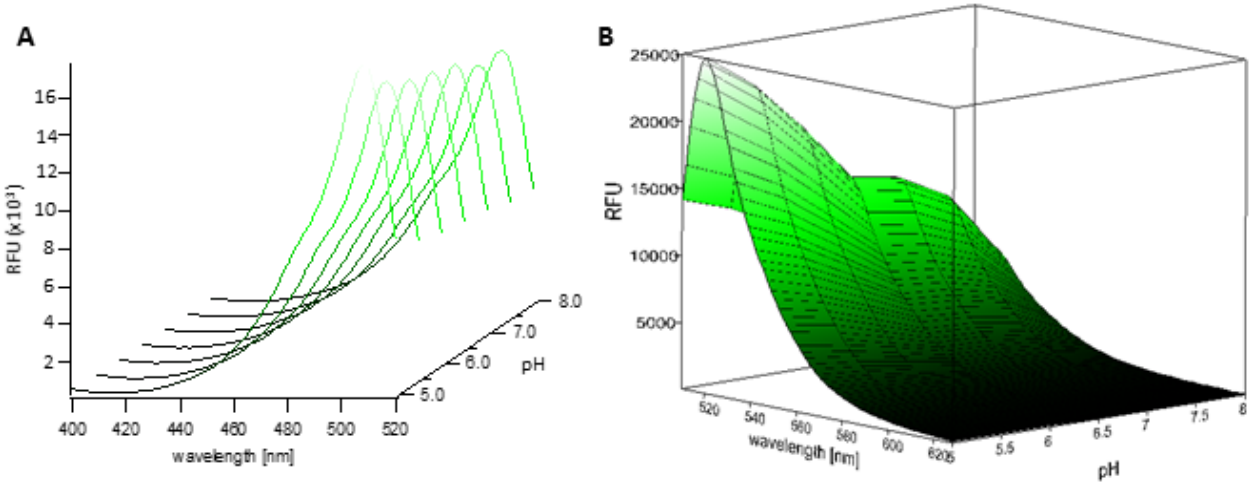

Figure 4.1 CQ_{GREEN} excitation and emission spectra at varying pH. Buffer solutions with varying pH ranging from 5 – 8, each containing 1 µM CQ_{GREEN} were prepared in triplicate and measured using a fluorimeter. Temperature was set to 37°C during measurements. **A**, excitation spectra with fixed emission at 540 ± 4.5 nm. **B**, emission spectra with fixed excitation at 488 ± 4.5 nm.

4.4.3 CQ_{GREEN} accumulates in the parasite cytosol.

The weak base properties of CQ and its diprotonation at low pH result in its high accumulation in the parasite's DV [81]. However, addition of a fluorescent group to CQ might alter the intracellular distribution of this molecule. In this study, the CQS strain 3D7 was treated with 25 nM, 50 nM, 500 nM and 2.5 µM CQ_{GREEN} in Ringer's solution or buffer solutions with pH 7.2 and pH 5.2, respectively. CQ_{GREEN} uptake and intracellular distribution was monitored in 5 min intervals for a total of 30 min using a confocal microscope and a stage-top incubator. Increasing CQ_{GREEN} concentrations resulted in stronger fluorescence signals, independent of the buffer solution used (Figure 4.2). The fluorescence signal was always stronger in the cytosol compared to the DV. Faint accumulation of CQ_{GREEN} in the DV was observed with any of the buffer solutions and CQ_{GREEN} concentrations.

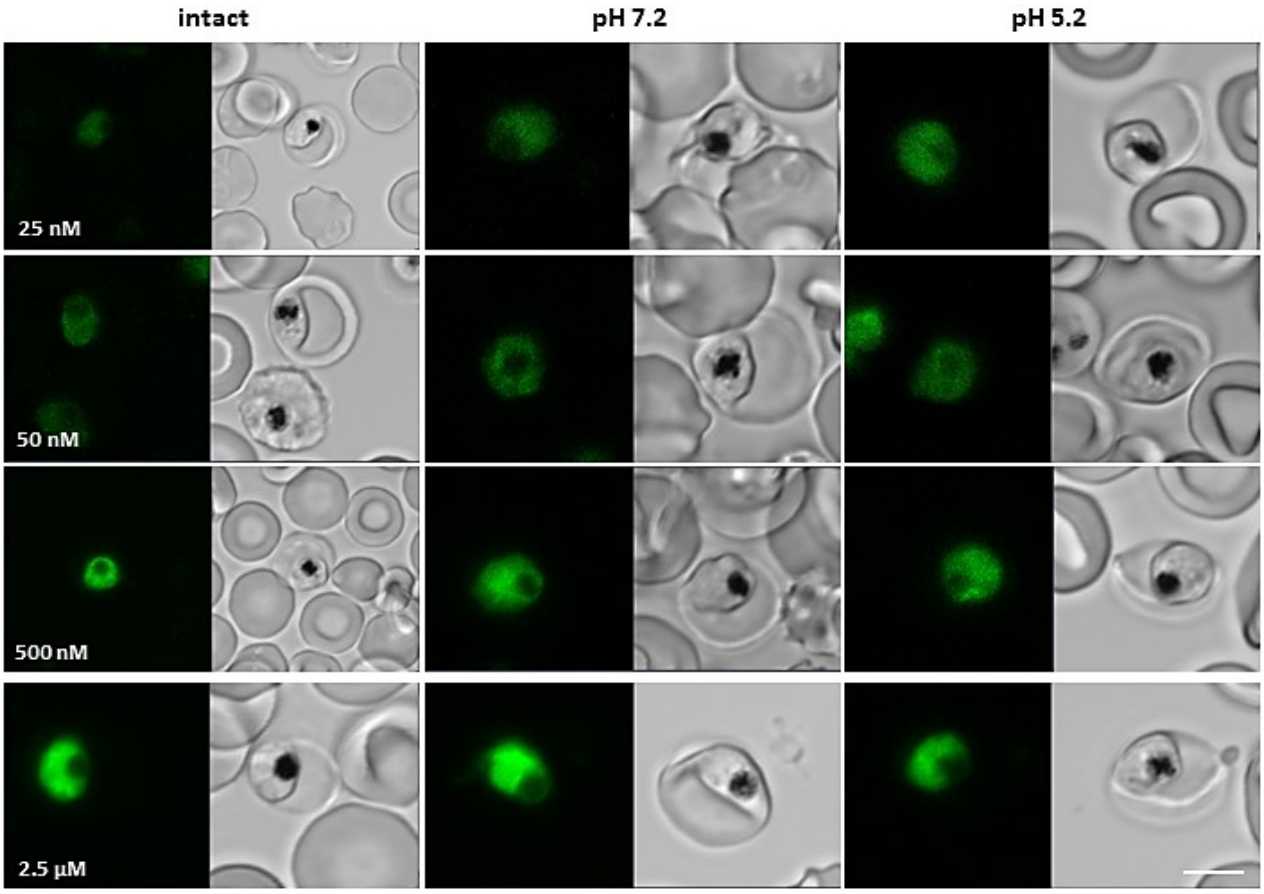

Figure 4.2 Live cell imaging of CQ_{GREEN} treated parasites. Synchronized trophozoite stage 3D7 parasites containing Ringer's or equilibration buffer solution for pH 7.2 and 5.2 were prepared for confocal microscopy. Different CQ_{GREEN} concentrations were added and uptake was monitored for 30 min, and emission range was set to 500-600 nm. Fluorescence increased with higher CQ_{GREEN} concentrations but no accumulation of CQ_{GREEN} could be detected in the parasite's digestive vacuole. Representative images of independent experiments. Scale bar, 5 µm.

Although CQ is expected to accumulate in the parasite's DV within minutes, addition of CQ_{GREEN} was extended for up to 7 h in 3D7 parasites at 37°C, 3% O_2, 5% CO_2, 92% N_2. It was previously reported that incubation of the CQ analogue CQ_{BLUE} at 3 µM for 8 h resulted in nonspecific localization throughout the parasite cytosol, while accumulation of CQ_{BLUE} in the DV was detected using a concentration of 300 nM [91]. Therefore, for this study, CQ_{GREEN} concentrations from 100 - 500 nM were used. Fluorescence signals obtained after 7 h incubation were very low for all tested CQ_{GREEN} concentrations (Figure 4.3). Accumulation of CQ_{GREEN} in the DV could be detected in very few parasites (approx. 5%) (Figure 4.3b+d). Furthermore, accumulation of CQ_{GREEN} in the DV was only seen in one parasite of a double-infected RBC (Figure 4.3b), suggesting that CQ_{GREEN} accumulation in the DV is not equally achieved in individual parasites. Moreover, the CQ_{GREEN}

fluorescence in the DV of the parasite in Figure 4.3b is only 2.8-fold higher compared to the cytosol, which is much lower than expected.

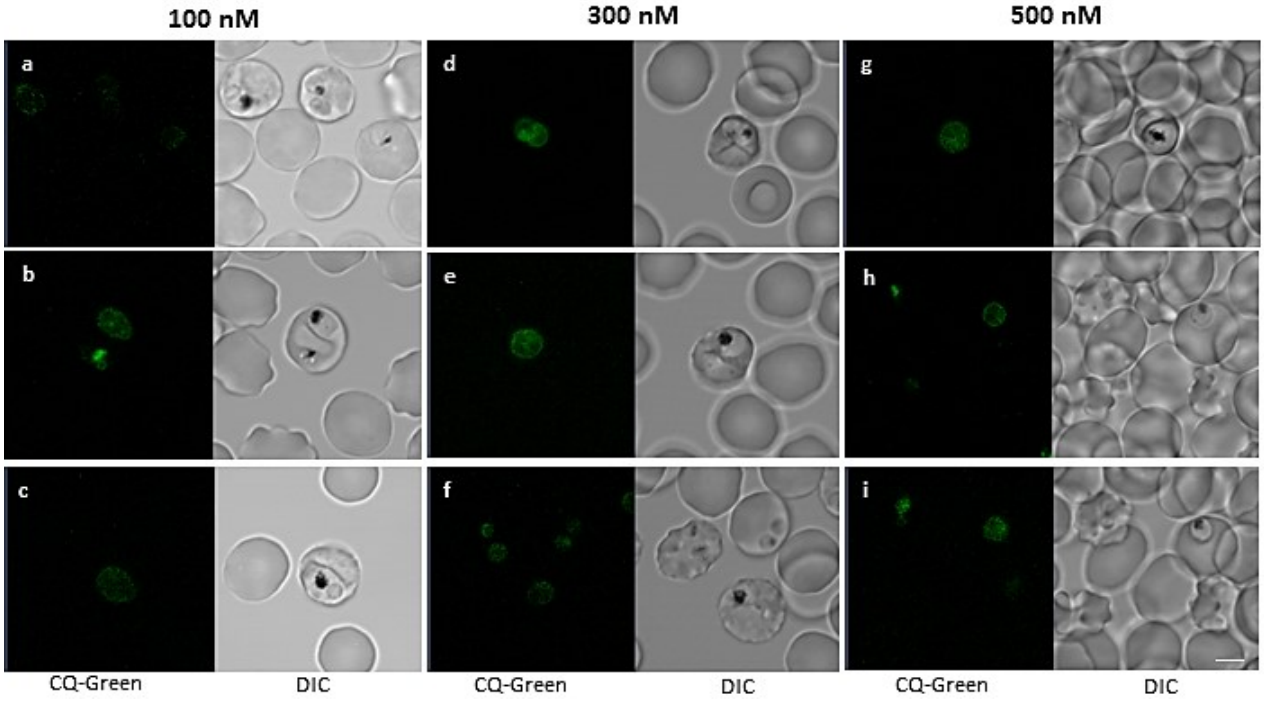

Figure 4.3 Long term incubation of CQ_{GREEN} treated parasites. Early trophozoite stage 3D7 parasites were incubated with 100 nM, 300 nM or 500 nM CQ_{GREEN} for 7 h in culture medium at 37°C, 3% O2, 5% CO2, and then transferred onto a microscope chamber. Faint fluorescence accumulation of CQ_{GREEN} in the DV could be detected in few parasites (approx. 5%). Experiments were done in triplicate on independent days. Scale bar, 5 µm.

4.4.4 No cleavage of the BODIPY moiety was observed in CQ_{GREEN}.

Next, we investigated if the BODIPY moiety of CQ_{GREEN} is cleaved and remains in the cytosol while CQ reaches the DV, where it can exert its antimalarial properties. It was previously demonstrated that cleavage of fluorescent molecules through proteases changes the environment of the reactive center loop, resulting in a spectral shift of the fluorescence peak [269, 270]. To evaluate if a spectral shift of the fluorescence peak occurs in CQ_{GREEN} after exposure to parasite proteases, uninfected or 3D7-infected cultures with a parasitemia of 2.5%, 5% or 10% were loaded with 500 nM CQ_{GREEN} for 1 h. Parasites were then washed to remove excess CQ_{GREEN} in the supernatant and were lysed before measuring fluorescence. Since live cells were loaded with the dye, any detected signal

should be derived from CQ_{GREEN} molecules taken up by the parasites. As a control, parasites were with free acid BODIPY-FL were analyzed using the same conditions.

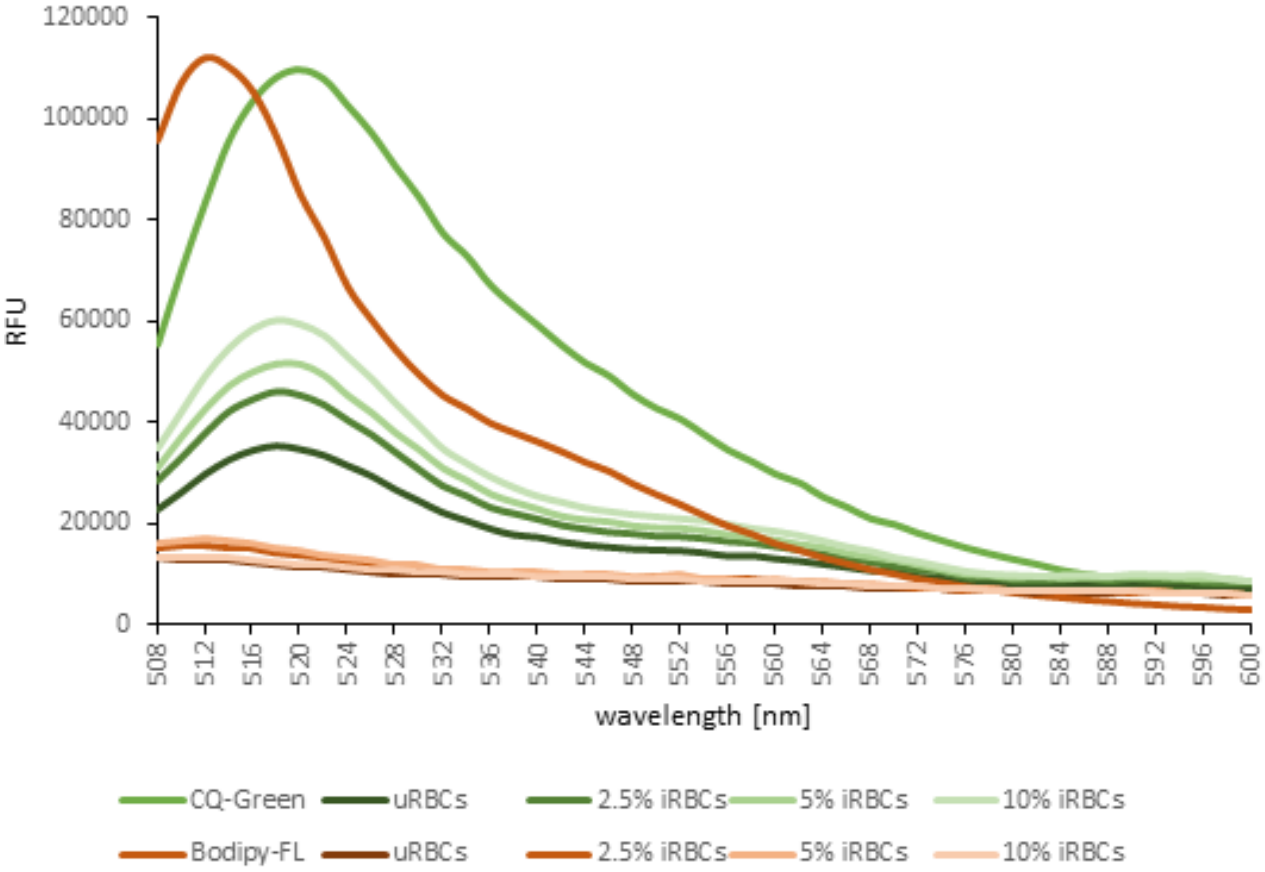

Figure 4.4 CQ_{GREEN} and BODIPY-FL fluorescence. CQ_{GREEN} and free acid BODIPY-FL were measured in solution or after incubation with, and lysis of, uninfected and infected red blood cells (uRBCs and iRBCs, respectively). No shift of CQ_{GREEN} fluorescence towards the BODIPY-FL peak was observed in uRBCs and iRBCs. Experiment was done twice in triplicate.

The fluorescence peak for the free acid BODIPY-FL control was measured at 512 nm, while the peak for CQ_{GREEN} was measured from 520 - 522 nm (Figure 4.4). This fluorescence shift is large enough to differentiate between free BODIPY and BODIPY conjugated to CQ. Treatment of uninfected RBCs (uRBCs) and infected RBCs iRBCs) with 500 nM BODIPY-FL for 1 h resulted in low fluorescence in all samples, indicating that BODIPY-FL is not readily accumulating in uRBCs or iRBCs. When parasites were treated with 500 nM CQ_{GREEN}, a proportional increase in CQ_{GREEN} fluorescence was observed with increasing parasitemia from 0% (uRBCs) to 10% (iRBCs), as expected. The

fluorescence peak was measured at 520 nm for CQ_{GREEN} in Ringer's solution alone (control) and remained constant at 518-520 nm for all CQ_{GREEN} treated uRBC and iRBC samples. Thus, either no cleavage of the BODIPY tag in CQ_{GREEN} occurred or the cleaved BODIPY moiety was not retained within the RBCs and a fluorescent signal was only obtained from uncleaved CQ_{GREEN}.

4.4.5 CQ_{GREEN} uptake differs between CQS and CQR strains.

Researchers have mainly focused on CQ accumulation in the DV, suggesting that enhanced CQ efflux from the DV through PfCRT confers drug resistance [271, 272]. CQ uptake in intact iRBCs has mainly been described as passive diffusion and subsequent accumulation in the DV due to the drug's weak base properties [32, 273]. Molecular mechanisms that influence CQ uptake and, therefore, reduce the drug influx in CQR strains compared to CQS strains may have been underestimated. CQ_{GREEN} offers the possibility to measure uptake in live cells. Although CQ_{GREEN} mainly accumulates and fluoresces in the parasite's cytosol, with weak fluorescence in the DV, it was still possible to measure its uptake rate in both compartments.

The rate of CQ_{GREEN} uptake was analyzed in two CQS strains (3D7 and HB3) and compared with two CQR strains (Dd2 and FCB). Fluorescence was measured from the parasite cytosol, DV, iRBC cytoplasm and uRBC. No increase in CQ_{GREEN} fluorescence beyond background levels was observed in the cytoplasm of infected or uninfected RBCs (Figure 4.5A). There was a rapid increase in fluorescence in the parasite cytosol and DV in the initial 150 seconds, followed by a slower, almost linear CQ_{GREEN} uptake. This is in agreement with previous studies, which showed that CQ uptake can be separated into a short period of very rapid uptake (< 30 sec) followed by a long, slower phase [3]. Addition of VP did not influence CQ uptake during the initial phase [274].

The rate of CQ_{GREEN} uptake into the parasite cytosol was approx. 2-fold higher in CQS strains compared to CQR strains (Figure 4.5B). For the DV, CQ_{GREEN} uptake rates were approx. 2.5-fold higher in CQS strains compared to CQR strains. CQ_{GREEN} uptake rates between CQS and CQR strains were statistically very significant for both the cytosol ($p < 0.0001$) and DV ($p < 0.0001$). Increased CQ_{GREEN} uptake rates for the DV of CQS strains suggest that active transport of CQ into the DV

occurred in addition to diffusion, which is absent in CQR strains. Addition of VP did not influence CQ_{GREEN} uptake in the parasite cytosol or DV in all CQR strains tested.

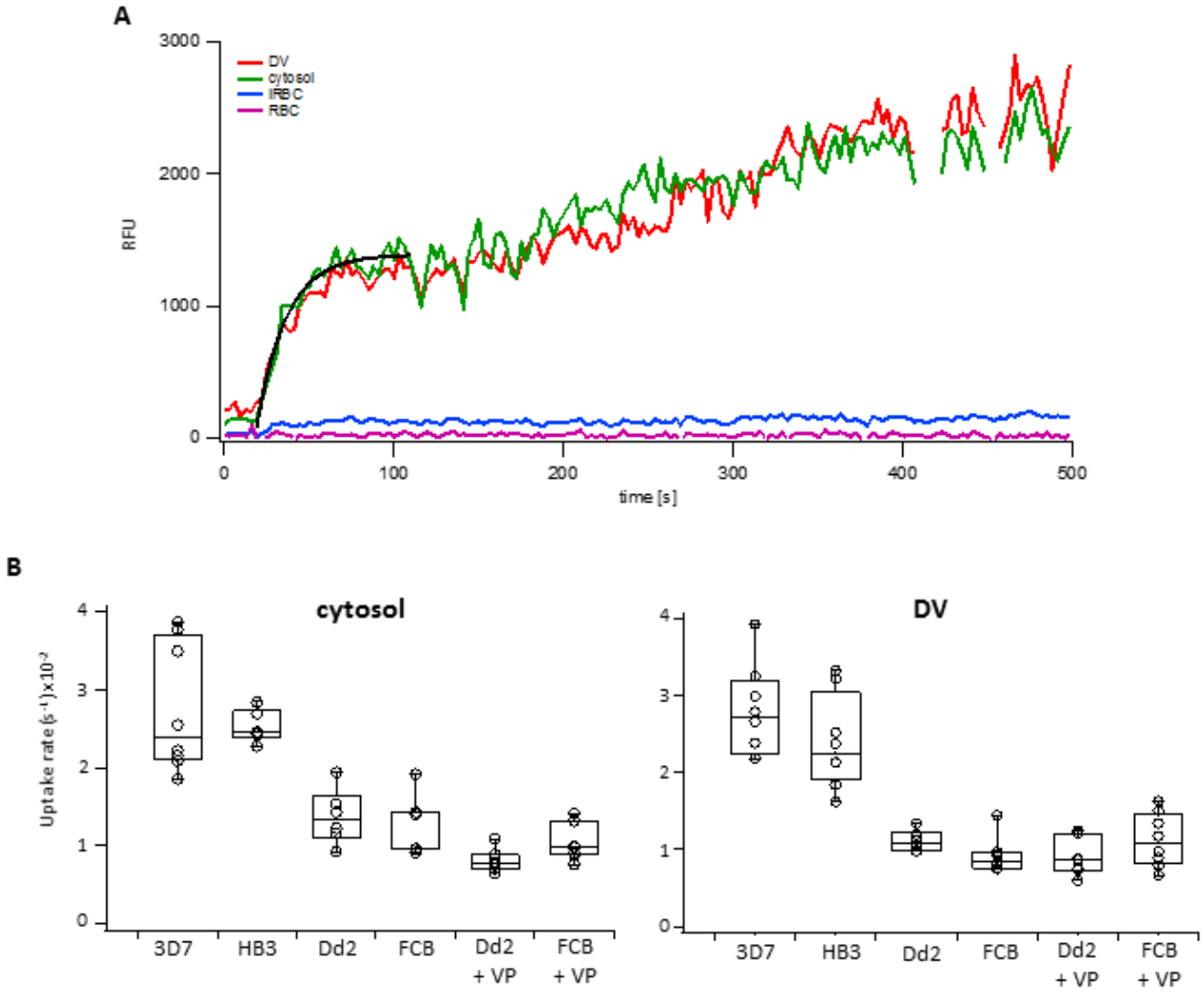

Figure 4.5 CQ_{GREEN} uptake in CQS and CQR strains. Trophozoite stage parasites were incubated with CQ_{GREEN} and fluorescence was recorded every 3 seconds. **A**, fluorescence was measured in the parasite cytosol, DV, infected RBC (iRBC) cytoplasm and uninfected RBC (uRBC). No accumulation of CQ_{GREEN} was observed for the uRBC and iRBC cytoplasms. Uptake rates were calculated for the parasite cytosol and DV during the saturation phase (black curve), which was followed by a linear uptake phase. **B**, CQR strains showed a slower uptake rate compared to CQS strains. Addition of VP did not influence the CQ_{GREEN} uptake rate of CQR strains. Experiments were done on three independent days.

4.5 Discussion

The exact mechanisms responsible for CQ resistance have eluded researchers for decades. It has long been described that CQR strains accumulate less CQ in the DV than CQS strains [89]. Nevertheless, CQR strains are still able to tolerate higher intracellular CQ concentrations than CQS strains [3, 4, 102]. Researchers have advocated that inhibition of hemozoin formation by CQ is not sufficient to explain its effect on parasite killing [23]. Furthermore, a possible role of CQ in the parasite's cytosol is proposed [79]. A fluorescently labeled CQ analogue could provide insight into the intracellular distribution of CQ that is not attributed to diffusion alone. This study set out to examine CQ uptake in live parasites using CQ_{GREEN}.

IC_{50} values were compared in CQS and CQR strains after exposure to CQ or CQ_{GREEN}. A decrease in the efficacy for CQ_{GREEN} may suggest that the CQ analogue does not reach its site of action, or binds to its target less efficiently. In CQS strains, CQ was twice as effective as CQ_{GREEN}. However, similar IC_{50} values were determined for CQ and CQ_{GREEN} in CQR strains. In a previous study by Loh and colleagues, IC_{50} values for CQ_{GREEN} were approx. 5-fold higher in 3D7 compared to CQ, and nearly doubled for the CQR strain K1 [92]. Thus, the parasites used for this study seemed to be more sensitive to CQ_{GREEN} exposure than reported in earlier publications. In both studies, drug resistance could be reversed by the chemosensitizer VP, suggesting that CQ_{GREEN} has a similar mode of action than CQ.

Although CQ_{GREEN} seemed slightly less effective than CQ in the IC_{50} assays, its BODIPY fluorescent tag makes it suitable for live cell imaging. This was confirmed by fluorimeter readings, where a strong fluorescence emission signal for CQ_{GREEN} was measured at a 488 nm excitation wavelength. Spectral scans showed a 1.6-fold increase in fluorescence at acidic pH, which should be taken into account when calculating the ratio between cytosolic and digestive vacuolar fluorescence. However, no accumulation of CQ_{GREEN} in the parasite's DV compared to the cytosol could be observed during live cell imaging at any of the tested CQ_{GREEN} concentrations, ranging from 25 nM to 2.5 µM. Considering that the CQ_{GREEN} IC_{50} was determined at 24 nM, any of the tested concentrations for live cell imaging should have killed the parasites and, therefore, theoretically have shown accumulation in the DV. Buffer solutions with varying pH showed that charge did not

play a role in the intraparasitic CQ_{GREEN} distribution. This was important to show since protonation of CQ, or its analogues, influence their membrane permeability [275, 276]. Although one study reported accumulation of CQ_{GREEN} in the DV [92], this was not observed here.

Fluorimeter measurements were performed to exclude a loss of fluorescence at low pH. Slightly higher fluorescence was observed for CQ_{GREEN} at acidic pH compared to neutral pH. Therefore, if CQ_{GREEN} accumulates in the DV, a fluorescent signal can be obtained. The absence of fluorescence signal in the DV suggests that CQ_{GREEN} either does not accumulate in the DV or the fluorescence is quenched through the presence of heavy metals such as iron [277]. Fluorescence quenching through FPIX, which harbors ferric iron (Fe^{3+}) in its center, has been reported in *P. falciparum* infected RBCs loaded with acridine orange [278, 279].

If CQ_{GREEN} does not accumulate in the DV, two possibilities may occur: i) cleavage of the fluorescent BODIPY moiety from CQ may occur in the parasite cytosol. This would allow CQ to accumulate in the DV, while the BODIPY moiety remains in the cytosol. In this case, the fluorescence signal does not specify the subcellular localization of CQ. ii) the BODIPY moiety alters the intrinsic properties of the protein and, therefore, prevents its accumulation in the DV. A simple way to elucidate whether the BODIPY moiety gets cleaved is determining fluorescence properties of conjugated versus free acid BODIPY-FL. Since there is a fluorescence shift between free acid BODIPY-FL alone (peak at 512 nm) and the BODIPY-tagged CQ_{GREEN} (peak at 520 nm), cleavage of the BODIPY moiety from CQ_{GREEN} during the cellular uptake would result in a fluorescence shift back to 512 nm when parasites are treated with CQ_{GREEN}. For this study, intact *P. falciparum*-infected RBCs were treated with CQ_{GREEN} to analyze the potential cleavage of the BODIPY moiety. Although a proportional increase in fluorescence with higher parasitemia was measured, no shift in the fluorescence peak was observed. Thus, CQ_{GREEN} remained intact and functional in live parasites prior to parasite lysis for fluorescence measurements.

Despite the unexpected localization of CQ_{GREEN} accumulation in the parasite cytosol instead of the DV, uptake rates were analyzed in two CQS and two CQR strains. Although the fluorescent signal obtained from the DV was weak compared to the cytosol, it was sufficient to calculate the uptake rate for this compartment. Interestingly, CQS strains had approx. 2-fold higher CQ_{GREEN} uptake rates

for the cytosol and 2.5-fold higher rates for the DV compared to CQR strains. Addition of verapamil to the CQR strains did not alter CQ_{GREEN} uptake rates, suggesting that PfCRT does not play a role in its uptake. This is consistent with the hypothesis that PfCRT is involved in CQ efflux but not its uptake [90]. Decreased CQ uptake rates in CQR strains compared to CQS strains may be explained through reduced availability or affinity to an intracellular target, such as free heme [280]. Thus, accumulation of CQ in the DV may contribute to parasite killing but additional drug targets in the parasite cytosol could also play a role.

4.6 Conclusion

Live cell imaging using fluorescently tagged antimalarial drugs provides a great tool to elucidate their intracellular localization and give insights into their uptake or efflux rates. The challenge using fluorescently labeled CQ analogues is their sensitivity to pH and altered intracellular localization, compared to unmodified CQ. If it is possible to find fluorescent groups that are more stable at different pH and do not influence the diffusion properties of the protein, this could provide a powerful tool in studying the activity of antimalarial drugs. Alterations between drug-sensitive and –resistance strains can be closely monitored to enhance our understanding of resistance mechanisms. Moreover, affinity of CQ, or its analogues, to cytosolic proteins may direct research on new antimalarial drug design away from the DV and increase the focus on cellular pathways in the parasite cytosol.

4.7 Chapter-related Acknowledgements

This study was supported in part by fellowships from the German Academic exchange Service (DAAD) (SJR) and the Centre for Host-Parasite Interaction (FRQNT) (SJR), and grants from the Natural Sciences and Engineering Research Council (NSERC) Discovery Grant (PR) and the Canada Foundation for Innovation (CFI) Leaders Opportunity Fund (PR).

— Chapter 5 —

Concluding Remarks and Future Direction

Concluding Remarks and Future Direction

Malaria remains one of the most important parasitic diseases worldwide. Among those malaria parasites that infect humans, *Plasmodium falciparum* poses the major threat since it may cause serious complications during the infection that can result in death. Emergence of resistance to commonly used antimalarial drugs is a main concern in the combat of *P. falciparum* infections.

Most malaria-endemic regions are in developing countries, where government spending on healthcare is generally low. Therefore, malaria treatment must not only be easy to use and cause little side effects but also be affordable. Chloroquine (CQ) meets all of these requirements. CQ has saved the lives of more people than any other antimalarial drug and has remained effective for decades until resistance arose. To date, its mechanisms of resistance have not been fully understood. If the parasite's resistance mechanisms to CQ could be determined, resistance could be reversed, making the drug once again effective.

The aim of this thesis was to gain insight into which regulatory mechanisms *P. falciparum* parasites have developed to survive under drug pressure. The *P. falciparum* multidrug resistance 1 transporter (PfMDR1) contains five amino acid mutations that are suggested to be involved in drug resistance. Three PfMDR1 mutation sites are located in a putative substrate binding pocket, namely residues 86, 1034 and 1042. In the second chapter (manuscript I) of this thesis, we described a possible functional role for residue 1042 in transport of the fluorescent substrate Fluo-4. Furthermore, competition studies with Fluo-4 and various antimalarial drugs revealed that *P. falciparum* strains from different genetic backgrounds but harboring the same PfMDR1 amino acid mutations displayed distinct Fluo-4 transport inhibition patterns. Altered Fluo-4 transport properties through differences in PfMDR1 protein expression levels were excluded by Western blot analysis. This suggests that substrate transport through PfMDR1 is highly regulated and its functional role may have been underestimated.

These findings emphasize the need to establish kinetic drug transport profiles for *P. falciparum* strains of different genetic background, even if they share the same PfMDR1 amino acid mutations. Since the PfMDR1 pump rate of Fluo-4 was determined for the drug-resistant strain Dd2 in intact

parasitized RBCs [213], this information can be used to design competition experiments using a fixed concentration of Fluo-4 and varying concentrations of antimalarial drugs. This system offers a great tool to investigate transport of currently used antimalarial drugs through PfMDR1. Furthermore, kinetic profiles of various polymorphisms in the PfMDR1 transporter can be used for the development of new antimalarial drugs.

In the third chapter (manuscript II) of this thesis, the mechanisms of CQ resistance were further investigated. CQ-sensitive (CQS) strains are known to accumulate higher concentrations of intracellular CQ compared to CQ-resistant (CQR) strains [3, 4]. In this chapter, we demonstrated that CQS strains undergo irreversible cell damage 4-6 hours earlier than CQR strains when exposed to equally lethal external CQ concentrations. This suggests that CQR strains can prevent irreversible cell damage longer and cope with higher CQ concentrations than CQS strains. Moreover, we described a novel phenotype for CQS strains after CQ exposure that was not observed in CQR strains. Hemozoin-containing compartments surrounded by a membrane bilayer were found in the cytosol of CQS strains after CQ exposure. They appeared before lysis of the DV membrane and leakage of DV contents into the cytosol took place. Furthermore, most parasites retained a functional mitochondrial membrane in the initial 4 hours after CQ exposure, while its loss is usually associated with apoptosis. These results suggest that CQS strains undergo a type of programmed cell death (PCD) that is distinct from classical apoptosis.

Only recently did researchers demonstrate that PCD pathways exist in unicellular eukaryotes [117-119]. An autophagic-like PCD pathway is proposed for *P. falciparum* strains that are exposed to CQ [125, 128]. Our findings confirm a potential role of a non-apoptotic pathway during CQ-induced cell death. This opens a wide field for exploring autophagy and its potential role in PCD after drug treatment of sensitive versus resistant parasites. Autophagy inhibitors or inducers, such as Bafilomycin-A1 and E-64, can be tested on *P. falciparum* parasites to determine if these substances have altered effects on strains of different genetic background. Understanding PCD in *Plasmodium* parasites will be highly beneficial in the design of new antimalarial drugs and provide a possibility to make drug-resistant strains more susceptible again.

The aim of the fourth chapter (manuscript III) of this thesis was to determine if there is a potential CQ target outside the DV. For this, a commercially available fluorescent CQ analogue, called LynxTag™-CQ_{GREEN} (CQ_{GREEN}) was used. CQ_{GREEN} highly accumulated in the parasite cytosol and to a much lesser extent in the DV. Changing the pH in all intracellular compartments to pH 7.2 or 5.2 did not influence intracellular distribution of CQ_{GREEN}, indicating that its accumulation in the cytosol occurs independent of pH. This suggests that CQ_{GREEN} has a high affinity to a cytosolic target. These results provide additional information that affinity of CQ, or its analogues, to a cytosolic target are underestimated. Therefore, involvement of cytosolic pathways to CQ resistance may play a greater role than previously thought.

The findings of this thesis suggest that future research on CQ resistance should focus on cytosolic molecules and pathways, which will likely complete our understanding of CQ resistance mechanisms in *P. falciparum*-infected red blood cells.

Bibliography

1. Laufer MK, Takala-Harrison S, Dzinjalamala FK, Stine OC, Taylor TE, Plowe CV: Return of chloroquine-susceptible *falciparum* malaria in Malawi was a reexpansion of diverse susceptible parasites. *J Infect Dis* 2010, 202:801-808.
2. Fidock DA, Nomura T, Talley AK, Cooper RA, Dzekunov SM, Ferdig MT, Ursos LMB, Singh Sidhu A, Naudé B, Deitsch KW, et al: Mutations in the *P. falciparum* digestive vacuole transmembrane protein PfCRT and evidence for their role in chloroquine resistance. *Molecular Cell* 2000, 6:861-871.
3. Geary TG, Jensen JB, Ginsburg H: Uptake of [^{3}H]chloroquine by drug-sensitive and -resistant strains of the human malaria parasite *Plasmodium falciparum*. *Biochemical Pharmacology* 1986, 35:3805-3812.
4. Cabrera M, Paguio MF, Xie C, Roepe PD: Reduced digestive vacuolar accumulation of chloroquine is not linked to resistance to chloroquine toxicity. *Biochemistry* 2009, 48:11152-11154.
5. WHO: World Malaria Report 2014. World Health Organization; 2014.
6. White NJ: Antimalarial drug resistance. *J Clin Invest* 2004, 113:1084-1092.
7. Smith DC, Sanford LB: Laveran's germ: the reception and use of a medical discovery. *Am J Trop Med Hyg* 1985, 34:2-20.
8. Ross R: On some peculiar pigmented cells found in two mosquitoes feeding on malarial blood. *Brit Med J* 1897, 2:1786-1788.
9. Sutherland CJ, Tanomsing N, Nolder D, Oguike M, Jennison C, Pukrittayakamee S, Dolecek C, Hien TT, do Rosario VE, Arez AP, et al: Two nonrecombining sympatric forms of the human malaria parasite *Plasmodium ovale* occur globally. *J Infect Dis* 2010, 201:1544-1550.
10. Singh B, Kim Sung L, Matusop A, Radhakrishnan A, Shamsul SS, Cox-Singh J, Thomas A, Conway DJ: A large focus of naturally acquired *Plasmodium knowlesi* infections in human beings. *Lancet* 2004, 363:1017-1024.

11. Chulay JD, Haynes JD, Diggs CL: *Plasmodium falciparum*: assessment of *in vitro* growth by [^{3}H]hypoxanthine incorporation. *Exp Parasitol* 1983, 55:138-146.
12. Reilly HB, Wang H, Steuter JA, Marx AM, Ferdig MT: Quantitative dissection of clone-specific growth rates in cultured malaria parasites. *Int J Parasitol* 2007, 37:1599-1607.
13. Wenk P, Renz A: Malaria: Wettrüsten oder Selbstkontrolle? *Naturwissenschaftliche Rundschau* 2014, 67:276-299.
14. Wipasa J, Elliott S, Xu H, Good MF: Immunity to asexual blood stage malaria and vaccine approaches. *Immunol Cell Biol* 2002, 80:401-414.
15. Nosten F, van Vugt M, Price R, Luxemburger C, Thway KL, Brockman A, McGready R, Kuile F, Looareesuwan S, White NJ: Effects of artesunate-mefloquine combination on incidence of *Plasmodium falciparum* malaria and mefloquine resistance in western Thailand: a prospective study. *Lancet* 2000, 356:297-302.
16. Noedl H, Se Y, Sriwichai S, Schaecher K, Teja-Isavadharm P, Smith B, Rutvisuttinunt W, Bethell D, Surasri S, Fukuda MM, et al: Artemisinin resistance in Cambodia: a clinical trial designed to address an emerging problem in Southeast Asia. *Clin Infect Dis* 2010, 51:e82-89.
17. Beez D, Sanchez CP, Stein WD, Lanzer M: Genetic predisposition favors the acquisition of stable artemisinin resistance in malaria parasites. *Antimicrob Agents Chemother* 2011, 55:50-55.
18. Ariey F, Witkowski B, Amaratunga C, Beghain J, Langlois A-C, Khim N, Kim S, Duru V, Bouchier C, Ma L, et al: A molecular marker of artemisinin-resistant *Plasmodium falciparum* malaria. *Nature* 2014, 505:50-55.
19. WHO: Practical chemotherapy of malaria. In *WHO Technical Report Series*, vol. No. 8051990.
20. Ginsburg H, Krugliak M: Chloroquine - some open questions on its antimalarial mode of action and resistance. *Drug Resist Updat* 1999, 2:180-187.
21. Ginsburg H, Famin O, Zhang J, Krugliak M: Inhibition of glutathione-dependent degradation of heme by chloroquine and amodiaquine as a possible basis for their antimalarial mode of action. *Biochemical Pharmacology* 1998, 56:1305-1313.

22. Zhang Y, Asante KS, Jung A: Stage-dependent inhibition of chloroquine on *Plasmodium falciparum* in vitro. *J Parasitol* 1986, 72:830-836.
23. Ginsburg H, Ward SA, Bray PG: An integrated model of chloroquine action. *Parasitology Today* 1999, 15:357-360.
24. Yayon A, Vande Waa JA, Yayon M, Geary TG, Jensen JB: Stage-dependent effects of chloroquine on *Plasmodium falciparum in vitro*. *J Protozool* 1983, 30:642-647.
25. Wunderlich J, Rohrbach P, Dalton JP: The malaria digestive vacuole. *Front Biosci (Schol Ed)* 2012, 4:1424-1448.
26. Ginsburg H, Geary TG: Current concepts and new ideas on the mechanism of action of quinoline-containing antimalarials. *Biochem Pharmacol* 1987, 36:1567-1576.
27. Ginsburg H, Nissani E, Krugliak M: Alkalinization of the food vacuole of malaria parasites by quinoline drugs and alkylamines is not correlated with their antimalarial activity. *Biochemical Pharmacology* 1989, 38:2645-2654.
28. Krogstad DJ, Schlesinger PH, Gluzman IY: Antimalarials increase vesicle pH in *Plasmodium falciparum*. *J Cell Biol* 1985, 101:2302-2309.
29. Yayon A, Cabantchik ZI, Ginsburg H: Identification of the acidic compartment of *Plasmodium falciparum*-infected human erythrocytes as the target of the antimalarial drug chloroquine. *EMBO J* 1984, 3:2695-2700.
30. Hoppe HC, van Schalkwyk DA, Wiehart UI, Meredith SA, Egan J, Weber BW: Antimalarial quinolines and artemisinin inhibit endocytosis in *Plasmodium falciparum*. *Antimicrob Agents Chemother* 2004, 48:2370-2378.
31. Hayward R, Saliba KJ, Kirk K: The pH of the digestive vacuole of *Plasmodium falciparum* is not associated with chloroquine resistance. *J Cell Sci* 2006, 119:1016-1025.
32. Yayon A, Cabantchik ZI, Ginsburg H: Susceptibility of human malaria parasites to chloroquine is pH dependent. *Proc Natl Acad Sci U S A* 1985, 82:2784-2788.
33. Kuhn Y, Rohrbach P, Lanzer M: Quantitative pH measurements in *Plasmodium falciparum*-infected erythrocytes using pHluorin. *Cell Microbiol* 2007, 9:1004-1013.
34. Fitch CD: Chloroquine resistance in malaria: a deficiency of chloroquine binding. *Proc Natl Acad Sci U S A* 1969, 64:1181-1187.

35. Bray PG, Howells RE, Ritchie GY, Ward SA: Rapid chloroquine efflux phenotype in both chloroquine-sensitive and chloroquine-resistant *Plasmodium falciparum*. A correlation of chloroquine sensitivity with energy-dependent drug accumulation. *Biochem Pharmacol* 1992, 44:1317-1324.

36. Bray PG, Mungthin M, Ridley RG, Ward SA: Access to hematin: the basis of chloroquine resistance. *Mol Pharmacol* 1998, 54:170-179.

37. Bray PG, Janneh O, Ward SA: Chloroquine uptake and activity is determined by binding to ferriprotoporphyrin IX in *Plasmodium falciparum*. *Novartis Found Symp* 1999, 226:252-260; discussion 260-254.

38. Sanchez CP, Stein W, Lanzer M: Trans stimulation provides evidence for a drug efflux carrier as the mechanism of chloroquine resistance in *Plasmodium falciparum*. *Biochemistry* 2003, 42:9383-9394.

39. Bray PG, Mungthin M, Hastings IM, Biagini GA, Saidu DK, Lakshmanan V, Johnson DJ, Hughes RH, Stocks PA, O'Neill PM, et al: PfCRT and the trans-vacuolar proton electrochemical gradient: regulating the access of chloroquine to ferriprotoporphyrin IX. *Molecular Microbiology* 2006, 62:238-251.

40. Fitch CD: *Plasmodium falciparum* in owl monkeys: drug resistance and chloroquine binding capacity. *Science* 1970, 169:289-290.

41. Zhang X, Shedden K, Rosania GR: A cell-based molecular transport simulator for pharmacokinetic prediction and cheminformatic exploration. *Mol Pharm* 2006, 3:704-716.

42. Trapp S, Rosania GR, Horobin RW, Kornhuber J: Quantitative modeling of selective lysosomal targeting for drug design. *Eur Biophys J* 2008, 37:1317-1328.

43. Jacobs GH, Oduola AM, Kyle DE, Milhous WK, Martin SK, Aikawa M: Ultrastructural study of the effects of chloroquine and verapamil on *Plasmodium falciparum*. *Am J Trop Med Hyg* 1988, 39:15-20.

44. Gligorijevic B, Bennett T, McAllister R, Urbach JS, Roepe PD: Spinning disk confocal microscopy of live, intraerythrocytic malarial parasites. 2. Altered vacuolar volume regulation in drug resistant malaria. *Biochemistry* 2006, 45:12411-12423.

45. Homewood CA, Warhurst DC, Peters W, Baggaley VC: Lysosomes, pH and the anti-malarial action of chloroquine. *Nature* 1972, 235:50-52.

46. Dzekunov SM, Ursos LM, Roepe PD: Digestive vacuolar pH of intact intraerythrocytic *P. falciparum* either sensitive or resistant to chloroquine. *Mol Biochem Parasitol* 2000, 110:107-124.

47. Einheber A, Palmer DM, Aikawa M: *Plasmodium berghei*: phase contrast and electron microscopical evidence that certain antimalarials can both inhibit and reverse pigment clumping caused by chloroquine. *Exp Parasitol* 1976, 40:52-61.

48. Fitch CD, Cai GZ, Chen YF, Ryerse JS: Relationship of chloroquine-induced redistribution of a neutral aminopeptidase to hemoglobin accumulation in malaria parasites. *Arch Biochem Biophys* 2003, 410:296-306.

49. Macomber PB, Sprinz H: Morphological effects of chloroquine on *Plasmodium berghei* in mice. *Nature* 1967, 214:937-939.

50. Orjih AU, Ryerse JS, Fitch CD: Hemoglobin catabolism and the killing of intraerythrocytic *Plasmodium falciparum* by chloroquine. *Experientia* 1994, 50:34-39.

51. Warhurst DC, Hockley DJ: The mode of action of chloroquine on blood stages of malaria parasites. *Parasitology* 1967, 57:23P.

52. Zarchin S, Krugliak M, Ginsburg H: Digestion of the host erythrocyte by malaria parasites is the primary target for quinoline-containing antimalarials. *Biochem Pharmacol* 1986, 35:2435-2442.

53. Zhang Y, Hempelmann E: Lysis of malarial parasites and erythrocytes by ferriprotoporphyrin IX-chloroquine and the inhibition of this effect by proteins. *Biochemical Pharmacology* 1987, 36:1267-1273.

54. Famin O, Ginsburg H: Differential effects of 4-aminoquinoline-containing antimalarial drugs on hemoglobin digestion in *Plasmodium falciparum*-infected erythrocytes. *Biochem Pharmacol* 2002, 63:393-398.

55. Chou AC, Fitch CD: Control of heme polymerase by chloroquine and other quinoline derivatives. *Biochem Biophys Res Commun* 1993, 195:422-427.

56. Zhang J, Krugliak M, Ginsburg H: The fate of ferriprotorphyrin IX in malaria infected erythrocytes in conjunction with the mode of action of antimalarial drugs. *Mol Biochem Parasitol* 1999, 99:129-141.

57. Goldie P, Roth EF, Jr., Oppenheim J, Vanderberg JP: Biochemical characterization of *Plasmodium falciparum* hemozoin. *Am J Trop Med Hyg* 1990, 43:584-596.
58. Yamada KA, Sherman IW: Plasmodium lophurae: composition and properties of hemozoin, the malarial pigment. *Exp Parasitol* 1979, 48:61-74.
59. Fitch CD, Chen YF, Cai GZ: Chloroquine-induced masking of a lipid that promotes ferriprotoporphyrin IX dimerization in malaria. *J Biol Chem* 2003, 278:22596-22599.
60. Sullivan DJ, Jr., Gluzman IY, Russell DG, Goldberg DE: On the molecular mechanism of chloroquine's antimalarial action. *Proc Natl Acad Sci U S A* 1996, 93:11865-11870.
61. Fitch CD: Ferriprotoporphyrin IX, phospholipids, and the antimalarial actions of quinoline drugs. *Life Sciences* 2004, 74:1957-1972.
62. Schmitt TH, Frezzatti WA, Jr., Schreier S: Hemin-induced lipid membrane disorder and increased permeability: a molecular model for the mechanism of cell lysis. *Arch Biochem Biophys* 1993, 307:96-103.
63. Chou AC, Fitch CD: Mechanism of hemolysis induced by ferriprotoporphyrin IX. *J Clin Invest* 1981, 68:672-677.
64. Dorn A, Vippagunta SR, Matile H, Jaquet C, Vennerstrom JL, Ridley RG: An assessment of drug-haematin binding as a mechanism for inhibition of haematin polymerisation by quinoline antimalarials. *Biochem Pharmacol* 1998, 55:727-736.
65. Slater AF, Cerami A: Inhibition by chloroquine of a novel haem polymerase enzyme activity in malaria trophozoites. *Nature* 1992, 355:167-169.
66. Leed A, DuBay K, Ursos LMB, Sears D, de Dios AC, Roepe PD: Solution structures of antimalarial drug−heme complexes. *Biochemistry* 2002, 41:10245-10255.
67. de Dios AC, Tycko R, Ursos LMB, Roepe PD: NMR studies of chloroquine−ferriprotoporphyrin IX complex. *The Journal of Physical Chemistry A* 2003, 107:5821-5825.
68. Fitch CD, Kanjananggulpan P: The state of ferriprotoporphyrin IX in malaria pigment. *J Biol Chem* 1987, 262:15552-15555.
69. Atamna H, Ginsburg H: Heme degradation in the presence of glutathione. A proposed mechanism to account for the high levels of non-heme iron found in the membranes of hemoglobinopathic red blood cells. *J Biol Chem* 1995, 270:24876-24883.

70. Famin O, Krugliak M, Ginsburg H: Kinetics of inhibition of glutathione-mediated degradation of ferriprotoporphyrin IX by antimalarial drugs. *Biochem Pharmacol* 1999, 58:59-68.
71. Platel DFN, Mangou F, Tribouley-Duret J: Role of glutathione in the detoxification of ferriprotoporphyrin IX in chloroquine resistant *Plasmodium berghei*. *Molecular and Biochemical Parasitology* 1999, 98:215-223.
72. Ambele MA, Egan TJ: Neutral lipids associated with haemozoin mediate efficient and rapid beta-haematin formation at physiological pH, temperature and ionic composition. *Malar J* 2012, 11:337.
73. Ambele MA, Sewell BT, Cummings FR, Smith PJ, Egan TJ: Synthetic hemozoin (beta-hematin) crystals nucleate at the surface of neutral lipid droplets that control their sizes. *Cryst Growth Des* 2013, 13.
74. Pandey AV, Babbarwal VK, Okoyeh JN, Joshi RM, Puri SK, Singh RL, Chauhan VS: Hemozoin formation in malaria: a two-step process involving histidine-rich proteins and lipids. *Biochemical and Biophysical Research Communications* 2003, 308:736-743.
75. Brunsveld L, Vekemans JAJM, Hirschberg JHKK, Sijbesma RP, Meijer EW: Hierarchical formation of helical supramolecular polymers via stacking of hydrogen-bonded pairs in water. *Proceedings of the National Academy of Sciences* 2002, 99:4977-4982.
76. Kuter D, Benjamin SJ, Egan TJ: Multiple spectroscopic and magnetic techniques show that chloroquine induces formation of the μ-oxo dimer of ferriprotoporphyrin IX. *J Inorg Biochem* 2014, 133:40-49.
77. Kuter D, Streltsov V, Davydova N, Venter GA, Naidoo KJ, Egan TJ: Solution structures of chloroquine-ferriheme complexes modeled using MD simulation and investigated by EXAFS spectroscopy. *J Inorg Biochem* 2015.
78. Chou AC, Fitch CD: Hemolysis of mouse erythrocytes by ferriprotoporphyrin IX and chloroquine. Chemotherapeutic implications. *J Clin Invest* 1980, 66:856-858.
79. Ginsburg H, Krugliak M: Chloroquine - some open questions on its antimalarial mode of action and resistance. *Drug Resistance Updates* 1999, 2:180-187.

80. Combrinck JM, Mabotha TE, Ncokazi KK, Ambele MA, Taylor D, Smith PJ, Hoppe HC, Egan TJ: Insights into the role of heme in the mechanism of action of antimalarials. *ACS Chem Biol* 2012.

81. Saliba KJ, Folb PI, Smith PJ: Role for the *Plasmodium falciparum* digestive vacuole in chloroquine resistance. *Biochem Pharmacol* 1998, 56:313-320.

82. Light WR, 3rd, Olson JS: The effects of lipid composition on the rate and extent of heme binding to membranes. *J Biol Chem* 1990, 265:15632-15637.

83. Famin O, Ginsburg H: The treatment of *Plasmodium falciparum*-infected erythrocytes with chloroquine leads to accumulation of ferriprotoporphyrin IX bound to particular parasite proteins and to the inhibition of the parasite's 6-phosphogluconate dehydrogenase. *Parasite* 2003, 10:39-50.

84. Menting JG, Tilley L, Deady LW, Ng K, Simpson RJ, Cowman AF, Foley M: The antimalarial drug, chloroquine, interacts with lactate dehydrogenase from *Plasmodium falciparum*. *Mol Biochem Parasitol* 1997, 88:215-224.

85. Diribe CO, Warhurst DC: A study of the uptake of chloroquine in malaria-infected erythrocytes. High and low affinity uptake and the influence of glucose and its analogues. *Biochem Pharmacol* 1985, 34:3019-3027.

86. Gluzman IY, Schlesinger PH, Krogstad DJ: Inoculum effect with chloroquine and *Plasmodium falciparum*. *Antimicrob Agents Chemother* 1987, 31:32-36.

87. Hammadi A, Ramiandrasoa F, Sinou V, Rogier C, Fusai T, Le Bras J, Parzy D, Kunesch G, Pradines B: Cellular uptake of a catechol iron chelator and chloroquine into *Plasmodium falciparum* infected erythrocytes. *Biochem Pharmacol* 2003, 65:1351-1360.

88. Macomber PB, O'Brien RL, Hahn FE: Chloroquine: physiological basis of drug resistance in *Plasmodium berghei*. *Science* 1966, 152:1374-1375.

89. Verdier F, Le Bras J, Clavier F, Hatin I, Blayo MC: Chloroquine uptake by *Plasmodium falciparum*-infected human erythrocytes during in vitro culture and its relationship to chloroquine resistance. *Antimicrob Agents Chemother* 1985, 27:561-564.

90. Cabrera M, Natarajan J, Paguio MF, Wolf C, Urbach JS, Roepe PD: Chloroquine transport in *Plasmodium falciparum*. 1. Influx and efflux kinetics for live trophozoite parasites using a novel fluorescent chloroquine probe. *Biochemistry* 2009, 48:9471-9481.

91. Ch'ng JH, Kotturi SR, Chong AG, Lear MJ, Tan KS: A programmed cell death pathway in the malaria parasite *Plasmodium falciparum* has general features of mammalian apoptosis but is mediated by clan CA cysteine proteases. *Cell Death Dis* 2010, 1:e26.

92. Loh CC, Suwanarusk R, Lee YQ, Chan KW, Choy KY, Renia L, Russell B, Lear MJ, Nosten FH, Tan KS, Chow LM: Characterization of the commercially-available fluorescent chloroquine-BODIPY conjugate, LynxTag-CQ_{GREEN}, as a marker for chloroquine resistance and uptake in a 96-well plate assay. *PLoS One* 2014, 9:e110800.

93. Fitch CD: Antimalarial schizontocides: ferriprotoporphyrin IX interaction hypothesis. *Parasitol Today* 1986, 2:330-331.

94. Lakshmanan V, Bray PG, Verdier-Pinard D, Johnson DJ, Horrocks P, Muhle RA, Alakpa GE, Hughes RH, Ward SA, Krogstad DJ, et al: A critical role for PfCRT K76T in *Plasmodium falciparum* verapamil-reversible chloroquine resistance. *EMBO J* 2005, 24:2294-2305.

95. Sidhu AB, Verdier-Pinard D, Fidock DA: Chloroquine resistance in *Plasmodium falciparum* malaria parasites conferred by *pfcrt* mutations. *Science* 2002, 298:210-213.

96. Wongsrichanalai C, Pickard AL, Wernsdorfer WH, Meshnick SR: Epidemiology of drug-resistant malaria. *Lancet Infect Dis* 2002, 2:209-218.

97. Raynes KJ, Bray PG, Ward SA: Altered binding of chloroquine to ferriprotoporphyrin IX is the basis for chloroquine resistance. *Drug Resistance Updates* 1999, 2:97-103.

98. Chen N, Russell B, Fowler E, Peters J, Cheng Q: Levels of chloroquine resistance in *Plasmodium falciparum* are determined by loci other than *pfcrt* and *pfmdr1*. *J Infect Dis* 2002, 185:405-407.

99. Anderson TJ, Nair S, Qin H, Singlam S, Brockman A, Paiphun L, Nosten F: Are transporter genes other than the chloroquine resistance locus (*pfcrt*) and multidrug resistance gene (*pfmdr*) associated with antimalarial drug resistance? *Antimicrob Agents Chemother* 2005, 49:2180-2188.

100. Mehlotra RK, Mattera G, Bockarie MJ, Maguire JD, Baird JK, Sharma YD, Alifrangis M, Dorsey G, Rosenthal PJ, Fryauff DJ, et al: Discordant patterns of genetic variation at two chloroquine resistance loci in worldwide populations of the malaria parasite *Plasmodium falciparum*. *Antimicrob Agents Chemother* 2008, 52:2212-2222.

101. Gligorijevic B, Purdy K, Elliott DA, Cooper RA, Roepe PD: Stage independent chloroquine resistance and chloroquine toxicity revealed via spinning disk confocal microscopy. *Mol Biochem Parasitol* 2008, 159:7-23.
102. Lehane AM, van Schalkwyk DA, Valderramos SG, Fidock DA, Kirk K: Differential drug efflux or accumulation does not explain variation in the chloroquine response of *Plasmodium falciparum* strains expressing the same isoform of mutant PfCRT. *Antimicrob Agents Chemother* 2011, 55:2310-2318.
103. Gaviria D, Paguio MF, Turnbull LB, Tan A, Siriwardana A, Ghosh D, Ferdig MT, Sinai AP, Roepe PD: A process similar to autophagy is associated with cytocidal chloroquine resistance in *Plasmodium falciparum*. *PLoS One* 2013, 8:e79059.
104. Siwo GH, Tan A, Button-Simons KA, Samarakoon U, Checkley LA, Pinapati RS, Ferdig MT: Predicting functional and regulatory divergence of a drug resistance transporter gene in the human malaria parasite. *BMC Genomics* 2015, 16:115.
105. Bray PG, Martin RE, Tilley L, Ward SA, Kirk K, Fidock DA: Defining the role of PfCRT in *Plasmodium falciparum* chloroquine resistance. *Mol Microbiol* 2005, 56:323-333.
106. Lehane AM, Hayward R, Saliba KJ, Kirk K: A verapamil-sensitive chloroquine-associated H^+ leak from the digestive vacuole in chloroquine-resistant malaria parasites. *J Cell Sci* 2008, 121:1624-1632.
107. Suwalsky M, Muñoz M, Mennickent S, Sotomayor CP, Bolognin S, Zatta P: Structural effects of verapamil on cell membranes and molecular models. *Journal of the Chilean Chemical Society* 2010, 55:1-4.
108. Bakkenist CJ, Kastan MB: DNA damage activates ATM through intermolecular autophosphorylation and dimer dissociation. *Nature* 2003, 421:499-506.
109. Kitagawa R, Bakkenist CJ, McKinnon PJ, Kastan MB: Phosphorylation of SMC1 is a critical downstream event in the ATM-NBS1-BRCA1 pathway. *Genes Dev* 2004, 18:1423-1438.
110. Maclean KH, Dorsey FC, Cleveland JL, Kastan MB: Targeting lysosomal degradation induces p53-dependent cell death and prevents cancer in mouse models of lymphomagenesis. *The Journal of Clinical Investigation* 2008, 118:79-88.
111. Tait SW, Ichim G, Green DR: Die another way--non-apoptotic mechanisms of cell death. *J Cell Sci* 2014, 127:2135-2144.

112. Shintani T, Klionsky DJ: Autophagy in health and disease: a double-edged sword. *Science* 2004, 306:990-995.
113. Geng Y, Kohli L, Klocke BJ, Roth KA: Chloroquine-induced autophagic vacuole accumulation and cell death in glioma cells is p53 independent. *Neuro-Oncology* 2010, 12:473-481.
114. Herzog C, Yang C, Holmes A, Kaushal GP: zVAD-fmk prevents cisplatin-induced cleavage of autophagy proteins but impairs autophagic flux and worsens renal function. *American Journal of Physiology - Renal Physiology* 2012, 303:F1239-F1250.
115. Hsin IL, Sheu G-T, Jan M-S, Sun H-L, Wu T-C, Chiu L-Y, Lue K-H, Ko J-L: Inhibition of lysosome degradation on autophagosome formation and responses to GMI, an immunomodulatory protein from *Ganoderma microsporum*. *British Journal of Pharmacology* 2012, 167:1287-1300.
116. Klionsky DJ, Elazar Z, Seglen PO, Rubinsztein DC: Does bafilomycin A1 block the fusion of autophagosomes with lysosomes? *Autophagy* 2008, 4:849-950.
117. van Zandbergen G, Luder CG, Heussler V, Duszenko M: Programmed cell death in unicellular parasites: a prerequisite for sustained infection? *Trends Parasitol* 2010, 26:477-483.
118. Reece SE, Pollitt LC, Colegrave N, Gardner A: The meaning of death: evolution and ecology of apoptosis in protozoan parasites. *PLoS Pathog* 2011, 7:e1002320.
119. Luder CG, Campos-Salinas J, Gonzalez-Rey E, van Zandbergen G: Impact of protozoan cell death on parasite-host interactions and pathogenesis. *Parasit Vectors* 2010, 3:116.
120. Cabon L, Martinez-Torres AC, Susin SA: [Programmed cell death comes in many flavors]. *Med Sci (Paris)* 2013, 29:1117-1124.
121. Eisenberg-Lerner A, Bialik S, Simon HU, Kimchi A: Life and death partners: apoptosis, autophagy and the cross-talk between them. *Cell Death Differ* 2009, 16:966-975.
122. Maiuri MC, Zalckvar E, Kimchi A, Kroemer G: Self-eating and self-killing: crosstalk between autophagy and apoptosis. *Nat Rev Mol Cell Biol* 2007, 8:741-752.
123. Hurd H, Grant KM, Arambage SC: Apoptosis-like death as a feature of malaria infection in mosquitoes. *Parasitology* 2006, 132 Suppl:S33-47.

124. Le Chat L, Sinden RE, Dessens JT: The role of metacaspase 1 in *Plasmodium berghei* development and apoptosis. *Mol Biochem Parasitol* 2007, 153:41-47.

125. Totino PRR, Daniel-Ribeiro CT, Corte-Real S, Ferreira-da-Cruz MdF: *Plasmodium falciparum*: Erythrocytic stages die by autophagic-like cell death under drug pressure. *Experimental Parasitology* 2008, 118:478-486.

126. Darzynkiewicz Z, Juan G, Li X, Gorczyca W, Murakami T, Traganos F: Cytometry in cell necrobiology: analysis of apoptosis and accidental cell death (necrosis). *Cytometry* 1997, 27:1-20.

127. Lockshin RA, Zakeri Z: Apoptosis, autophagy, and more. *Int J Biochem Cell Biol* 2004, 36:2405-2419.

128. Eickel N, Kaiser G, Prado M, Burda PC, Roelli M, Stanway RR, Heussler VT: Features of autophagic cell death in *Plasmodium* liver-stage parasites. *Autophagy* 2013, 9:568-580.

129. Warhurst DC, Thomas SC: Pharmacology of the malaria parasite--a study of dose-response relationships in chloroquine-induced autophagic vacuole formation in *Plasmodium berghei*. *Biochem Pharmacol* 1975, 24:2047-2056.

130. Maltese WA, Overmeyer JH: Methuosis: nonapoptotic cell death associated with vacuolization of macropinosome and endosome compartments. *Am J Pathol* 2014, 184:1630-1642.

131. Chan FK: Fueling the flames: Mammalian programmed necrosis in inflammatory diseases. *Cold Spring Harb Perspect Biol* 2012, 4.

132. Minina EA, Bozhkov PV, Hofius D: Autophagy as initiator or executioner of cell death. *Trends Plant Sci* 2014, 19:692-697.

133. Minina EA, Smertenko AP, Bozhkov PV: Vacuolar cell death in plants: Metacaspase releases the brakes on autophagy. *Autophagy* 2014, 10:928-929.

134. Warring SD, Dou Z, Carruthers VB, McFadden GI, van Dooren GG: Characterization of the chloroquine resistance transporter homologue in *Toxoplasma gondii*. *Eukaryot Cell* 2014, 13:1360-1370.

135. Dean M, Rzhetsky A, Allikmets R: The human ATP-binding cassette (ABC) transporter superfamily. *Genome Res* 2001, 11:1156-1166.

136. Ponte-Sucre A: ABC transporters in microorganisms: Research, innovation and value as targets against drug resistance. 01.08.2009 edn: Caister Academic Pr; 2009.
137. Perkins ME, Wu TW, Le Blancq SM: Cyclosporin analogs inhibit in vitro growth of *Cryptosporidium parvum*. *Antimicrobial Agents and Chemotherapy* 1998, 42:843-848.
138. Senior AE, al-Shawi MK, Urbatsch IL: The catalytic cycle of P-glycoprotein. *FEBS Lett* 1995, 377:285-289.
139. Qu Q, Russell PL, Sharom FJ: Stoichiometry and affinity of nucleotide binding to P-glycoprotein during the catalytic cycle. *Biochemistry* 2003, 42:1170-1177.
140. Smith PC, Karpowich N, Millen L, Moody JE, Rosen J, Thomas PJ, Hunt JF: ATP binding to the motor domain from an ABC transporter drives formation of a nucleotide sandwich dimer. *Mol Cell* 2002, 10:139-149.
141. Martin C, Berridge G, Higgins CF, Mistry P, Charlton P, Callaghan R: Communication between multiple drug binding sites on P-glycoprotein. *Mol Pharmacol* 2000, 58:624-632.
142. Martin C, Berridge G, Mistry P, Higgins C, Charlton P, Callaghan R: Drug binding sites on P-glycoprotein are altered by ATP binding prior to nucleotide hydrolysis. *Biochemistry* 2000, 39:11901-11906.
143. Martin C, Higgins CF, Callaghan R: The vinblastine binding site adopts high- and low-affinity conformations during a transport cycle of P-glycoprotein. *Biochemistry* 2001, 40:15733-15742.
144. Linton KJ, Higgins CF: Structure and function of ABC transporters: the ATP switch provides flexible control. *Pflugers Arch* 2007, 453:555-567.
145. Koenderink JB, Kavishe RA, Rijpma SR, Russel FG: The ABCs of multidrug resistance in malaria. *Trends Parasitol* 2010, 26:440-446.
146. Martin C, Berridge G, Higgins CF, Callaghan R: The multi-drug resistance reversal agent SR33557 and modulation of vinca alkaloid binding to P-glycoprotein by an allosteric interaction. *Br J Pharmacol* 1997, 122:765-771.
147. van Veen HW, Margolles A, Muller M, Higgins CF, Konings WN: The homodimeric ATP-binding cassette transporter LmrA mediates multidrug transport by an alternating two-site (two-cylinder engine) mechanism. *Embo j* 2000, 19:2503-2514.

148. Zelcer N, Huisman MT, Reid G, Wielinga P, Breedveld P, Kuil A, Knipscheer P, Schellens JH, Schinkel AH, Borst P: Evidence for two interacting ligand binding sites in human multidrug resistance protein 2 (ATP binding cassette C2). *J Biol Chem* 2003, 278:23538-23544.
149. Shapiro AB, Ling V: Positively cooperative sites for drug transport by P-glycoprotein with distinct drug specificities. *Eur J Biochem* 1997, 250:130-137.
150. Hanahan D, Weinberg RA: The hallmarks of cancer. *Cell* 2000, 100:57-70.
151. Krishna R, Mayer LD: Multidrug resistance (MDR) in cancer: Mechanisms, reversal using modulators of MDR and the role of MDR modulators in influencing the pharmacokinetics of anticancer drugs. *European Journal of Pharmaceutical Sciences* 2000, 11:265-283.
152. Borst P, Evers R, Kool M, Wijnholds J: The multidrug resistance protein family. *Biochimica et Biophysica Acta (BBA) - Biomembranes* 1999, 1461:347-357.
153. Lee CH, Bradley G, Zhang JT, Ling V: Differential expression of P-glycoprotein genes in primary rat hepatocyte culture. *J Cell Physiol* 1993, 157:392-402.
154. Shapiro AB, Ling V: Reconstitution of drug transport by purified P-glycoprotein. *J Biol Chem* 1995, 270:16167-16175.
155. Kavishe R, van den Heuvel J, van de Vegte-Bolmer M, Luty A, Russel F, Koenderink J: Localization of the ATP-binding cassette (ABC) transport proteins PfMRP1, PfMRP2, and PfMDR5 at the *Plasmodium falciparum* plasma membrane. *Malar J* 2009, 8:205.
156. Sauvage V, Aubert D, Escotte-Binet S, Villena I: The role of ATP-binding cassette (ABC) proteins in protozoan parasites. *Mol Biochem Parasitol* 2009, 167:81-94.
157. van der Velden M, Rijpma SR, Russel FG, Sauerwein RW, Koenderink JB: PfMDR2 and PfMDR5 are dispensable for *Plasmodium falciparum* asexual parasite multiplication but change in vitro susceptibility to anti-malarial drugs. *Malar J* 2015, 14:76.
158. Cowman AF, Karcz S, Galatis D, Culvenor JG: A P-glycoprotein homologue of *Plasmodium falciparum* is localized on the digestive vacuole. *J Cell Biol* 1991, 113:1033-1042.
159. Rohrbach P, Sanchez CP, Hayton K, Friedrich O, Patel J, Sidhu AB, Ferdig MT, Fidock DA, Lanzer M: Genetic linkage of *pfmdr1* with food vacuolar solute import in *Plasmodium falciparum*. *EMBO J* 2006, 25:3000-3011.
160. Reed MB, Saliba KJ, Caruana SR, Kirk K, Cowman AF: Pgh1 modulates sensitivity and resistance to multiple antimalarials in *Plasmodium falciparum*. *Nature* 2000, 403:906-909.

161. Price RN, Uhlemann AC, Brockman A, McGready R, Ashley E, Phaipun L, Patel R, Laing K, Looareesuwan S, White NJ, et al: Mefloquine resistance in *Plasmodium falciparum* and increased *pfmdr1* gene copy number. *Lancet* 2004, 364:438-447.

162. Sisowath C, Stromberg J, Martensson A, Msellem M, Obondo C, Bjorkman A, Gil JP: *In vivo* selection of *Plasmodium falciparum pfmdr1* 86N coding alleles by artemether-lumefantrine (Coartem). *J Infect Dis* 2005, 191:1014-1017.

163. Sidhu AB, Valderramos SG, Fidock DA: *pfmdr1* mutations contribute to quinine resistance and enhance mefloquine and artemisinin sensitivity in *Plasmodium falciparum*. *Mol Microbiol* 2005, 57:913-926.

164. Chen N, Chavchich M, Peters JM, Kyle DE, Gatton ML, Cheng Q: Deamplification of *pfmdr1*-containing amplicon on chromosome 5 in *Plasmodium falciparum* is associated with reduced resistance to artelinic acid in vitro. *Antimicrob Agents Chemother* 2010, 54:3395-3401.

165. Chavchich M, Gerena L, Peters J, Chen N, Cheng Q, Kyle DE: Induction of resistance to artemisinin derivatives in *Plasmodium falciparum*: Role of *pfmdr1* amplification and expression. *Antimicrob Agents Chemother* 2010.

166. Patel SK, George L-B, Prasanth Kumar S, Highland HN, Jasrai YT, Pandya HA, Desai KR: A computational approach towards the understanding of *Plasmodium falciparum* multidrug resistance protein 1. *ISRN Bioinformatics* 2013, 2013:15.

167. Ibraheem ZO, Abd Majid R, Noor SM, Sedik HM, Basir R: Role of different *pfcrt* and *pfmdr*-1 mutations in conferring resistance to antimalaria drugs in *Plasmodium falciparum*. *Malar Res Treat* 2014, 2014:950424.

168. Ferreira PE, Holmgren G, Veiga MI, Uhlen P, Kaneko A, Gil JP: PfMDR1: mechanisms of transport modulation by functional polymorphisms. *PLoS One* 2011, 6:e23875.

169. Loo TW, Bartlett MC, Clarke DM: Processing mutations disrupt interactions between the nucleotide binding and transmembrane domains of P-glycoprotein and the cystic fibrosis transmembrane conductance regulator (CFTR). *J Biol Chem* 2008, 283:28190-28197.

170. Oancea G, O'Mara ML, Bennett WF, Tieleman DP, Abele R, Tampe R: Structural arrangement of the transmission interface in the antigen ABC transport complex TAP. *Proc Natl Acad Sci U S A* 2009, 106:5551-5556.

171. Endicott JA, Ling V: The biochemistry of P-glycoprotein-mediated multidrug resistance. *Annu Rev Biochem* 1989, 58:137-171.

172. Duraisingh MT, Refour P: Multiple drug resistance genes in malaria -- from epistasis to epidemiology. *Mol Microbiol* 2005, 57:874-877.

173. Cowman AF, Galatis D, Thompson JK: Selection for mefloquine resistance in *Plasmodium falciparum* is linked to amplification of the *pfmdr1* gene and cross-resistance to halofantrine and quinine. *Proc Natl Acad Sci U S A* 1994, 91:1143-1147.

174. Ngo T, Duraisingh M, Reed M, Hipgrave D, Biggs B, Cowman AF: Analysis of *pfcrt*, *pfmdr1*, *dhfr*, and *dhps* mutations and drug sensitivities in *Plasmodium falciparum* isolates from patients in Vietnam before and after treatment with artemisinin. *Am J Trop Med Hyg* 2003, 68:350-356.

175. Pickard AL, Wongsrichanalai C, Purfield A, Kamwendo D, Emery K, Zalewski C, Kawamoto F, Miller RS, Meshnick SR: Resistance to antimalarials in Southeast Asia and genetic polymorphisms in *pfmdr1*. *Antimicrob Agents Chemother* 2003, 47:2418-2423.

176. Wilson CM, Volkman SK, Thaithong S, Martin RK, Kyle DE, Milhous WK, Wirth DF: Amplification of *pfmdr 1* associated with mefloquine and halofantrine resistance in *Plasmodium falciparum* from Thailand. *Mol Biochem Parasitol* 1993, 57:151-160.

177. Preechapornkul P, Imwong M, Chotivanich K, Pongtavornpinyo W, Dondorp AM, Day NP, White NJ, Pukrittayakamee S: *Plasmodium falciparum pfmdr1* amplification, mefloquine resistance, and parasite fitness. *Antimicrob Agents Chemother* 2009, 53:1509-1515.

178. Anderson TJ, Patel J, Ferdig MT: Gene copy number and malaria biology. *Trends Parasitol* 2009, 25:336-343.

179. White NJ, Pongtavornpinyo W: The *de novo* selection of drug-resistant malaria parasites. *Proc Biol Sci* 2003, 270:545-554.

180. Nair S, Nash D, Sudimack D, Jaidee A, Barends M, Uhlemann AC, Krishna S, Nosten F, Anderson TJ: Recurrent gene amplification and soft selective sweeps during evolution of multidrug resistance in malaria parasites. *Mol Biol Evol* 2007, 24:562-573.

181. Peel SA, Bright P, Yount B, Handy J, Baric RS: A strong association between mefloquine and halofantrine resistance and amplification, overexpression, and mutation in the P-

glycoprotein gene homolog (*pfmdr*) of *Plasmodium falciparum in vitro*. *Am J Trop Med Hyg* 1994, 51:648-658.

182. Pumpaibool T, Arnathau C, Durand P, Kanchanakhan N, Siripoon N, Suegorn A, Sitthi-Amorn C, Renaud F, Harnyuttanakorn P: Genetic diversity and population structure of *Plasmodium falciparum* in Thailand, a low transmission country. *Malar J* 2009, 8:155.

183. WHO: World Malaria Report 2005. 2005.

184. Mungthin M, Suwandittakul N, Chaijaroenkul W, Rungsrihirunrat K, Harnyuttanakorn P, Seugorn A, Na Bangchang K: The patterns of mutation and amplification of *Plasmodium falciparum pfcrt* and *pfmdr1* genes in Thailand during the year 1988 to 2003. *Parasitol Res* 2010.

185. Wongsrichanalai C, Sirichaisinthop J, Karwacki JJ, Congpuong K, Miller RS, Pang L, Thimasarn K: Drug resistant malaria on the Thai-Myanmar and Thai-Cambodian borders. *Southeast Asian J Trop Med Public Health* 2001, 32:41-49.

186. Price RN, Uhlemann AC, van Vugt M, Brockman A, Hutagalung R, Nair S, Nash D, Singhasivanon P, Anderson TJ, Krishna S, et al: Molecular and pharmacological determinants of the therapeutic response to artemether-lumefantrine in multidrug-resistant *Plasmodium falciparum* malaria. *Clin Infect Dis* 2006, 42:1570-1577.

187. Rogers WO, Sem R, Tero T, Chim P, Lim P, Muth S, Socheat D, Ariey F, Wongsrichanalai C: Failure of artesunate-mefloquine combination therapy for uncomplicated *Plasmodium falciparum* malaria in southern Cambodia. *Malar J* 2009, 8:10.

188. Poyomtip T, Suwandittakul N, Sitthichot N, Khositnithikul R, Tan-ariya P, Mungthin M: Polymorphisms of the *pfmdr1* but not the *pfnhe-1* gene is associated with *in vitro* quinine sensitivity in Thai isolates of *Plasmodium falciparum*. *Malar J* 2012, 11:7.

189. Dye C, Williams BG: Multigenic drug resistance among inbred malaria parasites. *Proc Biol Sci* 1997, 264:61-67.

190. Noedl H, Se Y, Schaecher K, Smith BL, Socheat D, Fukuda MM: Evidence of artemisinin-resistant malaria in western Cambodia. *N Engl J Med* 2008, 359:2619-2620.

191. Cerutti Junior C, Marques C, Alencar FE, Durlacher RR, Alween A, Segurado AA, Pang LW, Zalis MG: Antimalarial drug susceptibility testing of *Plasmodium falciparum* in Brazil using a radioisotope method. *Mem Inst Oswaldo Cruz* 1999, 94:803-809.

192. Boulos M, di Santi SM, Barradas Barata LC, Cotrim Segurado AA, Pacheco Dutra A, Fonseca de Camargo Neves VL: Some aspects of treatment, prophylaxis and chemoresistance of *Plasmodium falciparum* malaria. *Am J Trop Med Hyg* 1986, 46:8-14.

193. Griffing S, Syphard L, Sridaran S, McCollum AM, Mixson-Hayden T, Vinayak S, Villegas L, Barnwell JW, Escalante AA, Udhayakumar V: *pfmdr1* amplification and fixation of *pfcrt* chloroquine resistance alleles in *Plasmodium falciparum* in Venezuela. *Antimicrob Agents Chemother* 2010, 54:1572-1579.

194. Gama BE, de Oliveira NK, de Souza JM, Santos F, de Carvalho LJ, Melo YF, Rosenthal PJ, Daniel-Ribeiro CT, Ferreira-da-Cruz Mde F: Brazilian *Plasmodium falciparum* isolates: investigation of candidate polymorphisms for artemisinin resistance before introduction of artemisinin-based combination therapy. *Malar J* 2010, 9:355.

195. Humphreys GS, Merinopoulos I, Ahmed J, Whitty CJ, Mutabingwa TK, Sutherland CJ, Hallett RL: Amodiaquine and artemether-lumefantrine select distinct alleles of the *Plasmodium falciparum mdr1* gene in Tanzanian children treated for uncomplicated malaria. *Antimicrob Agents Chemother* 2007, 51:991-997.

196. Rosenthal PJ: The interplay between drug resistance and fitness in malaria parasites. *Molecular microbiology* 2013, 89:1025-1038.

197. Danquah I, Coulibaly B, Meissner P, Petruschke I, Müller O, Mockenhaupt FP: Selection of *pfmdr1* and *pfcrt* alleles in amodiaquine treatment failure in north-western Burkina Faso. *Acta Tropica* 2010, 114:63-66.

198. Alam MT, de Souza DK, Vinayak S, Griffing SM, Poe AC, Duah NO, Ghansah A, Asamoa K, Slutsker L, Wilson MD, et al: Selective sweeps and genetic lineages of *Plasmodium falciparum* drug-resistant alleles in Ghana. *J Infect Dis* 2011, 203:220-227.

199. Andriantsoanirina V, Ratsimbasoa A, Bouchier C, Tichit M, Jahevitra M, Rabearimanana S, Raherinjafy R, Mercereau-Puijalon O, Durand R, Menard D: Chloroquine clinical failures in *P. falciparum* malaria are associated with mutant *pfmdr-1*, not *pfcrt* in Madagascar. *PLoS One* 2010, 5:e13281.

200. Gowda DC, Davidson EA: Protein glycosylation in the malaria parasite. *Parasitol Today* 1999, 15:147-152.

201. Taguchi Y, Kino K, Morishima M, Komano T, Kane SE, Ueda K: Alteration of substrate specificity by mutations at the His61 position in predicted transmembrane domain 1 of human MDR1/P-glycoprotein. *Biochemistry* 1997, 36:8883-8889.

202. Sanchez CP, Rotmann A, Stein WD, Lanzer M: Polymorphisms within PfMDR1 alter the substrate specificity for anti-malarial drugs in *Plasmodium falciparum*. *Mol Microbiol* 2008, 70:786-798.

203. Sisowath C, Ferreira PE, Bustamante LY, Dahlstrom S, Martensson A, Bjorkman A, Krishna S, Gil JP: The role of *pfmdr1* in *Plasmodium falciparum* tolerance to artemether-lumefantrine in Africa. *Trop Med Int Health* 2007, 12:736-742.

204. Chaiyaroj SC, Buranakiti A, Angkasekwinai P, Looressuwan S, Cowman AF: Analysis of mefloquine resistance and amplification of *pfmdr1* in multidrug-resistant *Plasmodium falciparum* isolates from Thailand. *Am J Trop Med Hyg* 1999, 61:780-783.

205. Price RN, Cassar C, Brockman A, Duraisingh M, van Vugt M, White NJ, Nosten F, Krishna S: The *pfmdr1* gene is associated with a multidrug-resistant phenotype in *Plasmodium falciparum* from the western border of Thailand. *Antimicrob Agents Chemother* 1999, 43:2943-2949.

206. Lekostaj JK, Amoah LE, Roepe PD: A single S1034C mutation confers altered drug sensitivity to PfMDR1 ATPase activity that is characteristic of the 7G8 isoform. *Mol Biochem Parasitol* 2008, 157:107-111.

207. Duraisingh MT, Jones P, Sambou I, von Seidlein L, Pinder M, Warhurst DC: The tyrosine-86 allele of the *pfmdr1* gene of *Plasmodium falciparum* is associated with increased sensitivity to the anti-malarials mefloquine and artemisinin. *Mol Biochem Parasitol* 2000, 108:13-23.

208. Basco LK, Le Bras J, Rhoades Z, Wilson CM: Analysis of *pfmdr1* and drug susceptibility in fresh isolates of *Plasmodium falciparum* from subsaharan Africa. *Mol Biochem Parasitol* 1995, 74:157-166.

209. Duraisingh MT, von Seidlein LV, Jepson A, Jones P, Sambou I, Pinder M, Warhurst DC: Linkage disequilibrium between two chromosomally distinct loci associated with increased resistance to chloroquine in *Plasmodium falciparum*. *Parasitology* 2000, 121 (Pt 1):1-7.

210. Sibley CH: Understanding drug resistance in malaria parasites: Basic science for public health. *Mol Biochem Parasitol* 2014.

211. Sidhu AB, Uhlemann AC, Valderramos SG, Valderramos JC, Krishna S, Fidock DA: Decreasing *pfmdr1* copy number in *Plasmodium falciparum* malaria heightens susceptibility to mefloquine, lumefantrine, halofantrine, quinine, and artemisinin. *J Infect Dis* 2006, 194:528-535.

212. Safa AR, Stern RK, Choi K, Agresti M, Tamai I, Mehta ND, Roninson IB: Molecular basis of preferential resistance to colchicine in multidrug-resistant human cells conferred by Gly-185----Val-185 substitution in P-glycoprotein. *Proc Natl Acad Sci U S A* 1990, 87:7225-7229.

213. Friedrich O, Reiling SJ, Wunderlich J, Rohrbach P: Assessment of *Plasmodium falciparum* PfMDR1 transport rates using Fluo-4. *J Cell Mol Med* 2014.

214. Wellems TE, Panton LJ, Gluzman IY, do Rosario VE, Gwadz RW, Walker-Jonah A, Krogstad DJ: Chloroquine resistance not linked to *mdr*-like genes in a *Plasmodium falciparum* cross. *Nature* 1990, 345:253-255.

215. Trager W, Jensen JB: Human malaria parasites in continuous culture. *Science* 1976, 193:673-675.

216. Hall TA: BioEdit: a user-friendly biological sequence alignment editor and analysis program for Windows 95/98/NT. *Nucleic Acids Symp* 1999, 41:95-98.

217. Bacon DJ, Latour C, Lucas C, Colina O, Ringwald P, Picot S: Comparison of a SYBR green I-based assay with a histidine-rich protein II enzyme-linked immunosorbent assay for in vitro antimalarial drug efficacy testing and application to clinical isolates. *Antimicrob Agents Chemother* 2007, 51:1172-1178.

218. Le Nagard H, Vincent C, Mentre F, Le Bras J: Online analysis of in vitro resistance to antimalarial drugs through nonlinear regression. *Comput Methods Programs Biomed* 2011, 104:10-18.

219. Kaddouri H, Nakache S, Houze S, Mentre F, Le Bras J: Assessment of the drug susceptibility of *Plasmodium falciparum* clinical isolates from africa by using a *Plasmodium* lactate dehydrogenase immunodetection assay and an inhibitory maximum

effect model for precise measurement of the 50-percent inhibitory concentration. *Antimicrob Agents Chemother* 2006, 50:3343-3349.

220. Mawili-Mboumba DP, Kun JF, Lell B, Kremsner PG, Ntoumi F: *Pfmdr1* alleles and response to ultralow-dose mefloquine treatment in Gabonese patients. *Antimicrob Agents Chemother* 2002, 46:166-170.

221. Rason MA, Andrianantenaina HB, Ariey F, Raveloson A, Domarle O, Randrianarivelojosia M: Prevalent *pfmdr1* N86Y mutant *Plasmodium falciparum* in Madagascar despite absence of *pfcrt* mutant strains. *Am J Trop Med Hyg* 2007, 76:1079-1083.

222. Fox E, Bates SE: Tariquidar (XR9576): a P-glycoprotein drug efflux pump inhibitor. *Expert Rev Anticancer Ther* 2007, 7:447-459.

223. Witkowski B, Nicolau ML, Soh PN, Iriart X, Menard S, Alvarez M, Marchou B, Magnaval JF, Benoit-Vical F, Berry A: *Plasmodium falciparum* isolates with increased *pfmdr1* copy number circulate in West Africa. *Antimicrob Agents Chemother* 2010, 54:3049-3051.

224. Childs GE, Pang L, Wimonwattrawatee T, Pooyindee N, Nanakorn A, Limchitee S, Webster HK: *In vitro* mefloquine resistance of *Plasmodium falciparum* isolated from the Burmese border region of Thailand. *Southeast Asian J Trop Med Public Health* 1987, 18:438-443.

225. Oduola AM, Omitowoju GO, Gerena L, Kyle DE, Milhous WK, Sowunmi A, Salako LA: Reversal of mefloquine resistance with penfluridol in isolates of *Plasmodium falciparum* from south-west Nigeria. *Trans R Soc Trop Med Hyg* 1993, 87:81-83.

226. Fox E, Bates SE: Tariquidar (XR9576): a P-glycoprotein drug efflux pump inhibitor. *Expert Review of Anticancer Therapy* 2007, 7:447-459.

227. Eyase FL, Akala HM, Ingasia L, Cheruiyot A, Omondi A, Okudo C, Juma D, Yeda R, Andagalu B, Wanja E, et al: The role of *pfmdr1* and *pfcrt* in changing chloroquine, amodiaquine, mefloquine and lumefantrine susceptibility in western-Kenya P. falciparum samples during 2008-2011. *PLoS One* 2013, 8:e64299.

228. Duraisingh M, Drakeley C, Muller O, Bailey R, Snounou G, Targett G, Greenwood B, Warhurst D: Evidence for selection for the tyrosine-86 allele of the *pfmdr 1* gene of *Plasmodium falciparum* by chloroquine and amodiaquine. *Parasitology* 1997, 114:205-211.

229. Urbatsch IL, Sankaran B, Bhagat S, Senior AE: Both P-glycoprotein nucleotide-binding sites are catalytically active. *Journal of Biological Chemistry* 1995, 270:26956-26961.

230. Cowman AF, Crabb BS: A parasite genome sheds light on an old enemy. *Nat Biotechnol* 2002, 20:1098-1099.

231. Pillai DR, Hijar G, Montoya Y, Marouino W, Ruebush TK, 2nd, Wongsrichanalai C, Kain KC: Lack of prediction of mefloquine and mefloquine-artesunate treatment outcome by mutations in the *Plasmodium falciparum* multidrug resistance 1 (*pfmdr1*) gene for *P. falciparum* malaria in Peru. *Am J Trop Med Hyg* 2003, 68:107-110.

232. Murray CJ, Rosenfeld LC, Lim SS, Andrews KG, Foreman KJ, Haring D, Fullman N, Naghavi M, Lozano R, Lopez AD: Global malaria mortality between 1980 and 2010: a systematic analysis. *Lancet* 2012, 379:413-431.

233. Ridley RG: Malaria: Dissecting chloroquine resistance. *Current Biology* 1998, 8:R346-R349.

234. Le Bras J, Durand R: The mechanisms of resistance to antimalarial drugs in *Plasmodium falciparum*. *Fundam Clin Pharmacol* 2003, 17:147-153.

235. Dorn A, Stoffel R, Matile H, Bubendorf A, Ridley RG: Malarial haemozoin/beta-haematin supports haem polymerization in the absence of protein. *Nature* 1995, 374:269-271.

236. Fitch CD, Chevli R, Banyal HS, Phillips G, Pfaller MA, Krogstad DJ: Lysis *of Plasmodium falciparum* by ferriprotoporphyrin IX and a chloroquine-ferriprotoporphyrin IX complex. *Antimicrob Agents Chemother* 1982, 21:819-822.

237. Pagola S, Stephens PW, Bohle DS, Kosar AD, Madsen SK: The structure of malaria pigment beta-haematin. *Nature* 2000, 404:307-310.

238. Jensen M, Mehlhorn H: Seventy-five years of Resochin in the fight against malaria. *Parasitol Res* 2009, 105:609-627.

239. Djimde A, Doumbo OK, Cortese JF, Kayentao K, Doumbo S, Diourte Y, Dicko A, Su XZ, Nomura T, Fidock DA, et al: A molecular marker for chloroquine-resistant *falciparum* malaria. *N Engl J Med* 2001, 344:257-263.

240. Petersen I, Gabryszewski SJ, Johnston GL, Dhingra SK, Ecker A, Lewis RE, de Almeida MJ, Straimer J, Henrich PP, Palatulan E, et al: Balancing drug resistance and growth rates via compensatory mutations in the *Plasmodium falciparum* chloroquine resistance transporter. *Mol Microbiol* 2015.

241. Bennett TN, Paguio M, Gligorijevic B, Seudieu C, Kosar AD, Davidson E, Roepe PD: Novel, rapid, and inexpensive cell-based quantification of antimalarial drug efficacy. *Antimicrob Agents Chemother* 2004, 48:1807-1810.

242. Baniecki ML, Wirth DF, Clardy J: High-throughput *Plasmodium falciparum* growth assay for malaria drug discovery. *Antimicrob Agents Chemother* 2007, 51:716-723.

243. Valderramos SG, Valderramos JC, Musset L, Purcell LA, Mercereau-Puijalon O, Legrand E, Fidock DA: Identification of a mutant PfCRT-mediated chloroquine tolerance phenotype in *Plasmodium falciparum*. *PLoS Pathog* 2010, 6:e1000887.

244. Malmquist NA, Moss TA, Mecheri S, Scherf A, Fuchter MJ: Small-molecule histone methyltransferase inhibitors display rapid antimalarial activity against all blood stage forms in *Plasmodium falciparum*. *Proc Natl Acad Sci U S A* 2012, 109:16708-16713.

245. Ch'ng JH, Liew K, Goh AS, Sidhartha E, Tan KS: Drug-induced permeabilization of parasite's digestive vacuole is a key trigger of programmed cell death in *Plasmodium falciparum*. *Cell Death Dis* 2011, 2:e216.

246. Rohrbach P, Friedrich O, Hentschel J, Plattner H, Fink RH, Lanzer M: Quantitative calcium measurements in subcellular compartments of *Plasmodium falciparum*-infected erythrocytes. *J Biol Chem* 2005, 280:27960-27969.

247. Meslin B, Barnadas C, Boni V, Latour C, De Monbrison F, Kaiser K, Picot S: Features of apoptosis in *Plasmodium falciparum* erythrocytic stage through a putative role of PfMCA1 metacaspase-like protein. *J Infect Dis* 2007, 195:1852-1859.

248. Pasini EM, van den Ierssel D, Vial HJ, Kocken CH: A novel live-dead staining methodology to study malaria parasite viability. *Malar J* 2013, 12:190.

249. Ch'ng JH, Lee YQ, Gun SY, Chia WN, Chang ZW, Wong LK, Batty KT, Russell B, Nosten F, Renia L, Tan KS: Validation of a chloroquine-induced cell death mechanism for clinical use against malaria. *Cell Death Dis* 2014, 5:e1305.

250. Rombo L, Bergqvist Y, Hellgren U: Chloroquine and desethylchloroquine concentrations during regular long-term malaria prophylaxis. *Bulletin of the World Health Organization* 1987, 65:879-883.

251. Mockenhaupt FP, May J, Bergqvist Y, Ademowo OG, Olumese PE, Falusi AG, Großterlinden L, Meyer CG, Bienzle U: Concentrations of chloroquine and malaria parasites in blood in Nigerian children. *Antimicrobial Agents and Chemotherapy* 2000, 44:835-839.

252. Thomas D, Tovey SC, Collins TJ, Bootman MD, Berridge MJ, Lipp P: A comparison of fluorescent Ca^{2+} indicator properties and their use in measuring elementary and global Ca^{2+} signals. *Cell Calcium* 2000, 28:213-223.

253. Lovett JL, Sibley LD: Intracellular calcium stores in *Toxoplasma gondii* govern invasion of host cells. *J Cell Sci* 2003, 116:3009-3016.

254. Stagg MA, Malik AH, MacLeod KT, Terracciano CM: The effects of overexpression of the Na^{+}/Ca^{2+} exchanger on calcium regulation in hypertrophied mouse cardiac myocytes. *Cell Calcium* 2004, 36:111-118.

255. Hirase H, Qian L, Bartho P, Buzsaki G: Calcium dynamics of cortical astrocytic networks *in vivo*. *PLoS Biol* 2004, 2:E96.

256. Nyakeriga AM, Perlmann H, Hagstedt M, Berzins K, Troye-Blomberg M, Zhivotovsky B, Perlmann P, Grandien A: Drug-induced death of the asexual blood stages of *Plasmodium falciparum* occurs without typical signs of apoptosis. *Microbes Infect* 2006, 8:1560-1568.

257. Hain AU, Weltzer RR, Hammond H, Jayabalasingham B, Dinglasan RR, Graham DR, Colquhoun DR, Coppens I, Bosch J: Structural characterization and inhibition of the *Plasmodium* Atg8-Atg3 interaction. *J Struct Biol* 2012, 180:551-562.

258. Rigden DJ, Michels PA, Ginger ML: Autophagy in protists: Examples of secondary loss, lineage-specific innovations, and the conundrum of remodeling a single mitochondrion. *Autophagy* 2009, 5:784-794.

259. Tomlins AM, Ben-Rached F, Williams RA, Proto WR, Coppens I, Ruch U, Gilberger TW, Coombs GH, Mottram JC, Muller S, Langsley G: *Plasmodium falciparum* ATG8 implicated in both autophagy and apicoplast formation. *Autophagy* 2013, 9.

260. Wlodkowic D, Skommer J, Darzynkiewicz Z: Flow cytometry-based apoptosis detection. *Methods Mol Biol* 2009, 559:19-32.

261. Fivelman QL, Adagu IS, Warhurst DC: Effects of piperaquine, chloroquine, and amodiaquine on drug uptake and of these in combination with dihydroartemisinin against

drug-sensitive and -resistant *Plasmodium falciparum* strains. *Antimicrob Agents Chemother* 2007, 51:2265-2267.

262. Papakrivos J, Sa JM, Wellems TE: Functional characterization of the *Plasmodium falciparum* chloroquine-resistance transporter (PfCRT) in transformed *Dictyostelium discoideum* vesicles. *PLoS One* 2012, 7:e39569.

263. Ch'ng JH, Mok S, Bozdech Z, Lear MJ, Boudhar A, Russell B, Nosten F, Tan KS: A whole cell pathway screen reveals seven novel chemosensitizers to combat chloroquine resistant malaria. *Sci Rep* 2013, 3:1734.

264. Smilkstein M, Sriwilaijaroen N, Kelly JX, Wilairat P, Riscoe M: Simple and inexpensive fluorescence-based technique for high-throughput antimalarial drug screening. *Antimicrob Agents Chemother* 2004, 48:1803-1806.

265. Martin MM, Lindqvist L: The pH dependence of fluorescein fluorescence. *Journal of Luminescence* 1975, 10:381-390.

266. Shaner NC, Steinbach PA, Tsien RY: A guide to choosing fluorescent proteins. *Nat Methods* 2005, 2:905-909.

267. Urano Y, Asanuma D, Hama Y, Koyama Y, Barrett T, Kamiya M, Nagano T, Watanabe T, Hasegawa A, Choyke PL, Kobayashi H: Selective molecular imaging of viable cancer cells with pH-activatable fluorescence probes. *Nat Med* 2009, 15:104-109.

268. Karolin J, Johansson LBA, Strandberg L, Ny T: Fluorescence and absorption spectroscopic properties of dipyrrometheneboron difluoride (BODIPY) derivatives in liquids, lipid membranes, and proteins. *Journal of the American Chemical Society* 1994, 116:7801-7806.

269. Shore JD, Day DE, Francis-Chmura AM, Verhamme I, Kvassman J, Lawrence DA, Ginsburg D: A fluorescent probe study of plasminogen activator inhibitor-1. Evidence for reactive center loop insertion and its role in the inhibitory mechanism. *J Biol Chem* 1995, 270:5395-5398.

270. Lakowicz JR: *Principles of fluorescence spectroscopy.* 3 edn: Springer; 2006.

271. Sanchez H, Alonso JC: *Bacillus subtilis* RecN binds and protects 3'-single-stranded DNA extensions in the presence of ATP. *Nucleic Acids Res* 2005, 33:2343-2350.

272. Sanchez CP, Stein WD, Lanzer M: Is PfCRT a channel or a carrier? Two competing models explaining chloroquine resistance in *Plasmodium falciparum*. *Trends Parasitol* 2007, 23:332-339.

273. Krogstad DJ, Schlesinger PH: The basis of antimalarial action: non-weak base effects of chloroquine on acid vesicle pH. *Am J Trop Med Hyg* 1987, 36:213-220.

274. Martiney JA, Cerami A, Slater AFG: Verapamil reversal of chloroquine resistance in the malaria parasite *Plasmodium falciparum* is specific for resistant parasites and independent of the weak base effect. *Journal of Biological Chemistry* 1995, 270:22393-22398.

275. Chinappi M, Via A, Marcatili P, Tramontano A: On the mechanism of chloroquine resistance in *Plasmodium falciparum*. *PLoS One* 2010, 5:e14064.

276. Sanchez CP, Rohrbach P, McLean JE, Fidock DA, Stein WD, Lanzer M: Differences in trans-stimulated chloroquine efflux kinetics are linked to PfCRT in *Plasmodium falciparum*. *Mol Microbiol* 2007, 64:407-420.

277. Masuhara H, Shioyama H, Saito T, Hamada K, Yasoshima S, Mataga N: Fluorescence quenching mechanism of aromatic hydrocarbons by closed-shell heavy metal ions in aqueous and organic solutions. *The Journal of Physical Chemistry* 1984, 88:5868-5873.

278. Bray PG, Saliba KJ, Davies JD, Spiller DG, White MRH, Kirk K, Ward SA: Distribution of acridine orange fluorescence in *Plasmodium falciparum*-infected erythrocytes and its implications for the evaluation of digestive vacuole pH. *Molecular and Biochemical Parasitology* 2002, 119:301-304.

279. Bray PG, Saliba KJ, Davies JD, Spiller DG, White MRH, Kirk K, Ward SA: Further comments on the distribution of acridine orange fluorescence in *P. falciparum*–infected erythrocytes. *Molecular and Biochemical Parasitology* 2002, 119:311-313.

280. Bray PG, Janneh O, Raynes KJ, Mungthin M, Ginsburg H, Ward SA: Cellular uptake of chloroquine is dependent on binding to ferriprotoporphyrin IX and is independent of NHE activity in *Plasmodium falciparum*. *The Journal of Cell Biology* 1999, 145:363-376.

Annex

Permission for reproduction of figures:

Figure 1.1: modified from [14]. Reprinted by permission from Macmillan Publishers Ltd: IMMUNOLOGY & CELL BIOLOGY. Wipasa, J., et al. (2002). "Immunity to asexual blood stage malaria and vaccine approaches." *Immunol Cell Biol* 80(5): 401-414, copyright 2002

Figure 1.3: modified from [159]. Reprinted by permission from John Wiley and Sons: The EMBO Journal. Rohrbach, P., et al. (2006). "Genetic linkage of *pfmdr1* with food vacuolar solute import in *Plasmodium falciparum*." *EMBO J* 25(13): 3000-3011, copyright 2006.